

1 2 9 0



UNIVERSIDADE D  
COIMBRA

Beatriz Franco Azevedo

**INERTIZATION OF HEAVY METALS IN SOILS –  
UTILIZATION OF NANOTECHNOLOGIES AND  
NATURAL WASTES**

**Dissertation of Integrated Master's Degree in Chemical Engineering, Specialization in Process, Environment and Energy, with the orientation of Maria da Graça Bontempo Vaz Rasteiro, PhD and António Alberto Santos Correia, PhD, and presented to the Department of Chemical Engineering of the Faculty of Sciences and Technology of the University of Coimbra.**

September 2020



Beatriz Franco Azevedo

**INERTIZATION OF HEAVY METALS IN SOILS –  
UTILIZATION OF NANOTECHNOLOGIES AND  
NATURAL WASTES**

**Dissertation of Integrated Master's Degree in Chemical Engineering with the orientation of Maria da Graça Bontempo Vaz Rasteiro, PhD and António Alberto Santos Correia, PhD, and presented to the Department of Chemical Engineering of the Faculty of Sciences and Technology of the University of Coimbra.**

September 2020



## Acknowledgements

The academic path is never covered alone and for this reason I would like to name several people who have participated in this journey and made this possible and more enjoyable along the way. Thus I express my deepest thanks:

To Professor Doctor Maria da Graça Rasteiro for being my supervisor in this work, for the availability to answer all my questions and give guidance and suggestions when needed, and for the knowledge shared.

To Professor Doctor António Alberto Santos Correia for being my co-supervisor, for the guidance given in the geotechnical laboratory and the share of knowledge of the methodologies used, and for all the suggestions and willingness to assist throughout this journey.

To VTT Technical Research Centre of Finland (Finland) for providing the LigniOx-LB used in this study.

To Mr. José António Lopes for all the assistance in the geotechnical laboratory, for the shared knowledge and ideas and for all the relentless support and words of encouragement.

To Doctor Luís Alves and to Solange Magalhães for the company in the chemical engineering laboratory, for the willingness to answer all my questions, for all the support and words of encouragement given, and for the knowledge and good times shared.

To the Engineers Maria João and Ana, from the Chemical Process Engineering and Forest Products Research Centre for all the assistance given throughout this work.

To the Engineers Cátia Mendes and Beatriz Banaco for all the assistance given and for the knowledge and good times shared.

To my friends for all the support and encouragement given in this journey and all the patience in these last months. I would like to give a special thanks to Carolina Silva, Jéssica Fernandes and Mónica Reis for all the extra support and patience.

To my family for the unconditional support, strength and motivation given me throughout my life. Most importantly, I have to thank my parents and brother for making all this possible and providing me the tools and guidance to achieve all my goals.

To all, my deepest thanks!



## Abstract

The fast growth in population has overburdened Earth's resources and increased its levels of pollution. The constant search for new products and/or services has demanded for a higher level of production of industrial activities, which consequently results in greater emissions and discharges of pollutants to the air, water and soil. The heavy metals are a common and alarming contaminant due to their non-biodegradable and toxic nature. Thus, their disposal presents an environmental challenge.

There are several remediation techniques that may be used to effectively mitigate the heavy metals contaminants. However, the appropriate selection of the technique is crucial and depends on various factors, such as the type of pollutant and the area of contamination. According to the technique, it may be necessary to apply a reagent or an immobilization agent. Their adequate choice is also important as it highly affects the cost of the remediation, its efficiency and the targeted environment. Some of the desired characteristics are a high specific surface area, high porosity, high adsorption capacity and low toxicity. Nowadays, common adsorbents applied for remediation purposes are activated carbon, biochar from multiple feedstocks and nanomaterials.

In this work the focus was on the application of oak wood bark biochar and halloysite nanoclay to a soil contaminated with heavy metals (Cu, Cr, Ni and Zn) and the evaluation of their remediation potential. The experiments were done using percolation and suspension tests. In order to achieve a good dispersion of the adsorbents, three surfactants were tested, SDBS (anionic) and Pluronic F-127 (non-ionic) together and LigniOx-LB (anionic, being a natural surfactant obtained from a by-product).

First of all, the application of biochar and surfactants in different concentrations was assessed. Then, the effect of the time of contact was taken into consideration, evaluating the remediation performance for up to seven days. The shift in surfactant was the following parameter under evaluation. Lastly, the influence of the biochar diameter was taken into account.

Regarding the halloysite nanoclay, the first parameter analysed was its concentration. Following, the impact of the surfactants concentration was considered. Furthermore, the change in both the nanoclay and surfactants concentration was evaluated. The performance of LigniOx-LB was also investigated by applying two different concentrations.

Reviewing all the results obtained, the potential of both adsorbents to remediate the Baixo Mondego soft soil contaminated with heavy metals is clearly dependent on their

## ABSTRACT

---

concentration and effective dispersion, and on the organic matter content. Furthermore, it was concluded that the effective performance of the remediation agent is highly affected by the type of surfactant used for its dispersion and the time of contact, since a desorption effect occurred, over time, in various experiments, especially for Ni (II). The remediation techniques tested should be further investigated.

**Keywords:** Soil remediation; heavy metals; adsorption; biochar; halloysite nanoclay; surfactants, natural surfactants.



## Resumo

O rápido crescimento da população tem sobrecarregado os recursos da Terra e aumentado os níveis de poluição. A constante procura por novos produtos e/ou serviços tem aumentado o nível de produção das atividades industriais, o que conseqüentemente resulta numa maior emissão e descarga de poluentes para o ar, água e terra. Os metais pesados são um comum e alarmante contaminante devido à sua natureza não-biodegradável e tóxica. Deste modo, a sua descarga apresenta um desafio ambiental.

Existem várias técnicas de remediação que podem ser efetuadas para mitigar efetivamente os metais pesados como contaminantes. No entanto, a seleção apropriada da técnica é crucial e depende de vários fatores, como o tipo de poluente e a área de contaminação. De acordo com a técnica, pode ser necessário aplicar um reagente ou um agente de imobilização. A sua escolha adequada também é importante dado que afeta bastante o custo da remediação, a sua eficiência e o ambiente alvo. Algumas das características desejadas são a elevada área específica, elevada porosidade, elevada capacidade de adsorção e baixa toxicidade. Atualmente, adsorventes comumente aplicados para efeitos de remediação são o carvão ativado, biochar proveniente de múltiplas matérias-primas e nanomateriais.

Neste trabalho o foco é na aplicação de biochar de casca de carvalho e nanoargila num solo contaminado com metais pesados (Cu, Cr, Ni e Zn) e a avaliação do potencial de remediação destes materiais. As experiências foram realizadas com base em testes de percolação e em suspensão. De modo a atingir uma boa dispersão dos adsorventes, três surfatantes foram testados, SDBS (aniónico) e Pluronic F-127 (não-iónico) em conjunto e LigniOx-LB (aniónico, sendo um surfatante natural obtido através de um sub-produto).

Primeiramente, a aplicação de biochar e surfatantes em diferentes concentrações foi aferida. Seguidamente, o efeito do tempo de contacto foi tido em consideração, avaliando o desempenho da remediação até sete dias. A alteração de surfatante foi o parâmetro seguidamente sob avaliação. Por último, a influência do diâmetro do biochar foi tida em conta.

Relativamente à nanoargila, o primeiro parâmetro analisado foi a sua concentração. Seguidamente, o impacto da concentração de surfatante foi considerado. Para além disso, a alteração da concentração de nanoargila e surfatante foi avaliada. O desempenho do LigniOx-LB foi também investigado pela aplicação de duas concentrações diferentes.

Revendo todos os resultados obtidos, o potencial de ambos os adsorventes para remediar o solo mole do Baixo Mondego contaminado com metais pesados é claramente

dependente das concentrações dos aditivos e da dispersão efectiva dos mesmos e ainda do teor de matéria orgânica na suspensão de solo. Para além disso, foi concluído que o desempenho eficaz do agente de remediação é bastante afetado pelo tipo de surfatante usado para a sua dispersão e o tempo de contacto, dado que ocorreu um efeito de desadsorção, ao longo do tempo nalgumas experiências, especialmente para o Ni (II). No entanto, investigação adicional necessita de ser realizada.

**Palavras-chave:** Remediação de solos; metais pesados; adsorção; biochar; nanoargila; surfatantes, surfatante natural.

## Index

<b>Acknowledgements</b> .....	<b>i</b>
<b>Abstract</b> .....	<b>iii</b>
<b>Resumo</b> .....	<b>v</b>
<b>Index</b> .....	<b>vii</b>
<b>Figures Index</b> .....	<b>ix</b>
<b>Tables Index</b> .....	<b>xi</b>
<b>Acronyms and Symbols</b> .....	<b>xiii</b>
<b>Acronyms</b> .....	<b>xiii</b>
<b>Symbols</b> .....	<b>xiv</b>
<b>1. Introduction</b> .....	<b>1</b>
<b>2. State of the art</b> .....	<b>5</b>
<b>2.1. Heavy Metals</b> .....	<b>5</b>
2.1.1. Legislation .....	<b>8</b>
<b>2.2. Remediation of soils contaminated with haevy metals</b> .....	<b>10</b>
<b>2.3. Adsorbent particles</b> .....	<b>13</b>
2.3.1. Biochar .....	<b>13</b>
2.3.2. Carbon Nanoparticles .....	<b>22</b>
2.3.3. Nanoclays.....	<b>23</b>
2.3.4. Particles dispersion .....	<b>32</b>
<b>3. Materials and Methods</b> .....	<b>37</b>
<b>3.1. Materials</b> .....	<b>37</b>
3.1.1. Baixo Mondego soft soil.....	<b>37</b>
3.1.2. Heavy metals.....	<b>38</b>
3.1.3. Adsorbent particles .....	<b>38</b>
3.1.4. Surfactants .....	<b>40</b>
<b>3.2. Characterization Techniques</b> .....	<b>41</b>
3.2.1. Particle size.....	<b>41</b>
<b>3.3. Atomic Absorption Spectrometry</b> .....	<b>43</b>

<b>3.4. Experimental Procedure .....</b>	<b>44</b>
3.4.1. Heavy metals' adsorption by soil percolation.....	44
3.4.2. Heavy metals' adsorption by soil suspension.....	46
<b>3.5. Tests' Plan .....</b>	<b>47</b>
<b>4. Results and Discussion.....</b>	<b>49</b>
<b>4.1. Results of the heavy metals' adsorption by soil percolation tests .....</b>	<b>49</b>
<b>4.2. Results of the heavy metals' adsorption by soil suspension tests with the     application of oak wood bark biochar.....</b>	<b>51</b>
<b>4.3. Results of the heavy metals' adsorption by soil suspension tests with the     application of nanoclays .....</b>	<b>59</b>
<b>5. Conclusions and future work .....</b>	<b>69</b>
5.1. Conclusions .....	69
5.2. Future work.....	71
<b>Bibliography.....</b>	<b>73</b>
<b>Appendix A – Biochar dispersions' .....</b>	<b>85</b>
<b>Appendix B – Halloysite nanoclay dispersions' .....</b>	<b>86</b>
<b>Appendix C - Safety.....</b>	<b>88</b>
Copper (II) chloride dihydrate .....	88
Chromium (III) nitrate nonahydrate .....	88
Nickel (II) nitrate hexahydrate.....	89
Zinc sulfate heptahydrate .....	89
Sodium dodecylbenzenesulfonate .....	90
Pluronic F-127 .....	90
Halloysite nanoclay .....	90

## Figures Index

Figure 1: Contaminants influencing the solid matrix (Van Liedekerke et al., 2014). .....	5
Figure 2: Most commonly applied remediation techniques for soil contamination (Van Liedekerke, 2014). .....	10
Figure 3: Soil's grain size curve. ....	37
Figure 4: Thermogravimetric Analysis of the oak wood bark biochar. ....	39
Figure 5: Illustration of the halloysite nanoclay from Sigma-Aldrich (Halloysite nanoclay, n.d.). ....	40
Figure 6: Illustration of the percolation system by Matos (2017). ....	45
Figure 7: Evolution of the percentage of Zn (II) adsorbed over time in the soil suspension tests with the application of oak wood bark biochar. ....	55
Figure 8: Evolution of the percentage of Ni (II) adsorbed over time in the soil suspension tests with the application of oak wood bark biochar. ....	57
Figure 9: Evolution of the percentage of Zn (II) adsorbed over time in the soil suspension tests with the application of halloysite nanoclay. ....	62
Figure 10: Evolution of the percentage of Ni (II) adsorbed over time in the soil suspension tests with the application of halloysite nanoclay. ....	65
Figure A1: Comparison of the particle size distribution for the experiments performed with oak wood bark biochar with a size lower than 210 $\mu\text{m}$ using different surfactants and concentrations. ....	85
Figure A2: Comparison of the particle size distribution for the experiments performed with oak wood bark biochar with a size comprehended between 210 and 345 $\mu\text{m}$ using different surfactants and concentrations. ....	85
Figure B1: Particle size distribution of the dispersion of 0.01% (w/w) halloysite nanoclay with 0.03% (w/w) SDBS + Pluronic F-127. ....	86
Figure B2: Particle size distribution of the dispersion of 0.05% (w/w) halloysite nanoclay with 0.15% (w/w) SDBS + Pluronic F-127. ....	86
Figure B3: Particle size distribution of the dispersion of 1% (w/w) halloysite nanoclay with 3% (w/w) SDBS + Pluronic F-127. ....	86
Figure B4: Particle size distribution of 1% (w/w) halloysite nanoclay with 3% (w/w) LigniOx-LB. ....	87



## Tables Index

Table 1: Role in human health, sources of contamination and potential toxic effects of the heavy metals selected. ....	6
Table 2: Ranges of concentration (mg/kg) of the heavy metals selected, pH and organic matter of the Portuguese soil (Inácio et al., 2008). ....	7
Table 3: Limit values for heavy metals in soil and sludge established by the Council Directive 86/278/EEC of the European Union for agriculture use. ....	8
Table 4: Limit values for heavy metals in soil and sludge established by the 276/2009 Decree-Law. ....	8
Table 5: Intervention values for soil and groundwater established by Rijkswaterstaat Ministry of Infrastructures and Environment in 2013. ....	9
Table 6: Soil, groundwater and sediment standards established by the Ontario Ministry of the Environment on July 1, 2011. ....	9
Table 7: Advantages and disadvantages of the in situ and ex situ remediation techniques (Wuana & Okieimen, 2011). ....	11
Table 8: Comparison of different remediation techniques. ....	12
Table 9: Products of pyrolysis processes in different conditions (Tomczyk et al., 2020). ....	13
Table 10: Comparison of the adsorption capacity of biochar from different studies. ....	17
Table 11: Comparison of different clay groups and their respective specifications. ....	25
Table 12: Comparison of the adsorption capacity of nanoclays from different studies. ....	28
Table 13: Characteristics of the soil. ....	37
Table 14: Maximum concentration of heavy metals found in Portuguese soils by Inácio et al. (2008) and the heavy metals ion's and salt's information. ....	38
Table 15: Halloysite nanoclay's properties given by Sigma-Aldrich. ....	40
Table 16: Characteristics of the surfactants used. ....	41
Table 17: Key features of the ZetaSizer Nano ZS from Malvern Instruments (Merkus, 2009). ....	43
Table 18: AAS detection limits for each ion in the Atomic Absorption Spectrometer 3300 from Perkin Elmer. ....	44
Table 19: Salt mass added to 100 mL of ultrapure water to contaminate 100 g of soil. ....	44
Table 20: Salt and metal concentrations in the contaminated soil at t=0 (100 g of soil). ....	46

Table 21: Mass of salt used for the contamination of 61.67 g of wet soil and initial metallic ion concentration in the suspension tests. ....	46
Table 22: Overview of the performed tests in soil percolation. ....	47
Table 23: Overview of the performed tests in soil suspension. ....	48
Table 24: Adsorption capacities obtained in the percolation tests. ....	49
Table 25: Results obtained for the reference tests in the heavy metals' adsorption by soil suspension tests. ....	51
Table 26: Results of the reference test of Ni by adsorption in suspension test obtained by Gomes (2017). ....	52
Table 27: Results obtained in the adsorption by soil suspension tests with the application of oak wood bark biochar. ....	54
Table 28: Results obtained in the adsorption by soil suspension tests with the application of halloysite nanoclay. ....	61



## Acronyms and Symbols

### Acronyms

AAS	Atomic Absorption Spectrometry
AC	Activated Carbon
APA	Portuguese Environment Agency
BC	Biochar
CMC	Critical Micelle Concentration
CNTs	Carbon Nanotubes
CTAB	Cetyl Trimethyl Ammonium Bromide
CVD	Chemical Vapour Deposition
DLS	Dynamic Light Scattering
EC	Electrical Conductivity
EEA	European Environment Agency
HM	Heavy Metal
HNTs	Halloysite Nanotubes
IUPAC	International Union of Pure and Applied Chemistry
LDS	Laser Diffraction Spectroscopy
MWCNTs	Multi-walled Carbon Nanotubes
NC	Nanoclay
Pluronic	Pluronic F-127
PTEs	Potentially Toxic Elements
SDBS	Sodium Dodecylbenzene Sulfonate
SDS	Sodium Dodecyl Sulfate
SWCNTs	Single-walled Carbon Nanotubes
TGA	Thermogravimetric Analysis
TX-100	Octylphenol Ethoxylate
UCS	Unconfined Compressive Strength
USEPA	United States Environmental Protection Agency
WHO	World Health Organization
ZNS	ZetaSizer Nano ZS

**Symbols**

Al	Aluminium	-
C	Carbon	-
Ca	Calcium	-
Cd	Cadmium	-
CEC	Cation Exchange Capacity	cmol <sub>c</sub> /kg
C <sub>eq</sub>	Equilibrium Concentration	kg/m <sup>3</sup>
Cr	Chromium	-
Cr(NO <sub>3</sub> ) <sub>3</sub> ·9H <sub>2</sub> O	Chromium (III) Nitrate Nonahydrate	-
Cu	Copper	-
CuCl·2H <sub>2</sub> O	Copper (II) Chloride Dihydrate	-
D	Diffusion coefficient	m <sup>2</sup> /s
D[3,2]	Surface weighted mean	m
D[4,3]	Volume mean diameter	m
H	Hydrogen	-
k	Boltzmann constant	J/K
K	Potassium	-
l	Optical path length	
Mg	Magnesium	-
N	Nitrogen	-
Na	Sodium	-
Ni	Nickel	-
Ni(NO <sub>3</sub> ) <sub>2</sub> ·6H <sub>2</sub> O	Nickel (II) Nitrate Hexahydrate	-
O	Oxygen	-
OM	Organic Matter content	%
P	Phosphorus	-
Pb	Lead	-
S	Sulfur	-
T	Temperature	K
t	Time	s
μ	Dynamic viscosity	Pa.s
Zn	Zinc	-
ZnSO <sub>4</sub> ·7H <sub>2</sub> O	Zinc Sulfate Heptahydrate	-

## 1. Introduction

The fast growth in population over the last few decades has had a remarkable impact in the natural resources present on Earth, such as water and soil/land. Humankind has become greedy for growth and development and has jeopardized the quality and maintenance of these resources. Pollution has been continuously growing for decades, mainly due to the emissions and discharges of pollutants by the industrial sector and domestic activities, and people have stayed stagnant, making minor changes to their behaviour with negative impact on the environment. However, as the consequences of these activities become clearer, the social awareness rises.

The continuous advancements in technology have triggered the development of several subjects, including science and its various areas. Therefore, multiple methods and equipment were developed and updated allowing more accurate measurements. Furthermore, innovative methodologies were created and developed. These techniques allowed the close monitoring of the levels of potentially toxic elements present in nature, which is tremendously important in the assessment of the quality of soil, water and air to prevent harmful effects on the health of humans, animals and plants. Heavy metals are a common contaminant worth careful control due to their adverse effects and inorganic nature. Thus, the remediation of the already polluted sites and the prevention of further pollution are crucial.

To remediate a polluted site various factors have to be taken into consideration, such as the type and concentration of pollutant, the environmental component affected, the location and the possibly exposed receptors. According to these factors, the type of remediation suitable for a specific situation is studied in order to optimize the efficiency and prevent secondary pollution or waste, minimize the potentially harmful effects, and avoid the application of non-renewable resources and energy (Fortuna et al., 2011). The fulfilment of all these requirements results in a sustainable remediation.

Depending on the type of remediation performed, the application of a reagent or immobilization agent may be necessary. Hence, the study of the potentially applied agent is vital to avoid further pollution and secondary effects. Furthermore, the material used as the remediation agent highly affects the cost, efficiency and environmental friendliness of the remediation technique. A large specific surface area, high porosity, strong adsorption capacity and low toxicity are suitable characteristics for the remediation agents. Thus, some common adsorbents utilized are activated carbon and biochar. Various researchers have been studying the potential of biochar in the remediation of several types of pollutants. Moreover, the effect

of the type of feedstock and the pyrolysis conditions in the performance of biochar amendments are also subjects under study.

Nanomaterials have become an interesting remediation agent due to their attractive properties, i.e., high surface area and chemical reactivity and their possible synthesis in multiple shapes. Some nanomaterials already used for heavy metal remediation purposes are carbon-based materials (such as carbon nanoparticles and multi-walled carbon nanotubes), metal oxides and iron-oxide based nanosorbents, since they are recyclable and have a large surface area, low toxicity and a reduced production cost (Kalita & Baruah, 2020). Halloysite nanotubes are another example of a nanomaterial applied for the treatment of contaminants owing to their wide availability and subsequent low cost, and their exceptional physicochemical properties (Liu et al., 2019b; Liu et al., 2019c).

The main aim of this study was to assess the ability of oak wood bark biochar from the Portuguese wildfires and halloysite nanoclay previously dispersed to remediate a soil contaminated with heavy metals.

First of all, the effect of the concentration of biochar on its remediation performance was studied. Then, the influence of the time of contact was taken into consideration. Thirdly, the performance of surfactant type was evaluated. Finally, the impact of the size/diameter of biochar applied was assessed.

In regards to the remediation of soils contaminated with heavy metals by halloysite nanoclay, the first parameter under evaluation was the concentration of nanomaterials. Secondly, the concentration of surfactants applied to disperse them was assessed. The influence of the time of contact in the remediation process was also taken into account. Furthermore, the effects of the application of a different type of surfactant and its respective concentration were studied.

This work is separated into five chapters as shown below:

- Chapter 1 is the introduction, where the definition of the problem is made and the objectives are enumerated;
- Chapter 2 is the state of the art, comprising the description of the main theoretical basis and the results and conclusions obtained by other authors;
- Chapter 3 is the materials and methods, where all the materials, characterization techniques, experimental procedures and test plans are described;
- Chapter 4 is the presentation of the results, including a discussion and comparison of the results obtained with previous studies;

- Chapter 5 is the conclusions and future work, containing the list of the main conclusions and some proposals for future studies.



## 2. State of the art

### 2.1. Heavy Metals

The metallic chemical elements that present high atomic density ( $> 6 \text{ g/cm}^3$ ), high atomic mass ( $> 20$ ) and toxic properties are designated as heavy metals (Bakshi & Abhilash, 2020; Chowdhury et al., 2015; Li et al., 2019a; Heavy metals, n.d.). In biological terms, metals or metalloids are denominated as heavy when they are prejudicial to plants and animals even in small concentrations (Li et al., 2019a). Due to their long half-life, soil residence time (over a thousand years), bioaccumulation, bioamplification and carcinogenic properties, heavy metals are described as toxic (Selvi et al., 2019).

In a report from the European Environment Agency (EEA), in 2011, heavy metals represented 34.8% of the contaminants present in the solid matrix affecting soil and groundwater in Europe, as shown in Figure 1. Nevertheless, the effects of these contaminants in the environment and human health are dependent on properties like their solubility in water, bioavailability, potential for dispersion and carcinogenicity (Van Liedekerke et al., 2014). Since heavy metals are not biodegradable, they accumulate in the environmental matrices reaching hazardous concentrations (Selvi et al., 2019), hence their disposal presents an environmental challenge. The adsorption of heavy metals present in soil becomes slower over time as they reassign into distinct chemical forms with differing bioavailability, mobility and toxicity (Wuana & Okieimen, 2011). The mechanisms that control this distribution are the mineral precipitation and dissolution; ion exchange, adsorption and desorption, aqueous complexation, biological immobilization and plant uptake (Wuana & Okieimen, 2011), depending on parameters such as the pH, nature of the metal, temperature, water content, particle size distribution and clay content (Selvi et al., 2019).

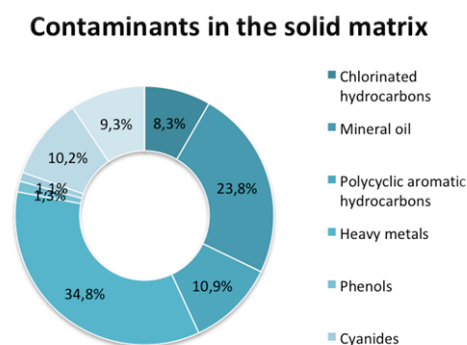


**Figure 1:** Contaminants influencing the solid matrix (Van Liedekerke et al., 2014).

Amongst several heavy metals that naturally occur in nature, thirteen of those are considered of importance to human and environmental health according to the World Health Organization (WHO), such as arsenic, cadmium, copper, chromium, lead, mercury, nickel and zinc (Heavy metals, n.d.). Additionally, the United States Environmental Protection Agency (USEPA) also registered these eight heavy metals as the most common in the environment (Selvi et al., 2019). In this study the focus will be on copper, chromium, nickel and zinc due to their common availability in Portuguese soils (Inácio et al., 2008).

Chromium is the 21<sup>st</sup> most abundant element in the terrestrial crust, nickel the 23<sup>rd</sup>, zinc the 24<sup>th</sup> and copper the 25<sup>th</sup> (Abundance of elements in Earth's crust, 2020). However, their concentration in nature has been alarmingly rising due to anthropogenic reasons, thus presenting potential adverse effects for flora and fauna. The contamination of the soil and aqueous systems with heavy metals can result in its entrance in the water cycle and food chain, therefore hindering the ecosystem (Awa & Hadibarata, 2020; Bakshi & Abhilash, 2020; Wuana & Okieimen, 2011). The sources of contamination, role in human health and potential toxic effects for the heavy metals selected are present in Table 1 (Alloway, 2013; Chowdhury et al., 2015; Ihsanullah et al., 2016; Pandey & Mishra, 2011; Wuana & Okieimen, 2011).

**Table 1:** Role in human health, sources of contamination and potential toxic effects of the heavy metals selected.

<b>Metal</b>	<b>Sources of contamination</b>	<b>Role in human health</b>	<b>Potential toxic effects</b>
Cr	Industrial wastewater discharge, electroplating, metal plating, coating operation and tanneries	Assists the body in metabolizing sugar, protein and fat	Allergic dermatitis, severe diarrhoea, vomiting, pulmonary congestions, liver and kidney damage and respiratory cancers
Cu	Pesticides industry, mining, electroplating, metal piping and chemical industry	Essential for the immune and nervous system, skeletal health and the formation of red blood cells	Anaemia, liver and kidney damage, stomach and intestinal irritation, increased blood pressure and respiratory rates
Ni	Combustion of fossil fuels, battery manufacturing, production of some alloys, zinc base casting, printing, electroplating and silver refineries	Not essential but its deprivation affects the carbohydrate and lipid metabolism	Growth decline, dry cough, bone nose and lung cancer, cyanosis, rapid respiration, shortness of breath, tightness of chest, chest pain, nausea and vomiting, dizziness and headache
Zn	Brass plating, wood pulp production, ground and newsprint paper production, steel works with galvanizing lines zinc and brass metal works, refineries and plumbing	Essential for DNA and protein synthesis, cell division and growth	Birth defects, stomach nausea, skin irritations, cramps, vomiting and anaemia



The environmental hazard of chromium is related to the higher toxicity and mobility of its hexavalent form rather than its trivalent form (Kumpiene et al., 2008; Tóth et al., 2016; Wuana & Okieimen, 2011). According to Tóth et al. (2016), copper is applied as a pesticide in vineyard and orchards, therefore being commonly found in the agricultural land of the Mediterranean region. Furthermore, in the same study about the presence of heavy metals in the agricultural soil of the European Union, Tóth et al. (2016) found that the most affected region with nickel was also the Mediterranean, although the bioavailability and mobility of this metal is one of the lowest amongst heavy metals (Tóth et al., 2016). Lastly, the authors concluded that zinc pollution was not significant in European Union's agriculture.

Inácio et al. (2008), performed a geochemical mapping of the Portuguese soil establishing the baselines for 20 elements for two soil fraction sizes ( $< 0.18$  and  $< 2.00$  mm) and threshold concentrations for 9 elements. Considering the standard Portuguese soil (14% clay and 6% organic matter in the finer fraction), Inácio et al. (2008) proposed an action value for the 9 elements, i.e., a concentration that if exceeded poses an inadmissible threat to the environment through the soil's contamination. The concentration range and action values for the heavy metals selected in the finer fraction ( $< 0.18$  mm) of the Portuguese soil are represented in Table 2, as well as the pH and organic matter (OM) range (Inácio et al., 2008).

**Table 2:** Ranges of concentration (mg/kg) of the heavy metals selected, pH and organic matter of the Portuguese soil (Inácio et al., 2008).

Element	Range	Action Value (mg/kg)
Cr	$< 1 - 336$	300
Cu	$< 1 - 245$	200
Ni	$< 1 - 880$	100
Zn	$0.5 - 589$	500
pH	$3.6 - 8.1$	-
OM (%)	$1.21 - 41.48$	-

As heavy metals have multiple applications, they can be released to the environment in many ways. Hence, the need to control and manage their concentration levels in different mediums emerges. Thus, each member state of the European Union established a concentration limit per heavy metal, respecting the Directive 86/278/EEC, as presented on the next section.

### 2.1.1. Legislation

Due to the toxic properties of heavy metals, they have concentration limits in soil, which have to be respected in order not to pollute the water cycle and food chain. Therefore, the European Union and the countries within it have proposed concentrations limits for the heavy metals in soil and sewage sludge used for agriculture.

On the 12<sup>th</sup> of June of 1986, the Council of the European Union established a “Council Directive on the protection of the environment, and in particular of the soil, when sewage sludge is used in agriculture” (Council Directive 86/278/EEC) which presented the limit values for the concentration of seven heavy metals in soil and in sludge for use in agriculture, as illustrated in Table 3 for the heavy metals studied. However, the values permissible for Cr were only added on the 18<sup>th</sup> of November of 1988.

**Table 3:** Limit values for heavy metals in soil and sludge established by the Council Directive 86/278/EEC of the European Union for agriculture use.

Parameter	Limit values in soil (mg / kg dry matter)		Limit values in sludge for use in agriculture (mg / kg dry matter)
	(6 < pH < 7) (*)		
Copper	50 – 140		1000 – 1750
Nickel	30 – 75		300 – 400
Zinc	150 – 300		2500 – 4000
Chromium	100 – 200		1000 – 1750

(\*) applicable to soils on which commercial food crops are being grown exclusively for animal consumption.  
Source: Council Directive of 12<sup>th</sup> of June of 1986

In Portugal, the current Decree-Law number 276/2009 transposes the European Council Directive and limits the concentration of heavy metals in soil and sludge for use in agriculture, as illustrated in Table 4.

**Table 4:** Limit values for heavy metals in soil and sludge established by the 276/2009 Decree-Law.

Parameter	Limit values in soil (mg / kg dry matter)			Limit values in sludge for use in agriculture (mg / kg dry matter)
	pH ≤ 5.5	5.5 ≤ pH ≤ 7.0	pH ≥ 7.0 (*)	
Copper	50	100	200	1000
Nickel	30	75	110	300
Zinc	150	300	450	2500
Chromium	50	200	300	1000

(\*) applicable to soils on which commercial food crops are being grown exclusively for animal consumption.

In the Netherlands, the Rijkswaterstaat Ministry of Infrastructures and Environment updated the Dutch soil remediation and groundwater target and intervention values on the 1<sup>st</sup> of July of 2013. The intervention values denote the concentrations that if exceeded, would impose a serious threat to humans, plants and animals. In Table 5 these values are present for the heavy metals under study.

**Table 5:** Intervention values for soil and groundwater established by Rijkswaterstaat Ministry of Infrastructures and Environment in 2013.

Substance	Intervention values	
	Soil (mg / kg dry matter)	Groundwater ( $\mu\text{g} / \text{L}$ )
Copper	190	75
Nickel	100	75
Zinc	720	800
Chromium	-	30
Chromium (III)	180	-
Chromium (VI)	78	-

Source: Rijkswaterstaat Ministry of Infrastructures and Environment

The Portuguese Environment Agency (APA) proposes to use the Ontario Standards to classify the quality of the soil depending on its location and surroundings. The Ontario Ministry of the Environment extensively detailed all the soil, groundwater and sediment standards for use under Part XV.1 of the Environmental Protection Act. In Table 6 are listed the site condition standards for use within 30 m of a water flows in a potable groundwater condition for the heavy metals under study.

**Table 6:** Soil, groundwater and sediment standards established by the Ontario Ministry of the Environment on July 1, 2011.

Contaminant	Soil (other than sediment) ( $\mu\text{g} / \text{g}$ )		Groundwater ( $\mu\text{g} / \text{L}$ )	Sediment ( $\mu\text{g} / \text{g}$ )
	Agricultural use	Residential/ Industrial/ Commercial use		
Copper	62	92	69	16
Nickel	37	82	100	16
Zinc	290	290	890	120
Chromium (total)	67	70	50	26

Source: Ontario Ministry of the Environment (2011)

## 2.2. Remediation of soils contaminated with heavy metals

The growing population and industrialization have been overloading the planet's resources, such as its agricultural land and water systems. The depletion or lack of quality of these resources is highly threatening for the environmental and human health (Awa & Hadibarata, 2020; Li et al., 2019a; Selvi et al., 2019). Considering the majority of the contaminated sites are located in developed countries, the awareness, motivation and promptness to tackle this environmental challenge have been rising (Khalid et al., 2017). Since the methods of self-purification or dilution of the heavy metals in the contaminated soil are ineffective and time-consuming and their self-remediation can take between 100 and 200 years, this option has been proven unviable (Raja & Husen, 2020). Therefore, multiple researches have been carried out to find efficient and feasible technologies to remediate contaminated sites (Khalid et al., 2017). In Van Liedekerke's report are shown the most commonly applied remediation techniques for soil contamination in some of the European countries in 2011, as illustrated in Figure 2 (Van Liedekerke, 2014). It can be seen that most countries resort to excavation and disposal, which is highly discouraged due to the large environmental invasion and toxic effects implied. Hence, there is still a lot of room for improvement in this environmental field.

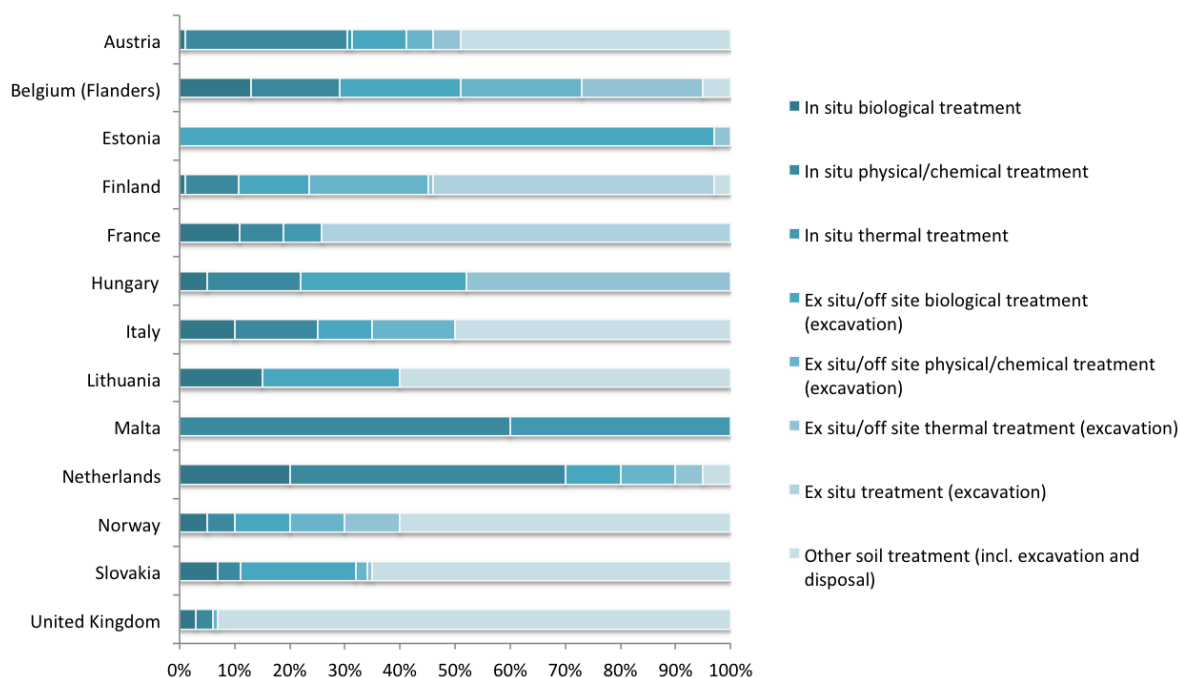


**Figure 2:** Most commonly applied remediation techniques for soil contamination (Van Liedekerke, 2014).

The appropriate selection of the remediation technique to apply in a contaminated site should fulfil some criteria. These parameters are the time required, the inherent costs

including energy costs, the effectiveness under high contaminant concentration, the feasibility to multi-metal contaminated sites remediation, the long-term effectiveness and the public acceptance and commercial availability (Dhaliwal et al., 2020; Khalid et al., 2017; Li et al., 2019a; Wuana & Okieimen, 2011).

The remediation techniques can be classified as in situ or ex situ according to the place of remediation. The former treatment occurs onsite, i.e., in the original place of contamination, not moving the contaminated soil. The latter treatment happens offsite, thus requiring the excavation and transport of the polluted soil to another location for further treatment (Li et al., 2019a; Wuana & Okieimen, 2011). The main advantages and disadvantages of the in situ and ex situ remediation techniques are shown in Table 7 (Wuana & Okieimen, 2011).

**Table 7:** Advantages and disadvantages of the in situ and ex situ remediation techniques (Wuana & Okieimen, 2011).

	<b>Advantages</b>	<b>Disadvantages</b>
<b>In situ</b>	Non-invasive Simple and rapid Low waste production Highly accepted Widely applicable for inorganic contaminants	Possibility of being only a temporary solution Constant monitoring May change soil physiochemical properties Only applicable in a given area
<b>Ex situ</b>	Fast and easy to apply Relatively low cost of investment and operation	Highly invasive Generates large amount of solid wastes By-product needs storage on a special landfill site Possible danger of additional release of contaminants Constant monitoring of the stored wastes Cost of transportation and CO <sub>2</sub> emissions

Moreover, the technologies may be divided in three groups according to their nature: physical, chemical or biological (Awa & Hadibarata, 2020; Dhaliwal et al., 2020; Khalid et al., 2017; Li et al., 2019a; Qayyum et al., 2020; Selvi et al., 2019). In the former group are included techniques such as the soil replacement, vitrification, electrokinetic remediation and soil washing. Immobilization and stabilization/solidification techniques are examples of chemical remediation. The latter group is constituted by phytostabilization, phytovolatilization and phytoextraction. To overcome disadvantages as high cost, low efficiency and the generation of toxic sludge, these techniques may be applied in combination, thus showing economic feasibility, versatility, on site adaptability, eventual short duration but higher efficiency for heavy metal removal (Selvi et al., 2019). The comparison of the different remediation techniques referred in the literature is illustrated in Table 8 (Awa & Hadibarata, 2020; Chen et al., 2019; Dhaliwal et al., 2020; Khalid et al.,

2017; Li et al., 2019a; Liu et al., 2019a; Pulimi & Subramanian, 2016; Qayyum et al, 2020; Selvi, et al., 2019; Xu et al., 2017).

**Table 8:** Comparison of different remediation techniques.

Method	Principle	Applicability	Advantages	Disadvantages
Soil replacement	Replace or partially replace the contaminated soil by non-contaminated soil	Small scale	Able to effectively isolate the contaminated soil and ecosystem, and appropriate for heavily contaminated soil.	Costly due to high labour work, production of dangerous waste and negative effect on soil
Vitrification	Application of high temperature to reduce HMs mobility in the contaminated soil	Small scale	Easy application, applicable to inorganic and organic contaminants and high efficiency	High cost due to energy requirement and limited application
Electrokinetic remediation	Application of a direct electric current through electro-migration, electro-osmosis, electrophoreses and electrolysis to remove the HMs from the matrix of the contaminated soil	Small scale	Easy application, economically effective and environmentally friendly	Requires soil with low permeability, failure to control the pH of the soil system and low efficiency
Immobilization	Reduction of HM's mobility, bioavailability and bioaccessibility through the application of immobilization agents or other materials forming stable and immobile complexes through adsorption, precipitation and complexation reactions	Small to medium scale	Fast and easy applicability, relatively low cost, applicable to a broad spectrum of inorganics and negligible effect on agricultural production	Temporary solution and permanent monitoring is necessary
Soil washing	Application of reagents to leach the contaminant from the soil	Small scale	High efficiency, cost-effective, rapid and meets specific criteria without long-term liability	Efficiency depends on the ability of extractant to dissolve the HM in soil and washing extractants may cause environmental issues
Phytostabilization	Use of plants to limit the mobility and bioavailability of contaminants through adsorption, precipitation and reduction of root	Small to medium scale	Economical and less disruptive	Temporary solution
Phytovolatilization	Use of plants to convert the contaminants into less toxic and volatile forms and releasing them to the atmosphere through transpiration	Small to medium scale	Economical and less disruptive	Transpiration rate of the plant affects the effectiveness, failure to completely remove the contaminants and no control after release to atmosphere
Phytoextraction	Use of plants to uptake, translocate and concentrate the contaminants from soil to the aboveground harvestable plant parts (shoots and leaves)	Large scale	Highly economical, eco-friendly and less disruptive	Bioavailability and adsorption rate of the metal limit the performance

In most of the different remediation techniques referred above it is common to use different types of adsorbent particles to improve the environment remediation effect, as explained below.

## 2.3. Adsorbent particles

### 2.3.1. Biochar

Biochar is produced by the pyrolysis of biomass. Different types of biomass have been used and studied for the production of biochar such as agricultural wastes (e.g. livestock manure, dairy manure, straw, sugar beet tailing), forest residues and residuals (e.g. bark, wood chips, pellets, sawdust, bamboo and coconut shell) and industrial by-products (e.g. sewage sludge, waste paper, press cakes) (Li et al., 2017; Tomczyk et al., 2020; Zhang, et al, 2013; Zheng et al., 2020). The woody biomass presents high bulk density, low water and ash content and, as a consequence, high calorific value. On the other hand, non-woody biomass has the exact opposite characteristics (Tomczyk et al., 2020).

Pyrolysis is the process in which biomass is heated at high temperature (typically 300-800°C) (Matin, et al., 2020) in the absence of oxygen (Cha et al., 2016; Li et al., 2017; Weber & Quicker, 2018; Zheng et al., 2020). This process produces a carbonaceous solid (biochar), bio-oil (mixture of hydrocarbons) and synthetic gas (mixed hydrocarbon gases), showing distinctive proportions depending on the temperature, heating rate, residence time and pressure, for example. Hence, pyrolysis can be classified according to the thermochemical technology used depending on these proportions (Cha et al., 2016; Tomczyk et al., 2020; Zheng et al., 2020). The type of feedstock and the pyrolysis temperature are the two main factors affecting the majority of the biochar's properties (Li et al., 2017; Lu et al., 2014; Tomczyk et al., 2020). In Table 9 are illustrated three technologies used to produce biochar and their conditions (Tomczyk et al., 2020).

**Table 9:** Products of pyrolysis processes in different conditions (Tomczyk et al., 2020).

Process	Pyrolysis temperature (°C)	Pressure	Residence time	Proportion of products in the pyrolysis process (%)		
				Bio-oil	Synthetic gas	Biochar
Fast Pyrolysis	400 – 600	Vacuum-atmospheric	Seconds	75.0	13.0	12.0
Slow pyrolysis	350 – 800	Atmospheric	Second-hours	30.0	35.0	35.0
Gasification	700 - 1500	Atmospheric-elevated	Second-minutes	5.0	85.0	10.0

Biomass is constituted by hemicellulose, cellulose and lignin, showing different proportions according to the material, and their thermal decomposition occurs in three different temperature stages (Cha et al., 2016; Tomczyk et al., 2020; Weber and Quicker, 2018; Zheng et al., 2020). Hemicellulose is characterized by a group of polysaccharides presenting a branched chain-structure, being the most reactive component of biomass (Weber & Quicker, 2018). Its thermal decomposition starts at about 200-260°C and produces volatile compounds, chars (solid product) and a few tars (condensable liquids) (Zheng et al., 2020). The mass loss verified is due to the conversion of unstable fractions whether by arrangement or fragmentation, which comprises dehydration, bond breakage, presence of free radicals, and the development of carboxyl and carbonyl groups (Zheng et al., 2020). The major changes in properties occur in this temperature range (Weber & Quicker, 2018). Secondly, between 240 and 350°C (Zheng et al., 2020), cellulose, an unbranched polysaccharide more thermally stable than hemicellulose (Weber & Quicker, 2018), begins to disintegrate through the depolymerisation of bonds between monomer units of biopolymers, therefore decreasing the degree of polymerization in the chains to produce volatile molecules (Zheng et al., 2020). Lastly, the decomposition of lignin, the three-dimensional macromolecule with several chemical bonds and functional groups presenting various thermal stabilities (Tomczyk et al., 2020; Weber & Quicker, 2018), occurs over a wide temperature range, 280-500°C, where the maximum rate decay occurs between 350 and 450°C (Zheng et al., 2020). In the final stage, carbon is the organic element that represents the bulk of biochar (Tomczyk et al., 2020). The graphitic structure of biochar is better developed by the condensation of benzene rings into polycyclic structures, which happens in the decomposition of the residual solid at a slow rate (Zheng et al., 2020). The ash content in biochar increases with the increase in pyrolysis temperature on account of the combustion of the organic matter residues, while the volatile and organic matter decrease (Cha et al., 2016; Tomczyk et al., 2020; Weber & Quicker, 2018; Zhang et al., 2013; Zheng et al., 2020).

Over the years, the interest in biochar's sorption capacity has been rising since it is an environmentally friendly and inexpensive material (Cha et al., 2016) and given its attractive properties, such as high porosity, high specific surface area, great content of surface functional groups and alkaline pH (Tomczyk et al., 2020; Zheng et al., 2020). Moreover, the attention keeps growing over its vast applications and benefits. Biochar application contributes to the improvement of soil quality and fertility, generation of bioenergy, remediation of soil and polluted water, carbon sequestration, waste management, and the reduction in the emission of greenhouse gases (GHGs) (Cha et al., 2016; Li et al., 2017; Tomczyk et al., 2020; Weber & Quicker, 2018; Zhang et al., 2013; Zheng et al., 2020).



The availability and mobility of heavy metals in the soil are highly affected by the soil properties, e.g. pH, soil organic matter, cation exchange capacity, moisture and temperature. However, the most relevant parameters are the pH and the soil organic matter, playing a key role in the efficacy of the heavy metals' remediation upon biochar application (Zheng et al., 2020). The form and solubility of the heavy metals present in soil is dictated by the soil pH (Xu et al., 2017; Zheng et al., 2020). Since biochar has an alkaline nature (Li et al., 2017; Zheng et al., 2020) due to carbonate groups and inorganic alkalis (Tomczyk et al., 2020), its application to the soil results in a pH increase contributing to the immobilization of the heavy metals (Zheng et al., 2020). This increase is attributed to the partition of alkali salts from organic materials (Tomczyk et al., 2020).

Due to the negative charges attributed to the presence of carboxyl and phenol groups in soil organic matter, the effective immobilization of heavy metals may occur by multiple interactions, such as complexation, ion exchange and electrostatic interaction. Furthermore, the higher the content of organic matter in the soil the better the stabilization of heavy metals. The application of biochar to the soil also increases its organic matter content, enhancing even more the heavy metals' stabilization (Zheng et al., 2020).

A crucial factor in the metal adsorption is the existence of surface functional groups e.g., carboxyl (-COOH), hydroxyl (-OH) and amino (-NH<sub>2</sub>). The presence of these groups on biochar's surface is highly dictated by the pyrolysis temperature and the type of feedstock. A higher degree of carbonization leads to the loss of functional groups by dehydration and deoxygenation, and therefore to a decrease in the atomic ratios of H/C, O/C and N/C (Li et al., 2017; Weber & Quicker, 2018; Tomczyk et al., 2020). However, the organization of the carbon layers improves with the increase in pyrolysis temperature (Tomczyk et al., 2020).

The alkalinity of biochar is intrinsically dependent on the type and number of functional groups and hence determines its neutralization capacity in soil (Weber & Quicker, 2018). The ability to receive protons is attributed to the unpaired negative charges of partially detached functional groups (e.g., carboxyl or hydroxyl) (Tomczyk et al., 2020). The biochar's alkalinity increases with the increase in pyrolysis temperature. Consequently, biochar's pH also increases due to the detachment of predominantly acidic functional groups, e.g. carboxyl, hydroxyl or formyl groups, resulting in a more basic remaining solid. Therefore, the pH value is an indicator of the degree of carbonization (Weber & Quicker, 2018).

The cation exchange capacity (CEC) represents the capability of a material of holding the exchangeable cations (e.g. Na<sup>+</sup>, K<sup>+</sup>, Ca<sup>2+</sup>, Mg<sup>2+</sup>). Therefore, this property is dependent on the surface structure and area of biochar (Tomczyk et al., 2020; Weber & Quicker, 2018). An

increase in temperature reduces the CEC of biochar since it removes surface functional groups and originates aromatic carbon (Tomczyk et al., 2020).

According to size, biochar's pores can be divided into categories such as micropores, mesopores and macropores (Weber & Quicker, 2018; Zheng et al., 2020). The porosity is temperature dependent and affects several other physical properties, such as the pore volume, bulk density, surface area and water holding capacity. The porosity of biochar develops with the temperature (Li et al., 2017; Weber & Quicker, 2018) as a result of the water loss (Li et al., 2017), i.e., the higher the pyrolysis temperature the better developed the pores will be. As a result, the pore volume increases, the bulk density decreases and the surface area increases (Li et al., 2017; Weber & Quicker, 2018). The increase in surface area is caused by the release or thermal cracking of the pore-blocking substances, the destruction of both aliphatic alkyls and ester groups and the uncovering of the aromatic lignin core (Tomczyk et al., 2020). The surface area and the size of the pores highly influence the number of active sites (Weber & Quicker, 2018), the type and number of functional groups with which it can bond and hence the adsorption capacity (Li et al., 2017). The continuous degradation of the organic materials and the development of channel structures may increase the volume of the pores (Tomczyk et al., 2020).

The hydrophobicity is the outcome of the surface functional groups (Weber & Quicker, 2018; Zheng et al., 2020). The materials can be hydrophobic or hydrophilic. In the first case, the structures are non-polar and exhibit weak interaction with water, while the second structures are polar, thus strongly interact with water by hydrogen bonding. As the increase in pyrolysis temperature removes more polar surface functional groups, it results in an increase of the hydrophobic nature of biochar, also increasing the aromaticity (Weber & Quicker, 2018).

The water holding capacity is dependent on biochar's porosity and bulk volume (Weber & Quicker, 2018). The increase in the biochar concentration resulted in a higher water holding capacity (Zhang et al., 2013).

In Table 10 are described ten different studies on the adsorption capacity of biochar towards different types of pollutants, showing the respective source of biochar, the conditions of the experiment and the results and main conclusions obtained.

**Table 10:** Comparison of the adsorption capacity of biochar from different studies.

Authors	Source of biochar	System	Results and conclusions
(Ali et al., 2020)	Biochar produced from rice straw.	<p>Evaluate the effectiveness of immobilizing agents (rice straw (RS), rice straw biochar (BI) and calcite (CC)) for Ni distribution and mobility.</p> <p>Soil samples:</p> <ul style="list-style-type: none"> <li>Collected from the surface layer from Jiangxia district</li> <li>Dried at room temperature</li> <li>Crushed to pass a 2 mm sieve for the incubation study</li> </ul> <p>Soil pH: 5.3</p> <p>Soil has a silty clay loam texture</p> <p>Conditions of biochar production:</p> <ul style="list-style-type: none"> <li>500°C for 2h</li> <li>0.25 mm pore size</li> </ul> <p>Incubation of 200 g of soil contaminated with NiSO<sub>4</sub>·6H<sub>2</sub>O to obtain 100 mg/kg Ni into normal cultivated soil for 2 months with 70% water holding capacity.</p> <p>After 2 months of incubation, RS, BI and CC at three concentrations (0, 1 and 2%) were applied into the spiked soil, reaching a total incubation period of 3 months.</p> <p>pH of heavy metal solution was adjusted to 5.</p> <p>Mixture of soil and metal solution was shaken for 24h at 120 rpm and centrifuged at 4500 rpm. Ni concentration in the aqueous phase was measured using FAAS.</p>	<ul style="list-style-type: none"> <li>Soil pH increased from 5.3 to 6.2 in the RS 2%, and to 6.4 in the BI 2% treated soil.</li> <li>Increasing the pH of an acidic soil decreases the metals' mobility and improves soil quality.</li> <li>Values of soil pH after a 3-month incubation period increased in the following order: CC 2% &gt; CC 1% &gt; BI 2% &gt; BI 1% &gt; RS 2% &gt; RS 1% &gt; control.</li> <li>Biochar exhibited the highest increase in soil electrical conductivity (EC) values.</li> <li>Values of soil EC after a 3-month period rose in the following order: BI 2% &gt; BI 1% &gt; RS 2% &gt; CC 2% &gt; CC 1% &gt; RS 1% &gt; control.</li> <li>Maximum increase in soil dissolved organic carbon was observed at 2% BI treatment.</li> <li>Prominent reduction (59-70.9%) was observed in the acid soluble portion of Ni when 1% and 2% of BI, respectively, was applied.</li> <li>Oxidizable fraction of Ni was increased by 65-73.7%, respectively, at 1 % and 2% BI addition.</li> <li>Ni concentration in different fractionations after a 3-month incubation period occurred in the order: BI 2% &gt; BI 1% &gt; RS 2% &gt; CC 2% &gt; CC 1% &gt; RS 1% &gt; control.</li> <li>Langmuir model showed a better fit than the Freundlich model to the adsorption process.</li> </ul>
(Chai et al., 2018)	Biochar produced from a rice straw.	<p>Removal of Cr by a straw-derived biochar.</p> <p>Conditions for biochar production:</p> <ul style="list-style-type: none"> <li>100-mesh sieve</li> <li>300°C for 2h</li> <li>Heating rate of 5°C/min</li> </ul> <p>Conditions:</p> <ul style="list-style-type: none"> <li>[SDBS]<sub>i</sub> = 50 - 200 mg/L</li> <li>Solution pH 2 ~ 11</li> </ul>	<ul style="list-style-type: none"> <li>Increasing the C<sub>eq</sub> increased the sorption amounts of Cr(VI) and Cr(III) by SB300.</li> <li>Decreasing the pH increased the removal of Cr(VI) by biochar.</li> <li>Surfactants immobilized on the sorbent's surface affect the characteristics of the surface and the sorption ability of a sorbent.</li> <li>Effect of SDBS on pH is critical.</li> <li>Increased pH inhibited the removal of Cr(VI) by SB300.</li> <li>SDBS promoted Cr(III) sorption but inhibited Cr(VI) sorption onto SB300.</li> </ul>

(Nascimento, 2018)	Biochar from oak wood bark and pinewood bark.	<p>Heavy metal removal (Ni and Zn) from contaminated soils using multi-walled carbon nanotubes (MWCNTs) and biochar from oak wood bark and pinewood bark.</p> <p>Soil water content of 68%.</p> <p>Biochar was sieved to &lt; 210 <math>\mu\text{m}</math>.</p> <p>Adsorbent (MWCNT or Biochar) suspension:</p> <ul style="list-style-type: none"> <li>• 0.03% (w/w) SBDS + Pluronic F-127</li> <li>• MWCNT: C (% w/w) of 0.01% or</li> <li>• Oak wood bark: C (% w/w) of 1, 3 and 5% or</li> <li>• Pinewood bark: C (% w/w) of 1, 3, 5 and 7%.</li> <li>• pH of 5 or 7</li> </ul>	<ul style="list-style-type: none"> <li>• Both MWCNTs and biochar addition improved the adsorption of HM ions.</li> <li>• Reference adsorption capacity for Ni and Zn (without pH adjustment) was 61.90% and 56.48%, respectively.</li> <li>• The application of 0.01% of MWCNT with 0.03% SDBS+Pluronic resulted in 71.64% of Ni adsorbed at pH 5, instead of 61.60% with no pH adjustment.</li> <li>• For Zn, the application of 0.01% of MWCNT with 0.03% SDBS+Pluronic increased the adsorption to 60.82% without pH adjustment, and to 58.17% at pH 5.</li> <li>• The highest sorption amounts of Ni and Zn obtained were 73.75% and 73.26%, respectively, for oak wood bark biochar at 3% with 0.03% SDBS+Pluronic and pH 5. For pinewood bark the highest Ni adsorption capacity was 66.05% at 5% with 0.03% SDBS+Pluronic and pH 5. For Zn was 61.98% at 3% with 0.03% SDBS+Pluronic at pH 5.</li> </ul>
(Figueredo et al., 2017)	Residues of sugarcane bagasse, eucalyptus bark and sewage sludge.	<p>Nutrients and contaminants (Zn, Cu, Cr, Ni) extraction in acid medium.</p> <p>Sugarcane bagasse and sewage size: 2 mm mesh sieve.</p> <p>Eucalyptus bark size: 2x3 cm pieces.</p> <p>Conditions:</p> <ul style="list-style-type: none"> <li>• Dried at 105°C for 24h in a muffle furnace</li> <li>• Pyrolysis temperature: 350 and 500°C</li> <li>• Heating rate of 25°C/min</li> <li>• 30 minutes</li> </ul>	<ul style="list-style-type: none"> <li>• Increase in pyrolysis temperature resulted in loss of oxygenated groups and increased carbon concentration in the biochars (BCs).</li> <li>• [C], H/C, O/C and C/N ratios highly influence metal sorption.</li> <li>• Loss of N with the increase in pyrolysis temperature is dependent on the composition of the raw material used.</li> <li>• A high pyrolysis temperature led to an even greater reduction in [C] and [N] of the BCs from sewage sludge but the opposite occurred in the BCs from plants as the [C] is higher.</li> <li>• In acid medium the chemical elements were released to the solution.</li> </ul>
(Li et al., 2017)	Revision	Heavy metal removal from aqueous solutions.	<ul style="list-style-type: none"> <li>• When biochar is applied to water for metal removal, solution pH strongly influences its surface charge.</li> <li>• Functional groups (carboxylic, amino and hydroxyl groups) play important roles in metal sorption.</li> <li>• Increasing temperature decreases the number of functional groups in biochar.</li> <li>• Change in solution pH impacts the complexation behaviour of functional groups.</li> <li>• Increasing biochar's surface area by incorporating nano-particles enhances its capacity for metal sorption.</li> </ul>

(Rizwan et al., 2016)	Biochar (BC) produced from rice straw (RS).	<p>Efficacy of RS and its derived biochar, single superphosphate (SSP) and MWCNT to immobilize the Pb- and Cu- contaminated soil. Soil was air dried for 2 weeks and passed through a 2 mm sieve. Condition for biochar production:</p> <ul style="list-style-type: none"> <li>• RS was air dried at room temperature and passed through a 10-mesh sieve</li> <li>• 500°C for 4h</li> <li>• Heating rate: 20°C/min</li> </ul> <p>MWCNT:</p> <ul style="list-style-type: none"> <li>• Outer diameter: 10 – 20 nm</li> <li>• Length: &gt; 5 <math>\mu</math>m</li> <li>• Specific surface area: 100 – 160 m<sup>2</sup>/g</li> </ul> <p>Contaminated soil was amended with RS 3 and 6% and its derived BC 3 and 6%, MWCNT 0.1, 0.5, and 1% (w/w) on dry soil basis, single superphosphate (SSP) 2500 and 5000 P<sub>2</sub>O<sub>5</sub> mg/kg and no amendment in the controlled soil. Samples were subjected to:</p> <ul style="list-style-type: none"> <li>• Incubation at 25°C for 45 days</li> <li>• Air dried and ground to pass through a &lt; 0.25 mm sieve</li> </ul>	<ul style="list-style-type: none"> <li>• pH and electrical conductivity (EC) had no significant change in MWCNT- and RS-treated soil.</li> <li>• BC showed the highest increase in soil pH (from 5.2 to 7) and EC (from 1.2 to 3 ms/cm) as compared to control when treated with 3 and 6% BC, respectively.</li> <li>• Addition of SSP slightly decreased the pH and increased the EC of soil.</li> <li>• Increasing the solution pH led to an increase in the amount of metal adsorption on biochar.</li> <li>• Increasing the MWCNT level resulted in a higher Pb and Cu immobilization.</li> <li>• Immobilization by MWCNT followed the order Pb &gt; Cu.</li> <li>• BC application was more effective to immobilize Cu and Pb than RS in contaminated soil.</li> <li>• Order of immobilization of Pb- and Cu-contaminated soil: BC &gt; SSP &gt; MWCNT &gt; RS.</li> <li>• RS was more effective in decreasing the bio-accessible Pb percentage and could be more effective by increasing incubation time.</li> <li>• SSP was more effective for Pb immobilization than Cu.</li> </ul>
(Lu et al., 2014)	Bamboo biochar and rice straw biochar.	<p>Effect of bamboo and rice straw biochars on the bioavailability of mixed metal contaminants. Conditions:</p> <ul style="list-style-type: none"> <li>• Soil was air dried</li> <li>• 2 mm stainless steel sieve</li> <li>• Bamboo biochar: 750°C with 3h retention time</li> <li>• Rice biochar: 500°C with 30 min retention time</li> <li>• 2 ground sizes: fine (&lt;0.25 mm) and coarse (&lt;1 mm)</li> </ul> <p>Plastic pots filled with 2 kg of soil and amended with 0.1% (w/w) and 5% (w/w) of bamboo or rice straw biochar. Pots with 70% of the field water holding capacity.</p>	<ul style="list-style-type: none"> <li>• Application of biochar increased the soil pH and electrical conductivity.</li> <li>• Particle size of biochar had no significant effect on the concentration reduction of Cd, Cu and Pb in plant shoots.</li> <li>• Cu and Pb concentration in shoots were more effectively reduced by rice straw biochar, whilst Cd was by bamboo biochar.</li> <li>• Fine biochars were more effective in reducing Zn concentration in shoots than coarse biochars, but not Cd, Cu and Pb concentrations.</li> <li>• Influence of biochar on heavy metal bioavailability varied with feedstock and application rate of biochars and was metal-dependent.</li> </ul>

(Hale et al., 2011)	Biochar produced from corn stover residues and Activated Carbon (AC) produced from anthracite coal.	<p>Adsorbent aging effect of biochar and AC (alone or mixed with soil) on the sorption of pyrene.</p> <p>Conditions for biochar production:</p> <ul style="list-style-type: none"> <li>• 600°C for 20 minutes</li> </ul> <p>AC size: 20 µm (80% of the particles smaller than 45 µm)  AC surface area: 859 to 792 m<sup>2</sup>/g  Biochar size: up to 2mm  Biochar surface area: 167 to 190 m<sup>2</sup>/g</p> <p>Sample aging:</p> <ul style="list-style-type: none"> <li>• Biochar and AC alone (20g)</li> <li>• Soil alone (100g)</li> <li>• Mixture of soil and biochar/AC (100g + 5% (w/w) Black Carbon amendment)</li> </ul> <p>Biological aging – exposing the materials to a:</p> <ul style="list-style-type: none"> <li>• Microbial inoculum</li> <li>• Nutrient solution</li> <li>• Glucose supplement</li> </ul> <p>Chemical aging – continual exposure of the materials to:</p> <ul style="list-style-type: none"> <li>• 60°C</li> <li>• 110°C</li> </ul> <p>Physical aging – samples subjected to 42 freeze – thaw cycles between -70°C (5h) and 20°C (19h).</p>	<ul style="list-style-type: none"> <li>• Decrease in pH for AC and biochar leads to an increase in surface acidity.</li> <li>• CEC of AC increased more strongly by aging than that of biochar.</li> <li>• Internal nanoporosity is the main factor determining sorption strength.</li> <li>• Grinding biochar to a smaller size did not significantly affect the sorption.</li> <li>• Aging had no significant effect on the sorption.</li> <li>• Soil exerts a minimal effect on the sorption to biochar.</li> </ul>
(Park et al., 2011)	Chicken manure-derived biochar (CM) and green waste-derived biochar (GW).	<p>Cd, Cu and Pb immobilization by monitoring NH<sub>4</sub>NO<sub>3</sub> extractable metal concentration.</p> <p>Biochar's treatment:</p> <ul style="list-style-type: none"> <li>• 550°C</li> <li>• Size: &lt; 250 µm</li> <li>• Outgassed in vacuum at 105°C for 8h</li> </ul> <p>Conditions:</p> <ul style="list-style-type: none"> <li>• 5% (w/w) of CM and GW</li> </ul> <p>Conditions of plant growth experiment:</p> <ul style="list-style-type: none"> <li>• 1, 5 and 15% of CM or GW</li> </ul>	<ul style="list-style-type: none"> <li>• Biochars showed high surface area enhancing the sorption of metals when incorporated into soils.</li> <li>• Wood biochars had higher total C, lower ash content, total N, P, K, S, Ca, Mg, Al, Na and Cu contents, and lower potential CEC and exchangeable cations than manure-derived biochars.</li> <li>• Biochars significantly increased Cd and Pb immobilization but were not effective for Cu.</li> <li>• Increasing level of biochar application had no significant effect on [Cu] of shoot.</li> <li>• CM was more effective in both the immobilization of metals and increasing plant growth than GW.</li> </ul>

(Trakal et al., 2011)	Biochar from stems of willow.	<p>Evaluate metals (Cd, Cu, Pb and Zn) sorption behaviour after biochar application into a metal-contaminated soil.</p> <p>Conditions:</p> <ul style="list-style-type: none"> <li>• 400°C</li> <li>• Heating rate: 10°C/min</li> <li>• Soil was air-dried</li> <li>• 2 mm sieve</li> </ul> <p>Six different concentrations: Cu, Pb and Zn (0.1, 0.5, 1, 2, 4 and 8 mmol) and Cd (0.05, 0.25, 0.5, 1, 2 and 4 mmol)</p>	<ul style="list-style-type: none"> <li>• Low desorption of Cu, a relatively low desorption of Cd and Pb and a high desorption of Zn.</li> <li>• The application of biochar to the soil had no significant effect on desorption.</li> <li>• Biochar application significantly reduced the desorbed Cd and Zn.</li> <li>• Soil pH decreased at increased metal concentrations during single- and multi-element sorption.</li> <li>• pH decrease during single-element sorption followed the order Cu &gt; Pb &gt; Zn &gt; Cd.</li> <li>• Soil sorption decreased in the following order Pb &gt; Cu &gt; Zn &gt; Cd.</li> <li>• Contaminated biochar had no additional negative effect on metal sorption.</li> <li>• Biochar application enhanced Cu and Pb sorption in all cases, whereas Cd and Zn sorption efficiency showed no significant changes.</li> <li>• Zn was predominantly desorbed during Cu and Pb single-metal sorption experiment.</li> <li>• Two different applied rates (1% and 2% w/w) had a negligible effect on metal sorption.</li> </ul>
(Beesley et al., 2010)	Hardwood-derived biochar.	<p>Biochar and greenwaste compost amendments effect on mobility, bioavailability and toxicity of inorganic and organic contaminants in a multi-element polluted soil.</p> <p>Conditions:</p> <ul style="list-style-type: none"> <li>• Soil was air dried at 20 – 25°C for 2 weeks</li> <li>• &lt; 2 mm sieve</li> </ul> <p>Soil was homogenised and thoroughly hand mixed with greenwaste compost and hardwood-derived biochar</p>	<ul style="list-style-type: none"> <li>• Biochar treatment was most effective at reducing the concentrations of total and bioavailable PAH groups.</li> <li>• Biochar and greenwaste compost equally increased shoot emergence (indicating phytotoxicity).</li> <li>• Biochar and compost decreased water-soluble phytotoxic element concentrations.</li> <li>• Total and bioavailable PAH concentrations were reduced by the application of biochar and compost alone.</li> <li>• Biochar and greenwaste compost work less effectively when added in combination.</li> </ul>

### 2.3.2. Carbon Nanoparticles

Usually, carbon nanotubes (CNTs) are produced by chemical vapour deposition (CVD) (Jawed et al., 2020) and they can be classified as single-walled carbon nanotubes (SWCNTs) or multi-walled carbon nanotubes (MWCNTs) (Dhasmana et al., 2019; Fiyadh et al., 2019; Jawed et al., 2020) according to their number of graphene sheets (Kalita & Baruah, 2020). Carbon nanotubes have a hollow cylindrical shape consisting of one or multiple graphene sheets rolled up (Fiyadh et al., 2019; Subramaniam, et al., 2019). According to the form of the sheets, the carbon nanotubes can be in zigzag, armchair or chiral (Fiyadh et al., 2019; Ihsanullah et al., 2016).

Carbon nanotubes are an attractive adsorbent for heavy metal removal from aqueous solution due to their high specific surface area, porosity, chemical and thermal stability and their simple large-scale synthesis (Dhasmana et al., 2019; Kalita & Baruah, 2020). Since MWCNTs have high dispersion ability, they present higher adsorption capacity when compared to SWCNTs (Kalita & Baruah, 2020). Moreover, MWCNTs can be produced in larger scales being much cheaper than SWCNTs. The surface of CNTs is characterized by the presence of functional groups, i.e. COOH, -C=O, and -OH, which provide active sites therefore improving the adsorption capacity. These surface functional groups react with the heavy metal's ions through electrostatic interaction (Kalita & Baruah, 2020). The attached functional groups influence the hydrophobic nature of carbon nanotubes, since the presence of polar groups on the surface makes CNTs dispersible in organic solvents (Fiyadh et al., 2019). Nonetheless, carbon nanotubes tend to be aggregated, difficult to operate and show poor dispersion ability due to the high surface area which favours van der Waals attractive forces (Fiyadh et al., 2019; Saikia et al., 2019).

The removal of heavy metals by carbon nanotubes can occur through electrostatic attraction, surface complexation, ligand exchange and sorption-precipitation between metal ions and functional groups present on CNT's surface (Jawed et al, 2020). The adsorption can occur in four distinct sites of the carbon nanotubes, such as the external surface, inner site, interstitial channel and the peripheral groove (Ihsanullah et al., 2016; Saikia et al., 2019). However, it is dependent on the reaction's pH. On one hand, at acidic pH the heavy metals are rapidly adsorbed as ions. On the other hand, at elevated pH, the heavy metals are present as hydroxides and their precipitation occurs (Jawed et al., 2020).

Gomes (2017) studied the performance of the surfactant TX-100 and three surfactants' combinations (SDBS + Pluronic F-127; SDBS + PolyDADMAC MMW; SDBS + TX-100),



previously studied individually by Matos (2016), in the dispersion of nanoparticles and their influence on the immobilizations of heavy metals. TX-100 and Pluronic F-127 are non-ionic surfactants, whereas SDBS is anionic and PolyDADMAC MMW is cationic. The efficiency of the dispersion of 0.01% (w/w) MWCNTs was evaluated with the application of 0.03% (w/w) of surfactants and followed the sequence: SDBS + Pluronic F-127 > SDBS + TX-100 > TX-100 > SDBS + PolyDADMAC MMW.

In the suspension tests Gomes (2017) achieved a better adsorption capacity of the heavy metals Pb, Cu, Zn and Ni when applying 0.01% (w/w) MWCNTs dispersed with 0.03% (w/w) of SDBS + Pluronic F-127, as the other combinations proved inefficient in the adsorption of heavy metals. The order of adsorption capacity obtained in the suspension test by Gomes (2017) after 24h was Pb (II) (99.6%) > Cu (II) (96.7%) > Zn (II) (59.7%) > Ni (II) (36.2%), which was attributed to the electronegativity of the heavy metals and the organic matter content of the soil under study.

Gomes (2017) also performed percolation tests and concluded that lead and copper reached an adsorption capacity higher than 99%. However, Zn (II) and Ni (II) corresponded to lower adsorption capacities in the reference tests performed by percolation than the ones obtained by suspension. The application of MWCNTs to the soil improved the adsorption capacity of the heavy metals, achieving 58% for Zn (II) with the application of 0.02% of SDBS and 0.01% of PolyDADMAC MMW and 37% for Ni (II) with 0.015% SDBS and 0.015% Pluronic F-127.

### **2.3.3. Nanoclays**

Over the years, as researchers demonstrated that clay and clay minerals have a layered structure and attractive properties, such as large specific surface area, high ion exchange capacity, low permeability, ability to swell and chemical and mechanical stability (Awasthi et al., 2019; Biswas et al., 2019; Kumar et al., 2019; Liu et al., 2019b), their applicability has grown. Nanoclays have been applied in the food industry (i.e. food packaging), animal feed, environmental remediation, agriculture, pharmaceutical and construction (Awasthi et al., 2019; Massaro et al., 2020; Soleimani & Amini, 2017).

Nanoclays are a natural, inexpensive, environmentally friendly and abundant material in nature (Anastopoulos et al., 2018; Awasthi et al., 2019; Biswas et al., 2019; Floody et al., 2009; Lisuzzo et al., 2020; Massaro et al., 2020; Radziemska & Mazur, 2016) formed by chemical weathering of various types of rocks (Massaro et al., 2020; Soleimani & Amini, 2017; Uddin, 2008) usually present in subtropical and wet tropical regions (Massaro et al., 2020).

The structure of clay minerals is organized in layers and each layer has two types of structural sheets, tetrahedral and octahedral. The first one is comprised of silica tetrahedrons ( $\text{SiO}_4$ ) linked to neighbouring tetrahedral by sharing three corners (Awasthi et al., 2019), subsequently showing a hexagonal network (Massaro et al., 2020; Uddin, 2008). The fourth oxygen of the tetrahedrons is commonly connected to Al, Mg or Fe in sixfold coordination and with hydroxyl groups, all belonging to the octahedral sheet (Gu et al., 2018; Massaro et al., 2020; Soleimani & Amini, 2017; Uddin, 2008). Structurally, two sheets constitute a layer and the space between the layers is designated as the interlayer (Awasthi et al., 2019; Uddin, 2008). The connection between layers by van der Waals or electrostatic force, hydrogen bonding or interlayer cations may form a clay crystallite (Uddin, 2008).

According to the arrangement of the tetrahedral and octahedral sheets, clays can be classified as 1:1, 2:1 and 2:1:1 phyllosilicates. The first type of phyllosilicates consists of one tetrahedral and one octahedral sheet for every clay layer, such as halloysite and kaolinite, whereas 2:1 phyllosilicates present two tetrahedral sheets with one octahedral sheet in the middle, like montmorillonite (smectite group) and illite. Finally, 2:1:1 phyllosilicates have an octahedral sheet adjacent to a 2:1 layer (Massaro et al., 2020; Uddin, 2008). The properties of the clay minerals vary according to its structure (Biswas et al., 2019). The formula, layer type and some properties of the kaolin, smectite and montmorillonite, illite and chlorine groups are indicated in Table 11 (Awasthi et al., 2019; Hillel, 2008; Uddin, 2008). The values shown for the properties are approximate values (Hillel, 2008).

**Table 11:** Comparison of different clay groups and their respective specifications.

	<b>Kaolin</b>	<b>Smectite and Montmorillonite</b>	<b>Illite</b>	<b>Chlorite</b>
Clay mineral	Dictite, nacrite, kaolinite and halloysite	Smectite and montmorillonite	Illite	Clinochlore, cookeite, donbassite, chamosite, nimite, sudoite and borocookeite
Formula	$Al_2Si_2O_5(OH)_4$	$(Ca,Na,H)(Al,Mg,Fe,Zn)_2(Si,Al)_4O_{10}(OH)_2 \cdot XH_2O$	$(K,H)Al_2(Si,Al)_4O_{10}(OH)_2 \cdot XH_2O$	$(Mg,Fe,Li)_6AlSi_3O_{10}(OH)_8$
Layer type	1:1	2:1	2:1	2:1
Layer charge	< 0.01	0.5 to 1.2	1.4 to 2.0	Variable
CEC / meq/100g	3 - 15	80 - 100	15 - 40	20 - 40
Planar diameter ( $\mu m$ )	0.1 - 4	0.01 - 1	0.1 - 2	0.1 - 2
Basic layer thickness / $\text{\AA}$	7.2	10	10	14
Particle thickness / $\text{\AA}$	500	10 - 100	50 - 300	100 - 1000
Specific surface / $m^2/g$	5 - 20	700 - 800	80 - 120	80
Area per charge / $\text{\AA}^2$	25	100	50	50

The sequence of tetrahedral and octahedral sheets influences the ion substitutions in the interlayer and therefore, the charge of the clay minerals and their swelling and cation exchange capacity. There are two types of charge, the structural charge, caused by ion substitutions in the interior of the layers which is permanent, and the surface charge, dictated by the pH value of the environment (Awasthi et al., 2019; Gu et al., 2018; Massaro et al., 2020; Soleimani & Amini, 2017). The surface adsorption capacity of clay minerals is associated with the charge chemistry at the surface (Awasthi et al., 2019). The sorption of pollutants by clay minerals can occur in two ways, either by their adsorption on planar external surfaces or by their exchange in the interlayers of the clay (Soleimani & Amini, 2017).

The structural properties of clay minerals are very important to determine the adsorption mechanism and selectivity towards contaminants. Therefore, the degree of adsorption in soils is highly dependent on the clay mineralogy in soil and clay content. The concentration of heavy metals in groundwater and soil is controlled by nanoclays and clay

minerals present in soil with metal hydroxides and organic matter (Soleimani & Amini, 2017).

The cation exchange capacity is the most significant feature of clay minerals and it is affected by the total layer charge (Soleimani & Amini, 2017). Moreover, when a clay mineral is added to a polluted site the CEC plays a vital role in its eco-toxicity control (Biswas et al., 2019). The clay present in soil is a considerable mean of transportation for pollutants and has the capability of adsorbing and transporting nutrients, metals and organic compounds (Soleimani & Amini, 2017).

The halloysite presents the following formula  $\text{Al}_2\text{Si}_2\text{O}_5(\text{OH})_4n\text{H}_2\text{O}$  ( $n = 0, 2$ ) and when in the hydrated form ( $n = 2$ ) there is one layer of water molecules between the multilayers (Glotov et al., 2019). Halloysite has a hollow tubular morphology (Anastopoulos et al., 2018; Gu et al., 2018; Hermawan et al., 2018; Lisuzzo et al., 2020; Liu et al., 2019b; Liu et al., 2019c; Massaro et al., 2020), which improves its adsorption capacity (Hermawan et al., 2018), with open-ended and regular pores (Radziemska & Mazur, 2016). In spite of its tubular shape, ions and molecules can hardly access the interlayer (Hermawan et al., 2018).

Halloysite nanotubes (HNTs) are the result of rolling kaolinite sheets, therefore exposing its negative charged external surface, comprised of siloxane (Si-O-Si) groups, and its positively charged inner lumen, composed by aluminol (Al-OH) groups (Glotov et al., 2019; Hermawan et al., 2018; Lisuzzo et al., 2020; Liu et al., 2019b; Massaro et al., 2020). Through the hydroxyl groups present on HNTs' surface, other chemical species can covalently bond (Liu et al., 2019b; Soleimani & Amini, 2017). However, the anions present in the solution, the pH and the ionic strength determine which metal ions adsorb on a particular reactive site. Clay minerals mainly adsorb organic cations due to their negatively charged outer surface (Soleimani & Amini, 2017). Nonetheless, their adsorption is limited as a consequence of electrostatic repulsion with the positively charged inner surface of halloysite (Glotov et al., 2019).

Whilst CNTs possess small and hydrophobic pores, halloysite has larger hydrophilic internal cavities allowing the lumen to be occupied with chemical and smaller particles (Glotov et al., 2019).

The application of halloysite nanotubes may be limited due to its weak interactions with other molecules by hydrogen or electrostatic bonds and hydrophobic effects (Massaro et al., 2020). Furthermore, their interlayer is barely reachable for ions and molecules. Thus, modifications may be performed to enhance their adsorption capacity (Hermawan et al., 2018). In Table 12 are described eight studies on the adsorption capacity of nanoclays

towards heavy metals. The source of the nanoclays, the conditions of the experiment and the results and conclusions are listed.

Throughout the years, various types of nanoclays with distinct compositions and properties have been employed for remediation purposes, as displayed in the few examples present in Table 12. Additionally, nanoclays have been applied with and without modifications in order to evaluate their performance. According to the studies present in Table 12, it is clear that the application of nanoclays to the soil increases its pH, therefore reducing the mobility of heavy metals and, as a consequence, increasing their immobilization. The clay material that exhibited the most promising results was the UltraHallopure halloysite nanotubes, showing a Ni (II), Zn (II), Pb (II) and Cu (II) removal percentage above 93% (Hermawan et al., 2018). The kaolinite clay used by Jiang et al. (2010) adsorbed 71% of Ni (II) when the equilibrium was attained and adsorbed 78% of Ni (II) at pH 7. However, the examples given in this work are only a few of the extensive research already done in the clay materials field for remediation purposes present in the literature.

**Table 12:** Comparison of the adsorption capacity of nanoclays from different studies.

Authors	Source of nanoclays	System	Results and conclusions
(Matin et al., 2020)	Fe <sub>3</sub> O <sub>4</sub> (nano-Fe (NF)) with a surface area of 24.8 m <sup>2</sup> /g and a pore diameter of 25.7 nm and natural sodium montmorillonite (nanoclay (NC)) with a surface area of 220-270 m <sup>2</sup> /g and a pore diameter of 6.0 nm	Investigation of the immobilization of five PTEs (Cd, Cr, Cu, Ni, and Zn) by a combination of two different biochars (almond shell (AB) and walnut shell (WB)) in three application rates (2.5%, 5%, and 10%) and two NP additions (NC and NF) of 1%. Almond and walnut shells conditions: <ul style="list-style-type: none"> <li>• Dried at 70°C</li> <li>• Almond pyrolysis: 500°C for 2h</li> <li>• Walnut pyrolysis: 400°C for 2h</li> <li>• Ground to pass through a 0.5-mm sieve.</li> </ul> Soil pH and CEC: 7.9 and 14.0cmol <sub>e</sub> /kg AB pH and CEC: 6.5 and 14.1cmol <sub>e</sub> /kg WB pH and CEC: 5.6 and 40.4cmol <sub>e</sub> /kg	<ul style="list-style-type: none"> <li>• Increasing the application rates of both biochars reduced leaching and stabilized PTEs in contaminated soils.</li> <li>• WB was more effective in immobilizing Cd, Cr, and Ni, while AB was more effective in immobilizing Zn.</li> <li>• Leaching was reduced by 46.2% for Ni and 58.5% for Zn with the combined addition of 10% WB and NC compared to 24.5% and 14.2% reduction with only WB addition, respectively.</li> <li>• The addition of NF to 10% AB originated a cumulative leaching of 39.8% and 28.7% of Ni and Zn, respectively, compared to 13.6% and 46.9% of Ni and Zn when NF was added to 10% WB, respectively.</li> <li>• Biochar application decreased the mobility indices (MI) of all PTEs, and in several cases NP addition reduced the MI further.</li> </ul>
(Liu et al., 2019c)	Halloysite nanotubes (HNTs-raw) supplied by Hongqiao Co., Ltd. (Hebei, China) HNT: <ul style="list-style-type: none"> <li>• Total pore volume: 0.2087 cm<sup>3</sup>/g;</li> <li>• Micropore volume: 0.0198 cm<sup>3</sup>/g;</li> <li>• Mesopore volume: 0.1889 cm<sup>3</sup>/g;</li> <li>• Surface area: 20.88 m<sup>2</sup>/g;</li> <li>• Density: 1.031 g/cm<sup>3</sup>.</li> </ul>	Potential application of HNTs@CRC materials on Co, Ni, Cu and Zn immobilization in contaminated river sediments. Conditions of experiment: <ul style="list-style-type: none"> <li>• Each type of amendment was mixed with the sediment separately at a ratio of 1:10 (w/w).</li> <li>• Samples prepared: <ol style="list-style-type: none"> <li>1. 0.5 g raw sediment without amendment (control);</li> <li>2. 0.5 g sediment with 0.05 g Ca(OH)<sub>2</sub>;</li> <li>3. 0.5 g sediment with 0.05 g HNTs-raw;</li> <li>4. 0.5 g sediment with 0.05 g HNTs@CRC (HNT@carbon with rich carboxylic groups);</li> <li>5. 0.5 g sediment with 0.04 g HNTs@CRC + 0.01 g Ca(OH)<sub>2</sub> (HNTs@CRC/Ca(OH)<sub>2</sub>).</li> </ol> </li> <li>• Each sample was added with 25 mL of deionized water and incubated for 1 week</li> <li>• 10 mL of the extraction fluid was mixed with 0.5 g of each solid sample and rotated at 30 ± 2 rpm for 18h at room temperature.</li> <li>• Centrifugation at 4000 rpm for 20 min</li> </ul>	<ul style="list-style-type: none"> <li>• For Ni, the residual fraction percentages raised from 27.84% to 28.76%, 32.38%, 31.52% and 38.35%, respectively, after applying Ca(OH)<sub>2</sub>, HNTs-raw, HNTs@CRC and HNTs@CRC/Ca(OH)<sub>2</sub> as amendments.</li> <li>• For Cu, the addition of HNTs-raw and Ca(OH)<sub>2</sub> caused a slight decrease in the residual percentages, but increased from 14.98% in the raw sediment to 17.13% and 33.47% with the addition of HNTs@CRC and HNTs@CRC/Ca(OH)<sub>2</sub> as amendments, respectively.</li> <li>• The residual fraction percentages of Zn increased from 20.26% (raw sediment) to 20.69%, 26.21% and 35.43% when amended with Ca(OH)<sub>2</sub>, HNTs@CRC and HNTs@CRC/Ca(OH)<sub>2</sub>, respectively.</li> <li>• HNTs@CRC effectively increased the residual fraction of the 4 HM.</li> <li>• After using HNTs@CRC/Ca(OH)<sub>2</sub> for sediment remediation, the immobilization effect was found to be enhanced by 7.95, 1.43, 2.36 and 1.82 times for Co, Ni, Cu and Zn, respectively.</li> <li>• High stabilization ratio for the 4 metals, especially for Zn in the amended sediment with HNTs@CRC/Ca(OH)<sub>2</sub>.</li> <li>• HNTs@CRC and HNTs@CRC/Ca(OH)<sub>2</sub> can be recognized as superior amendments for HM stabilization in contaminated river sediments.</li> <li>• The pH of the sediment was increased from 6.36 to 10.41 by adding HNTs@CRC/Ca(OH)<sub>2</sub>.</li> </ul>

(Hermawan, et al., 2018)	<p>Halloysite nanotubes: Matauri Bay (MB) and UltraHallopure (UHP)</p> <p>MB provided by Imery NZ (SiO<sub>2</sub>: 60.14% and Al<sub>2</sub>O<sub>3</sub>: 38.79%)</p> <p>UHP provided by I-Minerals Inc. (SiO<sub>2</sub>: 55.55% and Al<sub>2</sub>O<sub>3</sub>: 41.45%)</p> <p>Percentage of particles &lt; 0.075 mm:</p> <ul style="list-style-type: none"> <li>• MB: 25.2%</li> <li>• UHP: 41.7%</li> <li>• Fly ash (FA): 53.1%</li> <li>• Zeolite (Z): 9.81%</li> </ul>	<p>Identification of proper soil filter media that can remove heavy metal ions and has reasonably high hydraulic conductivity.</p> <p>Materials:</p> <ul style="list-style-type: none"> <li>• Fly ash (FA) with surface area of 0.6 m<sup>2</sup>/g</li> <li>• Zeolite (Z) with surface area of 17 m<sup>2</sup>/g</li> <li>• MB halloysite nanotubes:               <ul style="list-style-type: none"> <li>○ Surface area: 22 m<sup>2</sup>/g</li> <li>○ Length: 50 nm – 2 μm</li> <li>○ Outer diameter: 20 – 100 nm</li> <li>○ Inner diameter: 5 – 30 nm</li> </ul> </li> <li>• UHP halloysite nanotubes:               <ul style="list-style-type: none"> <li>○ Surface area: 47 m<sup>2</sup>/g</li> <li>○ Length: up to 4 μm</li> <li>○ Thinner than MB</li> </ul> </li> </ul> <p>Each PVC soil column contains 3 layers from bottom to top including drainage, transition and filter media.</p>	<ul style="list-style-type: none"> <li>• Increasing the percentage of fine material from 2% to 5% decreased the infiltration rate in all column types.</li> <li>• Infiltration rate followed the decreasing order: MB &gt; UHP &gt; Z &gt; FA.</li> <li>• Columns with 2% MB yielded the highest infiltration rate value (364 mm/h) while columns with 5% FA showed the slowest infiltration rate (98 mm/h).</li> <li>• Order of coarsest materials: MB &gt; UHP &gt; Z &gt; FA.</li> <li>• Material with larger particles gives higher infiltration rate.</li> <li>• 2% of additive material produces relatively higher infiltration rate than 5%.</li> <li>• All column types could remove Pb(II) and Cu(II) (removal &gt; 95%).</li> <li>• For Ni(II) removal, UHP and FA columns performed slightly better than columns with MB and Z.</li> <li>• Increasing the proportion of fine material from 2% to 5% slightly decreased the Ni(II) removal for columns containing MB and Z.</li> <li>• For Zn(II) removal, all columns showed removal percentages ≥ 95% except for MB (89% removal rate).</li> <li>• Increase in the fine material proportion has no considerable influence on Zn(II) removal.</li> <li>• Filter with 2% UHP was the best composition followed by 2% MB and control columns with no fine materials.</li> </ul>
(Radziemska & Mazur, 2016)	<p>Natural zeolite with phase composition of quartz 69.43% and aluminium oxide 13.04% obtained from Sokirnica, Ukraine.</p> <p>Raw halloysite obtained from the strip mine “Dunino”, Intermark Company (Legnica, Poland) and modified halloysite samples produced by the company by calcinations of the raw halloysite at 650°C.</p>	<p>Determination of the effects of soil contamination with Ni on the content of selected elements in the soil and examine the effectiveness of adding mineral reactive materials (raw halloysite, modified halloysite and natural zeolite) in decreasing Ni, Pb, Cr, Zn and Cu concentration in soils.</p> <p>Soil:</p> <ul style="list-style-type: none"> <li>• pH: 4.8</li> <li>• 4.05 mg<sub>Ni</sub>/kg, 10.90 mg<sub>Cr</sub>/kg, 8.49 mg<sub>Cu</sub>/kg, 24.20 mg<sub>Zn</sub>/kg and 5.44 mg<sub>Pb</sub>/kg.</li> </ul> <p>Doses of Ni in the amount of 0 (control), 80, 160, 240 and 320 mg/kg of soil were introduced in the form of chemically pure aqueous solutions of nickel sulphate heptahydrate (NiSO<sub>4</sub>·7H<sub>2</sub>O).</p> <p>Composition of soil: 2.0 – 0.05 mm: 86.6%; 0.002 – 0.05 mm: 11.2%; &lt; 0.002 mm: 2.2%</p>	<ul style="list-style-type: none"> <li>• Order of accumulation of HM in Ni-contaminated soil: Ni &gt; Zn &gt; Cr &gt; Cu &gt; Pb.</li> <li>• Modified halloysite was the most effective to neutralize the contamination and reduced Ni content by 12%.</li> <li>• Application of natural zeolite to soil with the highest contamination of Ni was the most beneficial and reduced Ni content in the soil by 13%.</li> <li>• The soil contents of Zn and Cu were significantly decreased by the highest doses of Ni.</li> <li>• Contamination at 320 mg<sub>Ni</sub>/kg<sub>soil</sub> led to the highest content increase in Ni, Pb and Cr in the control experiment.</li> <li>• Strongest effects on Cr were caused by natural zeolite, reducing its content.</li> <li>• The application of Ni decreased the concentration of Zn in soil in the control experiment, presenting a 7% decrease upon the application of the highest Ni concentration.</li> <li>• Modified halloysite reduced the average amount of Cu in soil by 30%.</li> </ul>

Świercz et al., 2016)	<p>Halloysite collected from the Dunino open-pit mine. Halloysite main constituents are Al (19.57%), Si (18.51%) and Fe (11.38%). The chemical analysis showed a negligible content of HM (Ni-0.05%, Cr – 0.04%, Cu - 0.01% and Zn – 0.01%).</p>	<p>Preliminary assessment of the use of halloysite in the process of phytoremediation of soils contaminated with HM and seeded with common orchardgrass. Raw halloysite was initially ground in a mortar, sieved through a 2 mm sieve, washed with distilled water and dried to the air-dry state.</p> <p>Experimental variants:</p> <ul style="list-style-type: none"> <li>• Z: mineral and organic soil contaminated with heavy metal</li> <li>• 0: (mucky) mineral and organic soil with the natural content of HM</li> <li>• I: soil Z with 10% halloysite</li> <li>• II: soil Z with 30% halloysite</li> <li>• III: soil Z with 50% halloysite</li> </ul> <p>Substrate humidity kept at 60% of field water capacity.</p> <p>Seeds of common orchardgrass were sown in an amount of 1g per pot.</p> <p>Pot experiment with a pot capacity of 5 m<sup>3</sup> and filled with a mixture of halloysite and soil, to the total weight of 2000 g.</p> <p>Soils were classified as neutral or slightly alkaline.</p>	<ul style="list-style-type: none"> <li>• Addition of halloysite to the soil increased soil pH and sorption capacity and limited HM mobility in soils.</li> <li>• Application of halloysite reduced the HM content in the contaminated soil.</li> <li>• Reducing the share of halloysite in soil inhibited Zn sorption.</li> <li>• Cr assumed a form hardly accessible to plants.</li> <li>• Content of HM had the following decreasing order: Zn &gt; Pb &gt; Cu &gt; Cr.</li> <li>• In the 0 control cultivation, the elevation of HM along with the crop yields followed the order: Zn &gt; Cu &gt; Pb &gt; Cr.</li> <li>• Increase of Pb, and decrease of Zn, Cu and Cr were observed in the biomass of common orchardgrass growing in the substrate enriched with halloysite.</li> <li>• Halloysite increased the quantity of biomass in comparison to the control cultivation.</li> <li>• Bioaccumulation factors indicate that the analysed plant absorbs Zn and Cu more intensively than Pb and Cr.</li> <li>• The stabilization of Cu and Zn in soils occurred most effectively with the 10% addition of halloysite, and for Cr with the 50% addition of halloysite.</li> </ul>
(Kananizadeh et al., 2011)	<p>Montmorillonite/Na<sup>+</sup> prepared by ATP Company with the interlayer spacing of 1.2 nm and density of 19 kN/m<sup>3</sup>.</p> <p>Clay's properties:</p> <ul style="list-style-type: none"> <li>• Liquid limit: 50.395%</li> <li>• Plastic limit: 32.14%</li> <li>• Plasticity index: 18.25%</li> <li>• Density: 20.26 kN/m<sup>3</sup></li> </ul>	<p>Investigation of nanoclay application in reducing soil permeability.</p> <p>Leachate's properties:</p> <ul style="list-style-type: none"> <li>• COD: 140 000 mg/L</li> <li>• pH: 7</li> <li>• Conductivity: 67.6 mS/cm</li> </ul> <p>Optimum water content: 27.16%</p> <p>Clay conditions:</p> <ul style="list-style-type: none"> <li>• Dried in a heating oven at ≈ 105°C for 24h</li> </ul> <p>Samples with 1, 2, 3, 4 and 5% nanoclay were saturated in H<sub>2</sub>O for 2 weeks and then subjected to a permeability test.</p> <p>Each test was done in triplicate and at different leachate pH of 4.8, 7 and 9.</p> <p>29% water content was selected for all samples.</p>	<ul style="list-style-type: none"> <li>• The increase in the NC content slightly decreases the plastic limit while slightly increases the liquid limit and plasticity index.</li> <li>• Permeability rapidly decreases by adding 3% NC and after that it seems to be less affected by NC content.</li> <li>• 4% NC was chosen as an additive as it increased compressive strength compared to raw samples and made the percentage of swelling increase.</li> <li>• NC helps the mixture remain dispersed.</li> <li>• Adding NC to the mixture decreased the permeability, which diminished the amount of HM that can penetrate into the mixture.</li> </ul>



(Jiang et al., 2010)	<p>Kaolinite clay supplied by the Kaolin Company of Long Yan, Fujian, China.</p> <p>Chemical composition: 53.7% SiO<sub>2</sub>; 43.6% Al<sub>2</sub>O<sub>3</sub>; 2.0% Fe<sub>2</sub>O<sub>3</sub>; 0.2% MnO; 0.5% K<sub>2</sub>O and 0.1% TiO<sub>2</sub></p>	<p>Investigation of the feasibility of kaolinite clay used as a low-cost adsorbent for the removal of Pb(II), Cd(II), Ni(II) and Cu(II) from aqueous solution.</p> <p>Kaolinite clay:</p> <ul style="list-style-type: none"> <li>• Sieved to pass 220 μm mesh</li> <li>• CEC: 95 mmol/kg</li> <li>• BET surface area: 3.7 m<sup>2</sup>/g</li> </ul> <p>Adsorption study:</p> <ul style="list-style-type: none"> <li>• 30°C at 150 rpm using 50 mL capped polyethylene bottles containing 20 mL of metal ion solutions and 0.5 g of kaolinite clay adsorbents</li> <li>• Contact time: 2 min to 4h</li> <li>• Centrifuged at 2500 rpm for 10 min</li> <li>• Contact time of 60 min was optimized and selected for the rest of the study.</li> </ul>	<ul style="list-style-type: none"> <li>• The equilibrium adsorption was reached within 30 min for all the metal ions and 92% of Pb(II), 68% of Cd(II), 71% of Ni(II) and 53% of Cu(II) were adsorbed on the kaolinite clay.</li> <li>• Kaolinite clay removal capacity followed the order: Pb(II) &gt; Ni(II) &gt; Cd(II) &gt; Cu(II).</li> <li>• The increase in the pH of the solution resulted in an increase of adsorption of all ions.</li> <li>• Increasing the initial metal ion concentration from 10 to 150 mg/L resulted in an increase in the metal ions adsorbed for single and multi-metal competitive adsorption.</li> <li>• Selectivity sequence of the adsorption: Pb(II) &gt; Cd(II) &gt; Ni(II) &gt; Cu(II).</li> <li>• Desorption of Cd(II) and Cu(II) were much easier than that of Pb(II) and Ni(II).</li> <li>• Experimental data were better fitted with Freundlich equation than Langmuir model.</li> <li>• Adsorption sites were non-uniform and nonspecific in nature.</li> <li>• Low surface area of the kaolinite clay is a result of the low percentage of kaolinite components in the clay.</li> </ul>
(Yavuz et al., 2003)	<p>Kaolinite from Turkey</p>	<p>Removal of Mn(II), Co(II), Ni(II) and Cu(II) from aqueous solution by adsorption on natural kaolinite.</p> <p>Conditions:</p> <ul style="list-style-type: none"> <li>• Kaolinite sieved to -200 mesh size and dried at 110°C</li> <li>• Known concentration of HM solutions were introduced into glass bottles (100 mL) containing accurately weighed amounts (1.00 g) of the adsorbent</li> <li>• Bottles were shaken at 25°C or 40°C using immersed water bath until equilibrium is reached</li> <li>• Centrifugation at 3500 rpm</li> </ul>	<ul style="list-style-type: none"> <li>• The equilibrium was attained after shaking for 2h.</li> <li>• Affinity order of kaolinite for metal ions: Cu(II) &gt; Ni(II) &gt; Co(II) &gt; Mn(II).</li> <li>• Cu(II) is the most adsorbed because of its smaller ionic radius (easily penetrates in the pores of the kaolinite) and its low solubility.</li> <li>• Formation of stable complex (between silanol or aluminol and HM cations) facilitates the adsorption of HM.</li> <li>• Better adsorption is obtained at higher temperature.</li> <li>• Conformed to the linear form of Langmuir adsorption equation.</li> </ul>

#### 2.3.4. Particles dispersion

The application of nanoparticles for environmental remediation requires them to be freely dispersed. However, one of their disadvantages is that they tend to aggregate or cluster (Kalita & Baruah, 2020), therefore exhibiting lower surface area and consequently hindering the adsorption capacity. To overcome this drawback, surfactants have been used as enhancing agents due to their ability to keep the nanoparticles dispersed and also because of their ability to solubilize contaminants present in the soil. They are a commonly applied additive in various remediation techniques, such as surfactant-enhanced soil washing, surfactant-enhanced electrokinetic remediation and surfactant-enhanced phytoremediation (Mao et al., 2015).

The structure of surfactants is denominated amphiphilic as two distinct parts characterize them: a hydrophobic tail and a hydrophilic head (Bisht, 2019; Mao et al., 2015; Shi et al., 2019; Zhang et al., 2019). The former is an insoluble alkyl chain presenting 8 to 22 carbons and demonstrating no affinity to water, while the latter is soluble and attracts water molecules (Bisht, 2019; Nakama, 2017). The application of surfactants can have differing purposes, such as solubilisation, emulsion stabilization, wetting, foaming, detergency and pharmaceutical formulations (Nakama, 2017; Siyal et al., 2020).

According to the charge present in the hydrophilic head, surfactants are classified as ionic, i.e. anionic or cationic, non-ionic, or amphoteric (Bisht, 2019; Liu et al., 2019a; Mao et al., 2015; Nakama, 2017; Shi et al., 2019; Siyal et al., 2020), with obvious impact on their properties. The most important surfactant's characteristics are the type of charge, solubility and the adsorption and physicochemical abilities (Bisht, 2019).

The concentration of surfactants has a direct influence in the form in which it is present (Mao et al., 2015). When surfactants are present at low concentration, they only occur as single molecules and they mostly gather at the liquid-liquid or solid-liquid interface (Bisht, 2019; Mao et al., 2015). The increase in concentration results in the replacement of the interfacial solvent by surfactant molecules, therefore lowering the polarity of the aqueous phase and the surface tension (Mao et al., 2015). The threshold concentration where surfactants form, spheroidal or ellipsoidal, micelles is denominated as the critical micelle concentration (CMC) (Bisht, 2019; Mao et al., 2015; Nakama, 2017). When the concentration of surfactants is higher than the CMC, surfactants and micelles are side-by-side in equilibrium (Bisht, 2019). The length of the hydrocarbon chain and the condition of the surfactant solution, for example, affect the CMC (Bisht, 2019). Generally, the CMC is lower for the

non-ionic surfactants and they can be employed in the remediation of contaminated soils due to their low toxicity and solubilisation capacity (Mao et al., 2015).

The micellization is an entropy-driven process that occurs in two stages, starting with the dehydration of the hydrocarbon tail and then its aggregation to the hydrocarbon tails of other surfactant molecules, consequently forming a micelle (Nakama, 2017; Shi et al., 2019). The entropy of water molecules caused by the release of free water prompts the micellization (Nakama, 2017). The entropy of the dehydration is much higher than the entropy of the aggregation (Nakama, 2017; Shi et al., 2019). Since micelles lack the capacity to exchange ions, the ion exchange mechanism does not have much influence above the CMC and therefore, the removal of heavy metals mainly occurs below the CMC (Liu et al., 2019a).

The addition of surfactants to thermodynamically stable aqueous solutions can cause solubilisation, if the surfactant's concentration is above the CMC. In this process, the lightly soluble materials dissolve due to the lipophilic group in the interior of the micelles (Mao et al., 2015; Nakama, 2017). The position of the solubilisation depends on the polarity of the solubilised substance. The temperature, structure and the addition of inorganic salts affect the surfactant's potential of solubilisation (Nakama, 2017).

The adsorption of surfactants in a solid-water interface may occur via physical or chemical adsorption, where the former is the result of van der Waals forces and the latter the consequence of ionic interactions or covalent bonds (Nakama, 2017). The mechanisms involved in the adsorption are hydrogen bonding, electrostatic and  $\pi$ - $\pi$  interactions and van der Waals forces, which are dependent on the distance and hence fairly weak and reversible (Nakama, 2017; Siyal et al., 2020). As the distance increases the van der Waals forces decrease. The adsorption mechanism depends on the nature of the surfactant and adsorbent (Siyal et al., 2020).

Li & Qiu (2019) and Zhang et al. (2019) have studied the dispersion of MWCNTs and CNTs, respectively. As Zhang et al. (2019) stated, the carbon nanotubes are prone to aggregate in aqueous solutions on account of the strong van der Waals forces along the tubes, thus reducing the sorption sites available for other compounds. To overcome this problem, CNTs have been dispersed by sonication though the dispersion obtained is not stable, even occurring re-aggregation (Zhang et al., 2019). Thereby, they studied the application of surfactants, such as, sodium dodecyl sulfate (SDS) (anionic), sodium dodecylbenzene sulfonate (SDBS) (anionic), cetyl trimethyl ammonium bromide (CTAB) (cationic) and octylphenol ethoxylate (TX-100) (non-ionic) (Li & Qiu, 2019; Zhang et al., 2019). Zhang et al. (2019) registered a decrease in the adsorption of the CNTs as the concentration of the anionic surfactants increased. The mechanism responsible for the adsorption of anionic

surfactants on CNTs is  $\pi$ - $\pi$  bonds with CNTs. The difference between SDBS and SDS is that the former has one more benzene ring, which favours its adsorption on CNTs (Zhang et al., 2019). In both studies, the better dispersion was obtained with the application of TX-100. Li & Qiu (2019) attributed to the contribution of the  $\pi$ - $\pi$  stacking interaction, provided by the benzene ring present in the tail of TX-100, and thus considerably increasing the binding and surface coverage of the surfactant molecules onto the graphite. The dispersion of MWCNTs by the non-ionic surfactant (TX-100) occurred through steric hindrance mechanism, while steric and electrostatic stabilization were responsible for the dispersion with the ionic surfactants (SDS) (Li & Qiu, 2019). However, Liu & Qiu (2019) found that the MWCNTs dispersed by SDS and TX-100 with SDS were more stable than those dispersed by only TX-100. Zhang et al. (2019) concluded that the most important factors affecting adsorption were the surface charge for anionic surfactants, the surfactant's concentration for cationic surfactants and the dispersion state for non-ionic surfactants.

Figueiredo (2014) characterized four surfactants and studied the most efficient surfactant's concentration for the dispersion of MWCNTs. Glycerox and Amber 4001 dispersed efficiently the MWCNTs. As Glycerox is a non-ionic surfactant, its molecules adsorb on the negative surface of the MWCNTs preventing aggregation by steric stabilization. Conversely, Amber 4001 is a cationic surfactant, therefore easily adsorbed on the MWCNTs' surface, and as charge repulsion occurs between surfactant molecules, aggregation is prevented. However, Figueiredo (2014) found that sodium acrylate and methacrylic acid (Disperse 31) and sodium acrylate (Disperse 32), both anionic, could not disperse the MWCNTs, showing the presence of aggregates. This is due to the surfactant and MWCNTs presenting the same charge, occurring electrostatic repulsions between them and, therefore, no adsorption and dispersion is possible. In conclusion, the best MWCNTs dispersion obtained by Figueiredo (2014) after applying ultrasonic energy was for 1% (w/w) of Glycerox, though there was no significant difference between the concentration of 1% and 3% (w/w).

Unconfined compressive strength (UCS) tests were performed by Figueiredo et al., (2015) to study the mechanical behaviour of the stabilized soil upon the addition of the previously dispersed suspensions of MWCNTs to the Portland cement, the responsible agent for soil stabilization. The maximum values of unconfined compressive strength were attained for higher concentrations of MWCNTs (0.01% (w/w)) due to the good dispersions achieved. The UCS tests showed that the application of small quantities of efficiently dispersed MWCNTs improved the mechanical properties of the soil stabilized with Portland cement. Finally, Figueiredo et al., (2015) concluded that the best surfactant was Amber 4001 as it

produced more satisfactory results in the UCS tests and obtained the best dispersion results with a lower concentration (1% (w/w)).



### 3. Materials and Methods

#### 3.1. Materials

##### 3.1.1. Baixo Mondego soft soil

The soil used in this study was collected at a depth of 2.5 m, in a portion of Quinta da Foja, near Santa Eulália, between 11 and 12 km of A14/IP3. The initial water content of the soil (80.9%) was measured according to the standard NP 84 (1965) and lowered to 71.30%. In order to classify and compare the soil’s characteristics to a previous study, some tests were carried out to determine the composition, organic matter content and the pH. The characterization of the soil, present in Table 13, was performed after the percolation tests, to clarify the results obtained.

**Table 13:** Characteristics of the soil.

		(Matos, 2016)	Present study
<b>Composition</b>	Clay (% w/w)	21	11
	Silt (% w/w)	59	72
	Sand (% w/w)	20	17
<b>Specific gravity of soil particles</b>	-	2.61	
<b>OM content</b>	(% w/w)	7.41	11.5
<b>pH</b>	-	5.34	5.25

The grain size composition of the soil was performed following the LNEC E 196 – 1966 specification. The curve obtained is illustrated in Figure 3 and the percentages of each soil component are present in Table 13. According to the Feret’s triangle, the soil can be classified as silt loam.

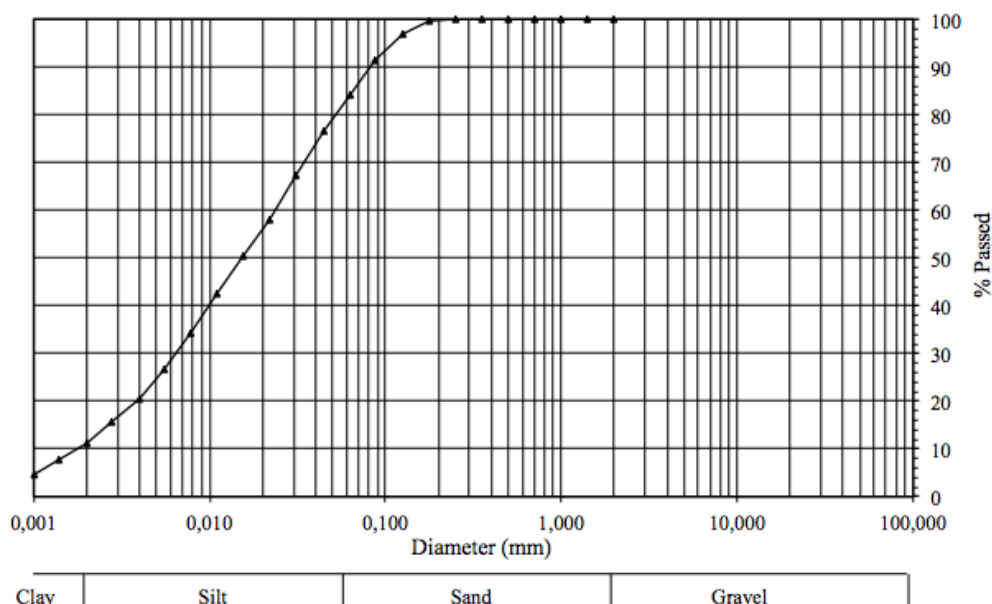


**Figure 3:** Soil's grain size curve.

To quantify the organic matter content in the soil, the Loss on Ignition (LOI) Method from BS 1377-3 (1990) was followed. In this test, four soil samples were weighted and oven-dried at 50°C for 24h. After their mass was registered, the samples were placed in a muffle furnace for 24h at 400°C and their final mass was measured. The mean of the percentage of mass lost is measured as the organic matter content.

The pH of the soil was measured according to the BS 1377-3 (1990). The test was performed in triplicate and the mean value obtained was 2.85. In order to have comparable results to previous studies, the pH of the soil was corrected to 5.25 by adding 4.78 mL of NaOH 3M per 100 g of soil.

### 3.1.2. Heavy metals

In this study, the adsorption capacity of four heavy metals was evaluated. The metals selected were Cu, Ni, Zn and Cr, as aforementioned. The first three metals have been used in previous studies, however Cr is a novel metal under study considering its high toxic potential. To recreate a real situation, the concentration of heavy metals used to contaminate the soil were the maximum found in Portuguese soils by Inácio et al. (2008), which are present in Table 14. The heavy metals were introduced in the salt form and information about the salts used is also shown in Table 14.

**Table 14:** Maximum concentration of heavy metals found in Portuguese soils by Inácio et al. (2008) and the heavy metals ion's and salt's information.

<b>Metal</b>	Copper	Chromium	Nickel	Zinc
<b>Concentration (mg/kg dry soil)</b>	245	336	880	589
<b>Metallic ion</b>	Cu (II)	Cr (III)	Ni (II)	Zn (II)
<b>Ion's Molecular Weight (g/mol)</b>	63.55	52.00	58.69	65.38
<b>Salt</b>	Copper (II) chloride dihydrate	Chromium (III) nitrate nonahydrate	Nickel (II) nitrate hexahydrate	Zinc (II) sulphate heptahydrate
<b>Salt's chemical formula</b>	CuCl <sub>2</sub> ·2H <sub>2</sub> O	Cr(NO <sub>3</sub> ) <sub>3</sub> ·9H <sub>2</sub> O	Ni(NO <sub>3</sub> ) <sub>2</sub> ·6H <sub>2</sub> O	ZnSO <sub>4</sub> ·7H <sub>2</sub> O
<b>Salt's Molecular Weight (g/mol)</b>	170.48	400.15	290.81	287.50

### 3.1.3. Adsorbent particles

#### 3.1.3.1. Biochar

The biochar used in this study is from oak wood bark, which was burnt in the October 2017 Portuguese wildfires, in the Oliveira do Hospital region. The bark was grinded in a hammer mill present in the Chemical Engineering Department of the Faculty of Sciences and



Technology of the University of Coimbra and sieved through two sieves (345 and 210  $\mu\text{m}$ ) collecting the particles with a size lower than 210  $\mu\text{m}$ , which was considered an appropriate size according to a previous study (Nascimento, 2018). A Thermogravimetric Analysis (TGA) was performed to evaluate the carbon content present in the biochar of oak wood bark. The result obtained by the analysis is shown in Figure 4.

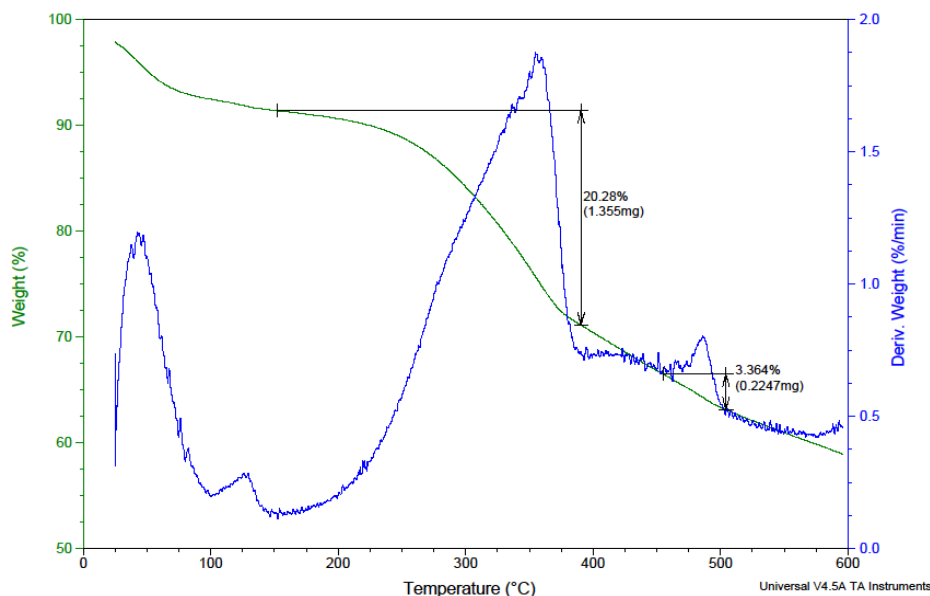


**Figure 4:** Thermogravimetric Analysis of the oak wood bark biochar.

The green line in Figure 4 represents the variation of the weight percentage of the biochar sample as a function of temperature, with an initial mass of 6.68 mg and a final mass of 3.959 mg, whereas the blue line illustrates the derivative of the weight percentage as a function of time.

The initial weight decrease registered until 150.48°C, is due not only to the loss of physisorbed water, but also to low molecular weight volatile compounds, solvents and trapped gases (Saadatkhah, et al., 2020). Between this temperature and 388.54°C, the major weight loss is recorded as a consequence of the carbonization of the organic matter present (20.28%) and the carbon oxidation in biochar. The stabilization of the carbon content occurred in the temperature range of 500 to 600°C, 59.27%, being the calculated carbon content of biochar.

In this work, the biochar with a size lower than 210  $\mu\text{m}$  was denoted as SO and the biochar with a size between 210 and 345  $\mu\text{m}$  was designated as MO.

### 3.1.3.2. Nanoclays

The nanoclays used in this study are denominated as halloysite nanoclay (kaolin clay) obtained from Sigma-Aldrich and are illustrated in Figure 5.

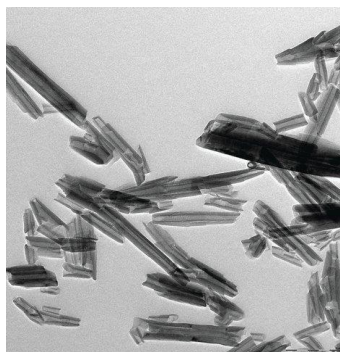


**Figure 5:** Illustration of the halloysite nanoclay from Sigma-Aldrich (Halloysite nanoclay, n.d.).

The nanoclays are a white powder and its formula and properties are listed in Table 15.

**Table 15:** Halloysite nanoclay's properties given by Sigma-Aldrich.

Properties	Value
Formula	$H_4Al_2O_9Si_2 \cdot 2H_2O$
Molecular weight (g/mol)	294.19
Appearance (form)	Powder
Specific gravity	2.53
Pore volume (mL/g)	1.26 – 1.34
Surface area (m <sup>2</sup> /g)	64
Refractive index n <sub>20/D</sub>	1.54
pH	4.5 – 7.0
Diameter (nm)	30 - 70
Length (μm)	1 - 3

#### 3.1.4. Surfactants

In this study, three different surfactants were used to evaluate their dispersion capacity. Sodium Dodecylbenzene Sulfonate (SDBS), anionic, and Pluronic F-127, non-ionic, both produced by MERCK (Germany), which were used together according to previous studies (Gomes 2017; Nascimento, 2018). The other surfactant, LigniOx-LB, produced through the LigniOx technology and provided by the VTT Technical Research Centre of Finland (Finland), has a lignin content of 18.5% (w/w).

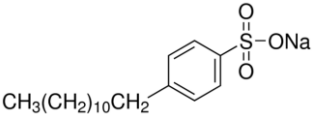
The LigniOx technology produces versatile dispersants through a lignin functionalization method based on alkali-O<sub>2</sub> oxidation. The aim of this simple and competitive technology, patented by the VTT, is the valorization of lignin, a valuable renewable resource widely available as a by-product of the lignocellulosic refineries, and the development of other upgrading methods (Kruus & Hakala, 2017).

As a result of the ionization of the phenolic groups, soda and kraft lignins are only soluble at basic pH, being necessary to increase the water solubility of lignin to attain desirable properties for dispersing applications. Therefore, at alkaline conditions, the addition

of molecular oxygen results in lignin depolymerisation and introduces acidic groups in lignin, consequently increasing its water solubility (Kalliola et al., 2015).

Both SDBS and Pluronic F-127 were characterised by Matos (2016) and have been used by Matos (2016), Gomes (2017) and Nascimento (2018) to disperse MWCNTs and Nascimento (2018) also used it to disperse biochar. Their characteristics and chemical structure are present in Table 16.

**Table 16:** Characteristics of the surfactants used.

Characteristics	SDBS	Pluronic F-127	LigniOx-LB
<b>Chemical structure</b>		$H(OCH_2CH_2)_x(OCH_2\overset{CH_3}{\underset{ }{C}})_y(OCH_2CH_2)_zOH$	
<b>Molecular Mass [kDa]</b>	363	9.49	4.50
<b>pH</b>	7.0 – 10.5	6.0 – 7.0	9.9
<b>Size – hydrodynamic diameter [nm]</b>	81.02	6.920	181.4
<b>Zeta Potential [mV]</b>	-66.97	-0.430	-24.0
<b>Charge</b>	Anionic	Non - ionic	Anionic

## 3.2. Characterization Techniques

### 3.2.1. Particle size

The measurement technique of the particle’s size is chosen accordingly to their size range. In this study, the selected techniques were the Laser Diffraction Spectroscopy (LDS) and the Dynamic Light Scattering (DLS) as they apply in the micrometre and nanometre range, respectively.

#### 3.2.1.1. Laser Diffraction Spectroscopy

The Laser Diffraction Spectroscopy technique was applied to evaluate the biochar’s dispersion in the suspension. For that purpose the equipment used was the Mastersizer Hydro 2000MU from Malvern Instruments (size range from 0.02 to 2000 microns) (Mastersizer, 2005). The principle behind this technique is a time-averaged measurement of the scatter pattern of a monochromatic laser light by particles in suspension, on a series of concentric photoelectric detectors (Hickey & Giovagnoli, 2018; Kastner & Perrie, 2016; Li et al., 2019b; Merkus, 2009; Pan et al., 2017). Subsequently, the scattering data is transmitted to a computer that applies a model-based matrix to obtain the particle size distribution (Li et al., 2019b; Merkus, 2009; Pan et al., 2017). The model employed correlates the diffraction angle with the particle size, since it assumes they are inversely proportional (Kastner & Perrie, 2016).

Therefore, small particles scatter light at large angles while large particles scatter light at small angles (Hickey & Giovagnoli, 2018; Kastner & Perrie, 2016; Li et al., 2019b). The most widely used theories are the Fraunhofer diffraction theory and the Mie Scattering theory.

The Mie theory is more complete and rigorous. However, to apply Mie's theory the material's and medium's refractive indices have to be known. The refractive index is a complex number and, thus, is characterized by two parts. On one hand, the real part of the index describes the refractive properties of the material and the medium and, on the other hand, the imaginary part represents the absorption properties of the particle material (Malvern Instruments, 2010; Merkus, 2009).

The Mastersizer software supplies the volume mean diameter ( $D[4,3]$ ), the surface weighted mean ( $D[3,2]$ ) and the distribution percentiles –  $D(10)$ ,  $D(50)$  and  $D(90)$  – which represent 10, 50 and 90% of the sample's volume, respectively, in the result's report (Kastner & Perrie, 2016; Malvern Instruments, 2010).

### **3.2.1.2. Dynamic Light Scattering**

The Dynamic Light Scattering technique measures the time-dependent intensity scattering fluctuation of the laser beam resulting of the interference with the particles in suspension (Kastner & Perrie, 2016; Merkus, 2009; Perry, et al., 2008; Schwaferts, et al., 2019). These oscillations are detected at a specific angle by a sensitive avalanche photodiode detector. Afterwards, the examination of the variations by a digital autocorrelator enables the construction of a correlation curve, which is fitted to an exponential function (Kastner & Perrie, 2016; Malvern, n.d.). Through this curve the diffusion coefficient ( $D$ ) can be obtained and, thus, the hydrodynamic diameter ( $d_H$ ) can be calculated by applying the Stokes-Einstein Equation (1) (Kastner & Perrie, 2016; Merkus, 2009):

$$d_H = \frac{kT}{3\pi\mu D} \quad (1)$$

where  $k$  represents the Boltzmann constant,  $T$  the absolute temperature and  $\mu$  the viscosity of the dispersion medium. Nevertheless, the Stokes-Einstein relationship is limited to spherical particles and may overestimate the diameter of larger particles due to the signal intensity being correlated to the diameter of the particle to the power 6 (Kastner & Perrie, 2016; Merkus, 2009; Schwaferts, et al., 2019).

In the suspension, the particles not only collide between themselves, but also with molecules, resulting in the Brownian motion of the particles (Kastner & Perrie, 2016). This motion and the particle's size affect the intensity fluctuations registered. As smaller particles

move more rapidly the intensity oscillations are faster than for larger particles (Kastner & Perrie, 2016; Merkus, 2009).

This technique was applied to assess the nanoclay's dispersion being performed in the ZetaSizer Nano ZS from Malvern Instruments and some of its specifications are listed in Table 17 (Merkus, 2009).

**Table 17:** Key features of the ZetaSizer Nano ZS from Malvern Instruments (Merkus, 2009).

Size range	0.3 to 10000 nm
Concentration range	Max 40% w/v Limits generally dependent on refractive index and particle size
Minimum sample volume (size measurement)	12 $\mu$ L
Measurement angles	13° and 173°
Parameters measured	Size, Zeta Potential, Molecular Weight Intensity, volume and number based particle size distribution
Application areas	Wide range of colloids, dispersions, suspensions

### 3.3. Atomic Absorption Spectrometry

The Atomic Absorption Spectrometry (AAS) analysis is performed in an Atomic Absorption Spectrometer 3300 from Perkin Elmer, from the Chemical Process Engineering and Forest Products Research Centre (CIEPQPF) in the Chemical Engineering Department of the Coimbra University. According to the type of atomizer used, flame or graphite furnace, the AAS is denominated as the flame AAS (FAAS) or the graphite furnace AAS (GFAAS) (officially designated as electrothermal – ETAAS – by IUPAC), respectively. In this study, the first technique was adopted to measure the heavy metal's concentration in the sample. The principle of the AAS consists on the absorption of monochromatic light by the analyte's atoms, at a specific wavelength determined by the monochromator, to an excited state for a short period of time (Borges & Holcombe, 2017; García & Báez, 2012; Skoog et al., 2007). For this analysis it is imperative that the analyte's atoms are free and in the gaseous phase (Borges & Holcombe, 2017; Skoog et al., 2007). Several methods can be used to obtain the calibration curve, which relates the absorbance with the analyte's concentration through the Beer-Lambert's Law (Borges & Holcombe, 2017; García & Báez, 2012; Skoog et al., 2007), as shown in Equation (2):

$$A = \epsilon lc \quad (2)$$

where  $\epsilon$  is the molar attenuation coefficient,  $l$  the optical path length and  $c$  the concentration of the attenuating species.

The samples were injected in the chamber, vaporized, and the amount of the different metals in the liquid samples collected during the absorption tests determined based on the absorbance measured (García & Báez, 2012; Skoog et al., 2007).

The detection limits of the Atomic Absorption Spectrometer 3300 from Perkin Elmer for the heavy metal's ions used in this study are present in Table 18.

**Table 18:** AAS detection limits for each ion in the Atomic Absorption Spectrometer 3300 from Perkin Elmer.

<b>Heavy Metal</b>	<b>Detection Limit (mg/L)</b>
Cu	0.002
Cr	0.003
Ni	0.009
Zn	0.002

### 3.4. Experimental Procedure

#### 3.4.1. Heavy metals' adsorption by soil percolation

The percolation tests occurred in the Civil Engineering Department of the Faculty of Sciences and Technology of the University of Coimbra.

Firstly, 100 g of soil are weighted and mixed in order to remove all the grains existent. The average moisture content of the soil is 71.30% ( $w_0$ ), on a dry soil basis, so the dry mass of soil is 58.38 g ( $P_{S0}$ ) and the mass of water ( $P_{w0}$ ) is 41.62 g. Then, the soil is contaminated with the heavy metals' solution and stirred to guarantee a homogenised soil. The mass of heavy metals' salt is dependent on the concentration in the soil targeted and on the molecular masses of the ion and salt. The mass of heavy metals' salt used to prepare 100 ml of solution is present in Table 19. To that mass it is added 100 mL of ultrapure water and then stirred at 150 rpm for 30 minutes.

**Table 19:** Salt mass added to 100 mL of ultrapure water to contaminate 100 g of soil.

<b>Salt</b>	<b>CuCl<math>\cdot</math>2H<math>_2</math>O</b>	<b>Cr(NO<math>_3</math>)<math>_3</math><math>\cdot</math>9H<math>_2</math>O</b>	<b>Ni(NO<math>_3</math>)<math>_2</math><math>\cdot</math>6H<math>_2</math>O</b>	<b>ZnSO<math>_4</math><math>\cdot</math>7H<math>_2</math>O</b>
<b>Mass (mg)</b>	38.37	150.9	254.6	151.2

The volume of heavy metals' solution added to 100 g of soil increased the moisture content of the soil to 80.87% ( $w_1$ ). Therefore, the new mass of water ( $P_{w1}$ ) per 100 g of soil is 47.21 g and, consequently, the volume of heavy metals' solution to add is 5.589 mL. Lastly,

the suspension of biochar or nanoclays is added to the mixture and stirred. As the volume of the suspension needs to increase the final moisture content to 115%, it is necessary to add 19.92 mL of the suspension of biochar / nanoclays.

The contaminated soil is split between two samples of approximately  $54 \pm 2$  g each. Each sample is placed in a PVC tube with 35 mm of height and internal diameter, with two perforated disks, one at the top and the other at the bottom. A moistened filter paper is placed at the top of the system. It is imperative to guarantee that there are no bubbles in the soil so that the water is prevented from passing through them. The set up, according to the scheme in Figure 6, is made of 8 PVC tubes and was constructed by Matos (2016).

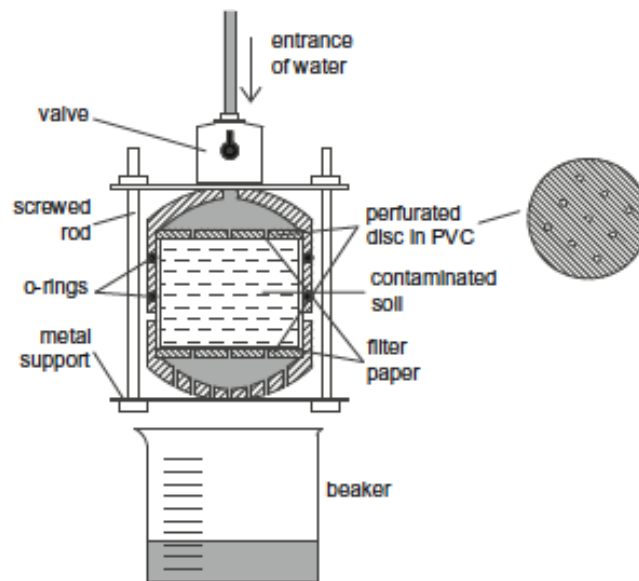


**Figure 6:** Illustration of the percolation system by Matos (2017).

The system is under a constant pressure of 50 kPa, which is kept by a regulated system constituted by a pressure regulator, an air compressor and an air – water interface. Before the percolation test starts, it is necessary to turn on the system for approximately 1 hour so the system reaches equilibrium. After that, the system operates until the lixivate volume reaches that of the sample, 33.67 mL.

When the sample volume is obtained, 15 mL of the lixivate are filtered through a syringe equipped with a nylon filter with a diameter of 25 mm and a pore size of  $0.45 \mu\text{m}$ , and placed in falcon tubes which go for Atomic Absorption Spectroscopy for metal quantification. The adsorption percentage is obtained by the difference between the initial concentration of metal in the soil, present in Table 20, and the concentration determined by AAS.

**Table 20:** Salt and metal concentrations in the contaminated soil at t=0 (100 g of soil).

<b>Metallic ion</b>	<b>Salt Concentration (mg/L)</b>	<b>Metal Concentration (mg/L)</b>
Cu (II)	571.5	213.0
Cr (III)	2248	292.2
Ni (II)	3792	765.2
Zn (II)	2252	512.2

### 3.4.2. Heavy metals' adsorption by soil suspension

The suspension tests occurred in the Chemical Engineering Department of the Faculty of Sciences and Technology of the University of Coimbra.

To perform the adsorption test using a suspension of soil, a suspension volume of 200 mL is required, which is obtained by mixing 150 mL of dispersed nanomaterial's suspension and 50 mL of water used to contaminate the soil. The suspension is continuously stirred for 24 hours at 150 rpm. However, to guarantee an initial homogenised suspension, an agitation of 300 rpm is executed for the first minute. Throughout the test, 5 samples of 15 mL of soil suspension are collected to a falcon tube using a syringe, after 20 minutes, 1h, 2h, 4h and 24h. Then, the samples go to a centrifuge for 20 minutes at 3000 rpm, to separate the supernatant. The centrifuge used is the Universal 23 model from Hettich. Subsequently, the supernatant, after centrifugation, is collected with a syringe and filtered through a 0.45 µm syringe nylon filter to another falcon tube. Lastly, the samples are analysed by AAS to quantify the amount of heavy metal present.

For this test, there are needed 36 g of dry soil, which represent 61.67 g of soil since its water content on a dry soil basis is 71.30%. To achieve the 50 mL of water content in the soil referred to previously, the heavy metals used to contaminate the soil are diluted in 24.33 mL of ultrapure water for 30 minutes at 150 rpm. The heavy metal's mass is calculated regarding the targeted maximum concentration found in the Portuguese soils by Inácio et al. (2008). The ion and salt's mass per 36 g of dry soil and the metallic ion initial concentration in the suspension are presented in Table 21.

**Table 21:** Mass of salt used for the contamination of 61.67 g of wet soil and initial metallic ion concentration in the suspension tests.

<b>Metallic Ion</b>	<b>Ion mass per 36 g of dry soil (mg)</b>	<b>Salt mass per 36 g of dry soil (g)</b>	<b>Initial concentration in the suspension (mg/L)</b>
<b>Cu (II)</b>	8.82	0.024	44.10
<b>Cr (III)</b>	12.1	0.093	60.48
<b>Ni (II)</b>	31.7	0.157	158.4
<b>Zn (II)</b>	21.2	0.093	106.0



Firstly, the heavy metal solution is added to the soil. The test begins when the 150 mL suspension of dispersed adsorbent is added to the soil. In the reference test, the 150 mL correspond to ultrapure water.

### 3.5. Tests' Plan

The experimental goal for this study was to evaluate the heavy metal's adsorption by soil percolation with the application of natural wastes (biochar) and nanomaterials (nanoclay). The parameters under study are the time of contact and the concentration and type of adsorbent and surfactant used for the treatment of soil contaminated with copper, chromium, nickel and zinc. The dispersion of the adsorbent with the application of surfactants was characterized for every concentration and the particle's size distributions of the dispersions are present in the Appendix A and B. The overview of the tests performed is listed in Table 22.

**Table 22:** Overview of the performed tests in soil percolation.

Oak wood bark biochar	Surfactant	Time of contact	Denomination
-	-	1 day	Ref-1day
-	-	1 day	Ref-1day <sup>ad</sup>
-	-	1 day	Ref-1day-pull <sup>ad</sup>
-	-	1 day	Ref-1day-push <sup>ad</sup>
-	-	1 day	Ref-1day-pull+push <sup>ad</sup>
-	-	1 day	Ref-1day-6h-percolation <sup>ad</sup>
3%	0.03% SDBS + Pluronic	1 day	SO3-1day
3%	0.03% SDBS + Pluronic	7 days	SO3-7days

ad- pH was adjusted

Note: Pull and push are referring to the application of the nylon filter.

The tests denoted with pull or/and push are referring to the action performed with the filter in the syringe, while in the test Ref-1day-6h-percolation the soil was left to percolate for 6 hours, 4 more hours than the other samples. The SO3-1day and SO3-7days refer to the percolations tests performed after one day and seven days of contamination, respectively, with the application of 3% (w/w) of oak wood bark biochar previously dispersed with 0.03% (w/w) SDBS + Pluronic F-127.

Due to the unexpected results obtained in the percolation tests, which will be discussed in the next chapter, further experiments were performed in a soil suspension as summarized in Table 23.

**Table 23:** Overview of the performed tests in soil suspension.

Oak wood biochar < 0.210 mm	Oak wood biochar 0.210 mm < size < 0.345 mm	Nanoclays	Surfactant		Nomenclature
			SDBS + Pluronic (SP)	LigniOx (L)	
-	-	-	-	-	Ref
3%	-	-	0.03%	-	SO3SP0.03
5%	-	-	0.05%	-	SO5SP0.05
3%	-	-	-	0.03%	SO3L0.03
-	3%	-	0.03%	-	MO3SP0.03
-	5%	-	0.05%	-	MO5SP0.05
-	3%	-	-	0.03%	MO3L0.03
-	-	0.01%	0.03%	-	NC0.01SP0.03
-	-	0.05%	0.03%	-	NC0.05SP0.03
-	-	0.05%	0.15%	-	NC0.05SP0.15
-	-	1%	3%	-	NC1SP3
-	-	1%	-	0.01%	NC1L0.01
-	-	1%	-	3%	NC1L3

The preparation of the suspension of biochar / nanoclays is in accordance to the conditions of each experiment, i.e., in the SO3SP0.03 test the 150 mL suspension is constituted by 0.015% (w/w) of SDBS (0.0225 g) and 0.015% (w/w) of Pluronic F-127 (0.0225 g) previously dispersed, as aforementioned, and 3% (w/w) of the smaller oak wood bark biochar (4.5 g).

## 4. Results and Discussion

This chapter contains the presentation of the results obtained and its discussion and comparison with previous studies performed by other authors. Firstly, the results of the heavy metals' adsorption by soil percolation tests with and without the application of oak wood bark biochar are presented and examined. Secondly, the addition of oak wood bark biochar is evaluated by the results of the heavy metals' adsorption by soil suspension tests. Finally, the results obtained upon the application of halloysite nanoclay on the suspension tests are displayed and discussed.

### 4.1. Results of the heavy metals' adsorption by soil percolation tests

The adsorption of contaminants by soil percolation provides a more accurate representation of a field situation, since the soil is in its usual state. In these tests, the water is percolated, under pressure, through the contaminated soil as it naturally occurs in nature. Therefore, the influence of the parameters under study, i.e., concentration of biochar and surfactant, time of contact and the size of the oak wood bark biochar, can be evaluated by percolation tests.

At the start of the experiment, the concentration of the heavy metals present in the soil is the maximum concentration found by Inácio et al. (2008) in the Portuguese soils, present in Table 20 (section 3.4.1). The adsorption capacities obtained at the end of the percolation tests, defined as when the volume of the lixivate is equal to the volume of the sample, for the four heavy metals under study, are present in Table 24.

**Table 24:** Adsorption capacities obtained in the percolation tests.

	% Ni	% Zn	% Cu	% Cr
Ref-1day	96.09	92.52	99.87	99.41
Ref-1day <sup>ad</sup>	99.22	98.82	-	-
Ref-1day-pull <sup>ad</sup>	-	98.41	-	-
Ref-1day-push <sup>ad</sup>	98.78	-	-	-
Ref-1day-pull+push <sup>ad</sup>	-	98.43	-	-
Ref-1day6h-percolation <sup>ad</sup>	-	99.35	-	-
SO3-1day	96.73	-	-	-
SO3-7days	97.09	94.39	99.88	99.72

According to the results achieved, it was concluded that the affinity of soil towards the heavy metals' ions followed the order: Cr (III) > Cu (II) > Ni (II) > Zn (II), which is in agreement with the literature (Fontes & Gomes, 2003). This may be due to several cumulative effects: the atomic radii of the heavy metals, which show the following order Cr (166 pm) > Ni (149 pm) > Cu (145 pm) > Zn (142 pm) (Clementi et al., 1967); to their Pauling electronegativity, presenting the following sequence Ni (II) (1.91) > Cu (II) (1.90) > Cr (III) (1.66) > Zn (II) (1.65) (Pauling, 1973), and to the affinity towards organic matter.

The adsorption capacity of the four heavy metals improved slightly with the addition of oak wood bark biochar, previously dispersed through the application of surfactants, and with the increment of the days of contact. This is possibly due to the increment in the soil's pH imposed by the addition of biochar and the respective decrease in the mobility of the heavy metals' ions, which consequently promotes their immobilization (Zheng et al., 2020). Nevertheless, the increase is less significant for Cr (III) and Cu (II), since they were almost entirely adsorbed by the soil particles. Thus, the following experiments were only done for nickel and/or zinc. Subsequently, the application of 3% (w/w) of oak wood bark biochar and 0.03% (w/w) of SDBS + Pluronic F-127 with one day of contact was studied for Ni (II) only (SO3-1day). It showed a small increase in the adsorption capacity in comparison to the reference test (Ref-1day), yet lower than the one achieved with seven days of contact (SO3-7days), displaying a small increase in the immobilization with the increase in the contact time.

Considering the high adsorption capacities obtained for Ni (II) and Zn (II) in the reference experiments, contrary to what was expected and obtained in previous studies, various studies were performed to investigate the error's source. Firstly, the soil pH was measured according to BS 1377-3 (1990), as formerly described in section 3.1.1. The test showed the soil pH was 2.85, instead of 5.34, as obtained previously by other authors using the same soil (Gomes, 2017; Matos, 2016; Nascimento, 2018). Therefore, 4.78 mL of NaOH 3M were added per 100 g of soil to guarantee a pH of 5.25. After this pH correction, another percolation test was carried out, which presented an even higher adsorption capacity, as expected since heavy metals show higher mobility at lower pH (Ali et al., 2020; Zheng et al., 2020). Secondly, the influence of the time of the percolation test was examined. One sample was left to percolate for 6 hours (4 more hours compared to the normal percolation tests), showing an increase in the adsorption capacity as the collected sample was more diluted with water compared to the other samples. Thirdly, the influence of the use of the nylon 0.45  $\mu\text{m}$  filter to filter the collected samples, before being submitted to Atomic Absorption measurements, was tested. Three tests were done: one with the filter in the syringe when pulling and pushing the lixiviate into the falcon tube, another when only pulling and the last

when only pushing. The adsorption capacities obtained show that the way the nylon filter is used has no influence on the results. The results were included in Table 24.

According to all the results attained in the percolation tests, the influence of the soil's grain size composition on adsorption and since it was not possible to collect a new soil sample from the same region, it became apparent the advantage of performing the tests in a suspension state, as the composition of the soil would have a lower influence on the adsorption capacity results. In the percolation study performed by Hermawan et al. (2018), the authors have verified that the presence of soil's larger particles (sand type) resulted in a higher infiltration rate. Thus, as in this study the low percentage of sand present in the soil is not sufficient to achieve good percolation conditions, it was obvious that there had been changes in the soil grain size when compared with previous studies conducted in the lab. Thus, the decision was that all parameters under study should be evaluated through soil suspension tests, as the soil composition (grain size) may have a lower influence on adsorption efficacy.

#### 4.2. Results of the heavy metals' adsorption by soil suspension tests with the application of oak wood bark biochar

First of all, the reference adsorption tests were executed along 7 days, collecting 15 mL samples of the suspension after 20 minutes, 1h, 2h, 4h, 24h, 3 days and 7 days since the beginning of the experiment, as detailed in section 3.4.2. The reference tests were performed for the four heavy metals individually. The results achieved are present in Table 25. In the beginning of the experiment, the concentration of each of the heavy metals present in the suspension is the maximum concentration found by Inácio et al. (2008) in the Portuguese soils.

**Table 25:** Results obtained for the reference tests in the heavy metals' adsorption by soil suspension tests.

Test t (min)	Reference Cr		Reference Cu		Reference Ni		Reference Zn	
	C (mg/L)	%	C (mg/L)	%	C (mg/L)	%	C (mg/L)	%
0	60.48	0	44.1	0	158.4	0	106.02	0
20	0.039	99.9	0.565	98.7	50.1	68.4	65.2	38.5
60	0.036	99.9	0.576	98.7	49.6	68.7	86.1	18.8
120	0.036	99.9	0.588	98.7	-	-	-	-
240	0.040	99.9	0.578	98.7	40.9	74.2	103.6	2.3
1440	0.045	99.9	0.678	98.5	41.7	73.7	67.5	36.3
3 days	0.054	99.9	1.177	97.3	92.9	41.4	71.77	32.3
7 days	0.032	99.9	0.239	99.5	105.8	33.2	86.1	18.8

The soil affinity towards the heavy metals' ions showed the following order: Cr (III) > Cu (II) > Ni (II) > Zn (II) as obtained in the soil percolation tests and as expected according to previous studies (Fontes & Gomes, 2003; Matos, 2016). According to Yousra et al. (2019), the adsorption affinity of the soil colloids towards heavy metals is favoured by a higher valence, i.e., the heavy metal ions with higher valence are more adsorbed by the soil particles, which explains the higher affinity of the soil towards Cr (III). The increase registered in the reference values for Cu (II) compared to previous studies (Gomes, 2017; Nascimento, 2018) may be explained by the rise in the organic matter content of the soil, as copper is the heavy metal with the highest affinity towards the organic matter (Lin & Xu, 2020; Rafaey et al., 2017). As Elbana et al. (2018) stated, the sorption of Cu (II) and Zn (II) is highly correlated with the soil pH, cation exchange capacity, amorphous oxides and clay and organic matter content.

Observing the results obtained in the reference test of Ni (II), present in Table 25, it should be emphasised that they significantly differ from previous studies where the same soil was used (Gomes, 2017; Matos, 2016; Nascimento, 2018), being unreasonably high. It must be stressed that this did not happen for the other heavy metals tested. Since the justification for this behaviour was not found and it was not possible to repeat these tests, as this discrepancy was only detected close to the end of the execution of the experimental part (the author had other courses that required full attention) the decision made was to use the reference values for Ni (II) obtained in the previous studies, which did not differ significantly between them. Therefore, the reference values considered hereafter are the ones obtained by Gomes (2017), presented in Table 26, as the conditions of the suspension are similar and the pH of the suspension was not adjusted. When accessing the effect of the time of contact for Ni (II) it will be necessary to consider the results obtained in the reference test of the present study, displayed in Table 25.

**Table 26:** Results of the reference test of Ni by adsorption in suspension test obtained by Gomes (2017).

Test	Reference Ni	
	t (min)	C (mg/L) %
0	158.4	0
20	109.1	42.6
60	86.3	45.5
240	90.2	43.0
1440	115.9	26.8

In the soil suspension tests' with the addition of oak wood bark biochar four parameters were evaluated. Firstly, the impact of the concentration of oak wood bark biochar and SDBS + Pluronic F-127 were assessed. Secondly, the effect of the time of contact was examined. Then, the performance of surfactant type, SDBS + Pluronic F-127 or LigniOx-LB, was evaluated. At last, the influence of the size range of oak wood bark biochar was analysed. The concentrations of the heavy metal present in the suspension (initially and as time passed) are shown in Table 27, as well as its adsorption percentage.

## RESULTS AND DISCUSSION

**Table 27:** Results obtained in the adsorption by soil suspension tests with the application of oak wood bark biochar.

Test	Ref Zn		SO3SP0.03		SO5SP0.05		SO3L0.03		MO3SP0.03		MO5SP0.05		MO3L0.03	
	t (min)	C (mg/L)	%	C (mg/L)	%	C (mg/L)	%	C (mg/L)	%	C (mg/L)	%	C (mg/L)	%	C (mg/L)
0	106.02	0	106.02	0	106.02	0	106.02	0	106.02	0	106.02	0	106.02	0
20	65.20	38.5	42.32	60.1	34.10	67.8	73.60	30.6	59.45	43.9	59.55	43.8	57.65	45.6
60	86.10	18.8	46.04	56.6	40.65	61.7	33.85	68.1	62.95	40.6	60.70	42.7	60.95	42.5
120	-	-	47.23	55.5	42.01	60.4	40.40	61.9	62.65	40.9	61.23	42.2	61.30	42.2
240	103.60	2.3	47.16	55.5	43.43	59.0	41.60	60.8	63.46	40.1	60.65	42.8	60.95	42.5
1440	67.50	36.3	35.62	66.4	42.49	59.9	32.65	69.2	62.04	41.5	62.55	41.0	59.70	43.7
3 days	71.77	32.3	48.03	54.7	-	-	-	-	-	-	-	-	-	-
7 days	86.10	18.8	35.25	66.8	-	-	-	-	-	-	-	-	-	-

Test	Ref Ni*		SO3SP0.03		SO5SP0.05		SO3L0.03		MO3SP0.03		MO5SP0.05		MO3L0.03	
	t (min)	C (mg/L)	%	C (mg/L)	%	C (mg/L)	%	C (mg/L)	%	C (mg/L)	%	C (mg/L)	%	C (mg/L)
0	158.4	0	158.4	0	158.4	0	158.4	0	158.4	0	158.4	0	158.4	0
20	109.1	42.6	37.3	76.5	47.6	69.9	41.3	73.9	92.2	41.8	96.6	39.0	94.5	40.3
60	86.3	45.5	58.3	63.2	41.8	73.6	51.2	67.7	97.4	38.5	111.1	29.9	102.3	35.4
120	-	-	62.5	60.5	51.9	67.2	58.4	63.1	98.9	37.6	113.8	28.2	103.2	34.8
240	90.2	43.0	66.6	58.0	52.9	66.6	60.3	61.9	103.8	34.5	115.6	27.0	104.5	34.0
1440	115.9	26.8	65.4	58.7	54.5	65.6	62.5	60.5	106.4	32.8	118.4	25.3	110.9	30.0
3 days	-	-	62.4	60.6	-	-	-	-	-	-	-	-	-	-
7 days	-	-	37.1	76.6	-	-	-	-	-	-	-	-	-	-

\*reference test obtained by Gomes (2017)



The results acquired for the evolution of the percentage of Zn (II) adsorbed throughout one day in the tests executed with the application of oak wood bark biochar are illustrated in Figure 7.

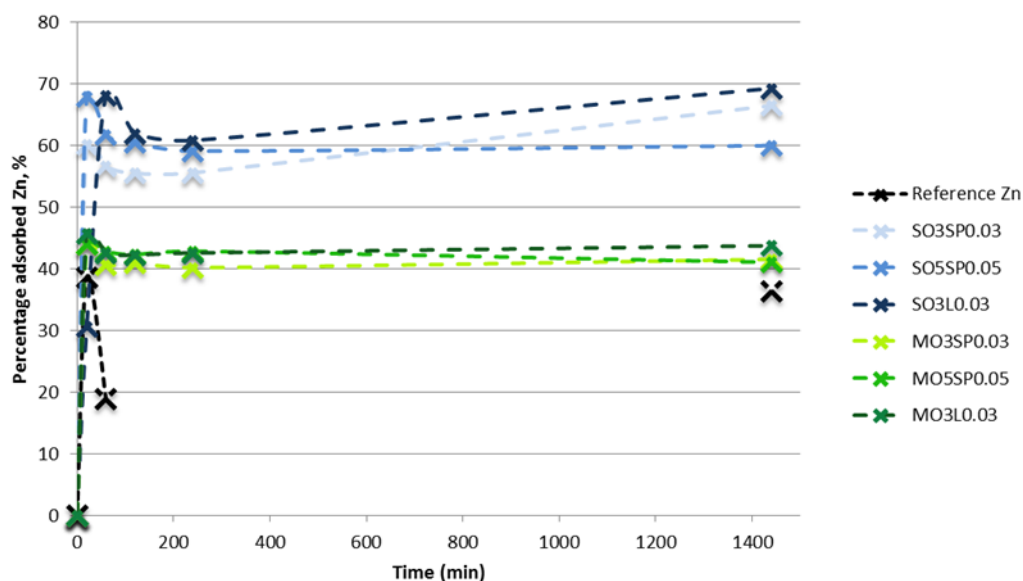


**Figure 7:** Evolution of the percentage of Zn (II) adsorbed over time in the soil suspension tests with the application of oak wood bark biochar.

Reviewing all the results obtained for the adsorption of Zn (II), it should be highlighted that the tests performed, using oak biochar as additive, efficiently retained Zn (II) and the equilibrium concentration was achieved after approximately 2 hours of adsorption.

The results obtained for Zn (II) on the test with 3% (w/w) of oak wood bark biochar previously dispersed with 0.03% of SDBS + Pluronic F-127 clearly show a significant improvement in the adsorption capacity in comparison to the reference test, having increased after 24h of contact from 36.3% to 66.4%. Furthermore, after 3 and 7 days the adsorption capacity of Zn (II) increased from 32.3% and 18.8% in the reference test to 54.7% and 66.8% in the SO3SP0.03 test, respectively. This may be due to the alkaline nature of biochar, as its introduction in acidic soils increases the pH of soil and, therefore, reduces the mobility and bioavailability of the heavy metals, since they are converted to less available fractions, and thus increases its adsorption capacity (Beesley et al., 2010; Guo et al., 2008; Jiang et al., 2010; Lu et al., 2014; Matin et al., 2020; Rizwan et al., 2016; Zhang et al., 2013; Zheng et al., 2020).

Nascimento (2018) performed a percolation test with the same concentration of oak wood bark biochar and SDBS + Pluronic F-127, with and without pH adjustment to 5, and obtained a Zn (II) adsorption capacity of 73.26% and 57.74%, respectively. Hence, the adsorption capacity achieved after one day in the SO3SP0.03 suspension test is higher than

the one obtained by Nascimento (2018) without pH adjustment but lower than the test with pH 5. This may be due to the difference in the soil initial state, its grain size composition and pH. The soil used by Nascimento (2018) presented a higher content of smaller particles and thus, it may explain the better adsorption capacity achieved in her study.

The increase in concentration of biochar and SDBS + Pluronic F-127 (from SO3SP0.03 to SO5SP0.05) did not favour the adsorption capacity of Zn (II) after 24h. The highest retention (67.8%) was registered after 20 min of adsorption and henceforward desorption occurred. The slight increase in the adsorption capacity for low contact times may be due to the higher number of active sites provided by the addition of more biochar and surfactant and to a greater enhancement of the soil pH, as observed by Rizwan et al. (2016), which have a stronger influence at the beginning of the adsorption process.

The shift in surfactant, from a mixture of SDBS + Pluronic F-127, anionic and non-ionic respectively, to LigniOx-LB, an anionic surfactant, originated a better adsorption capacity for Zn (II) after 1 day of adsorption, 66.4% compared to 69.2%, respectively. This may be attributed to a higher total quantity in weight of anionic surfactant, increasing the number of negative active sites available to form complexes with the heavy metal cations. Furthermore, since the application of LigniOx-LB increases the total organic matter content present in the suspension, and zinc has a strong affinity towards it, it may also explain the better adsorption obtained when compared to the other surfactants (Fontes & Gomes, 2003). Moreover, lignin is constituted by two main functional groups, carboxylic and phenolic groups, though it is richer in the latter which is also the one that presents higher affinity for metals ions (Guo et al., 2008). According to Guo et al. (2008), the phenolic-type sites have a binding strength in the following order: Pb (II) > Cu (II) > Cd (II) > Zn (II) > Ni (II).

The application of oak wood bark biochar with a higher size produced less effective results, although still higher than the reference test. The trend observed for the Zn (II) adsorption capacity was the same for both size ranges, i.e., the highest adsorption capacity was registered for the 3% (w/w) concentration of biochar and 0.03% (w/w) LigniOx-LB, followed by the 3% (w/w) concentration of biochar and 0.03% (w/w) SDBS + Pluronic F-127 and then the 5% (w/w) concentration of biochar and 0.05% (w/w) SDBS + Pluronic F-127. After 24h, the adsorption capacity of Zn (II) was 43.7%, 41.5% and 41%, respectively, for the three formulations referred above. The lower surface area of the bigger size oak wood bark biochar may justify the results achieved (Lu et al., 2014). In addition, the dispersions obtained for the larger size oak wood bark biochar, presented in Figure A2 in Appendix A, show a higher mean diameter and various peaks with distinct sizes suggesting a lower dispersion quality.

The data collected for the evolution of the percentage of Ni (II) adsorbed over one day of contact time in the tests performed with the application of oak wood bark biochar are illustrated in Figure 8.

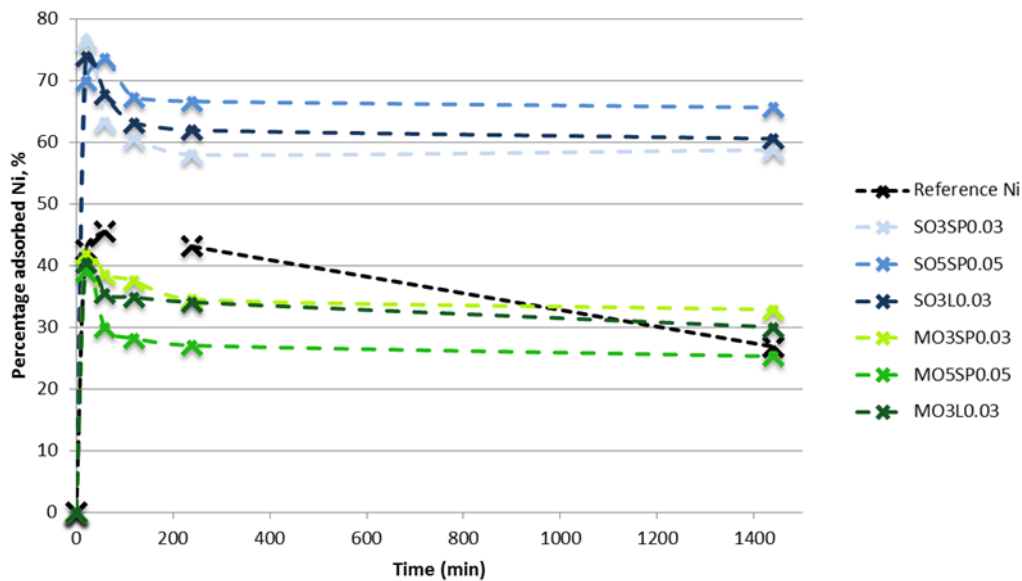


**Figure 8:** Evolution of the percentage of Ni (II) adsorbed over time in the soil suspension tests with the application of oak wood bark biochar.

Throughout the tests performed to study the adsorption capacity of Ni (II), it is clear that desorption occurred, as the highest retention was usually registered after 20 minutes from the beginning of the experiment and the lowest after 1 day of contact time. The equilibrium concentration was reached after approximately 2 hours since the beginning of the experiment.

In the SO3SP0.03 experiment, the adsorption capacity of Ni (II) increased after the fourth hour from 58% to 58.7%, 60.6% and 76.6% on the first, third and seventh day, respectively. It is noteworthy that the adsorption capacity reached on the seventh day is only 0.1% higher than the one obtained after 20 minutes of adsorption. The possible explanation for the improvement verified in the adsorption capacity of Ni (II) is the increase in the soil's pH, induced by the addition of biochar, and consequently the decrease in the mobility of the heavy metals' ions, as stated aforementioned previously for the results of Zn (II). Ali et al. (2020) attributed the immobilization capacity of biochar to its high specific surface area, alkaline nature and the presence of functional groups, which can form complexes with Ni through a ligand exchange of hydroxyl groups. Furthermore, they suggested that a larger content of cellulose present in the biochar could result in a higher aromaticity and alkalinity, thus improving the adsorption capacity by biochar.

In the percolation test performed by Nascimento (2018), with the same concentration of adsorbent and surfactants, the Ni (II) adsorption capacity attained was 73.75% and 56.14%

with and without adjusting the pH to 5, respectively. Thus, the immobilization of Ni (II) obtained in the SO3SP0.03 suspension test after 24h is, once again, lower than the one obtained with pH 5 and higher than the achieved without pH adjustment. Again, this may be due to the different composition of the soil, its pH and its initial state. Nevertheless, the adsorption capacities attained in the SO3SP0.03 suspension test after 20 minutes and 7 days, 76.5% and 76.6%, respectively, are both higher than the adsorption capacity reached by Nascimento (2018) in the percolation tests. This result suggests that the increase in the time of contact could also enhance the immobilization of Ni (II) obtained in percolation tests.

The increase in the concentrations of oak wood bark biochar and SDBS + Pluronic F-127 to 5% (w/w) and 0.05% (w/w), respectively, originated a slightly better adsorption capacity of Ni (II) after 1 day of contact, 73.6%, as it could be expected. However, after 1 hour of the start of the experiment, a desorption effect of Ni (II) was observed. In the study performed by Ali et al. (2020) the application of 2% of biochar, instead of 1%, resulted in an increase of the soil's pH, electrical conductivity and dissolved organic carbon and thus, in a higher adsorption capacity, as aforementioned in Table 10 in section 2.3.1.

The change of surfactant from SDBS + Pluronic F-127 to LigniOx-LB (from SO3SP0.03 to SO3L0.03), increased the final adsorption capacity of Ni (II) from 58.7% to 60.5%, respectively. Nonetheless, the maximum percentage of Ni (II) adsorbed with the application of LigniOx-LB, 73.9%, was slightly lower than the one obtained with SDBS + Pluronic F-127, 76.5%, after 20 minutes of adsorption for both tests. A possible justification for the better performance of LigniOx-LB is the greater organic matter content and the presence of carboxylic and phenolic groups provided by this surfactant (Guo et al., 2008), as previously mentioned in the discussion of the results obtained for Zn (II).

The efficiency of the adsorption of Ni (II) in the soil suspension is highly affected by the size of the biochar applied, as it is presented in Figure 8. In all cases tested, increasing the size of the biochar decreased the adsorption efficiency. The trend verified for the bigger size oak wood bark biochar, in the case of Ni (II) adsorption is not similar to the one obtained for the smaller size biochar, contrary to what occurred for Zn (II). The final retention capacity achieved for Ni (II) followed the order: MO3SP0.03 (32.8%) > MO3L0.03 (30.0%) > MO5SP0.05 (25.3%), after 24h of adsorption. This might be due to the poorer dispersions obtained for the bigger size biochar, presented in Figure A2 in Appendix A. The experiments with 3% (w/w) of biochar and 0.03% (w/w) of surfactants show multiple peaks with distinct sizes, while the test with 5% (w/w) of biochar and 0.05% (w/w) of SDBS + Pluronic F-127 has a large peak for larger sizes suggesting a lower surface area as a result of particle aggregation.

Matin et al. (2020) studied the immobilization of Ni and Zn by two biochars (almond and walnut biochar) for three biochar concentrations (2.5%, 5% and 10%) in an alkaline soil. The authors concluded the increase in biochar's concentration produced better results. As mentioned in Table 12, almond biochar was more effective in immobilizing Zn, i.e., 10.2%, 23.3% and 31.3% with addition of 2.5%, 5% and 10% of almond biochar, respectively, whereas walnut biochar was more effective in immobilizing Ni, i.e., 11.1%, 24.7% and 24.5% with addition of 2.5%, 5% and 10% of walnut biochar, respectively. However, the application of 10% of almond biochar reduced the cumulative leaching by 29.7%. Thus, all the experiments performed in the present study show a higher immobilization of Ni (II) and Zn (II) than the ones obtained by Matin et al. (2020), except in the test MO5SP0.05 for Ni (II). This may be due to the different temperature of the pyrolysis of the feedstock, which highly affects the properties of biochar, i.e., surface area, cation exchange capacity and alkalinity, and to the properties of the soil, such as its pH, organic matter content and composition. Furthermore, the almond and walnut shells used by Matin et al. (2020) were pyrolyzed at 500°C and 400°C, respectively, and although the temperature of the pyrolysis of the oak wood bark is not known, the temperature of a wildfire is usually between 600°C and 800°C. Therefore, the oak wood bark biochar may have better developed pores and a higher pore volume, surface area, alkalinity and pH (Weber & Quicker, 2018), as mentioned in section 2.3.1, and thus, a higher adsorption capacity.

#### **4.3. Results of the heavy metals' adsorption by soil suspension tests with the application of nanoclays**

In the soil suspension tests with the addition of halloysite nanoclay six parameters were evaluated. Initially, the effect of the concentration of nanoclay was assessed. Secondly, the impact of the concentration of SDBS + Pluronic F-127 was considered. Then, the outcome of the increase in concentration of both nanoclay and SDBS + Pluronic F-127 was evaluated. Next, the effect of the time of contact was examined. Afterwards, the performance of another surfactant, LigniOx-LB, was assessed. Finally, the influence of the concentration of LigniOx-LB was investigated. All the tests were performed for Zn (II) and Ni (II). The initial concentration of each heavy metal present in the suspension is the maximum concentration found by Inácio et al. (2008) in the Portuguese soils. In Table 28 are presented the initial concentrations of the heavy metals and the concentrations of the heavy metals in the suspension, as time progressed, measured through AAS for each time a sample was collected, as well as its respective adsorption percentage for every experiment performed. The

dispersions of the halloysite nanoclay alone, with the different surfactants, are displayed in Appendix B.

**Table 28:** Results obtained in the adsorption by soil suspension tests with the application of halloysite nanoclay.

Test	Ref Zn		NC0.01SP0.03		NC0.05SP0.03		NC0.05SP0.15		NC1SP3		NC1L0.01		NC1L3	
	t (min)	C (mg/L)	%	C (mg/L)	%	C (mg/L)	%	C (mg/L)	%	C (mg/L)	%	C (mg/L)	%	C (mg/L)
0	106.02	0	106.02	0	106.02	0	106.02	0	106.02	0	106.02	0	106.02	0
20	65.20	38.5	80.65	23.9	83.30	21.4	77.81	26.6	61.56	41.9	87.60	17.4	20.60	80.6
60	86.10	18.8	84.35	20.4	86.01	18.9	77.85	26.6	65.55	38.2	89.61	15.5	35.70	66.3
120	-	-	83.80	21.0	85.90	19.0	80.89	23.7	66.37	37.4	90.55	14.6	34.60	67.4
240	103.60	2.3	84.94	19.9	86.24	18.7	81.40	23.2	66.68	37.1	91.74	13.5	33.10	68.8
1440	67.50	36.3	87.06	17.9	83.19	21.5	79.82	24.7	68.85	35.1	92.63	12.6	27.80	73.8
3 days	71.77	32.3	93.35	12.0	-	-	79.15	25.3	41.10	61.2	-	-	-	-
7 days	86.10	18.8	-	-	-	-	37.05	65.1	-	-	-	-	-	-

Test	Ref Ni		NC0.01SP0.03		NC0.05SP0.03		NC0.05SP0.15		NC1SP3		NC1L0.01		NC1L3	
	t (min)	C (mg/L)	%	C (mg/L)	%	C (mg/L)	%	C (mg/L)	%	C (mg/L)	%	C (mg/L)	%	C (mg/L)
0	158.4	0	158.4	0	158.4	0	158.4	0	158.4	0	158.4	0	158.4	0
20	109.1	42.6	97.1	38.7	106.3	32.9	102.9	35.0	73.5	53.6	120.3	24.1	95.3	39.8
60	86.3	45.5	101.4	36.0	111.6	29.5	110.1	30.5	78.9	50.2	120.8	23.7	94.6	40.3
120	-	-	104.6	34.0	114.6	27.7	111.4	29.7	82.9	47.7	122.7	22.5	93.7	40.8
240	90.2	43.0	105.0	33.7	119.0	24.9	110.4	30.3	86.0	45.7	127.9	19.3	88.6	44.1
1440	115.9	26.8	115.4	27.1	127.4	19.6	111.5	29.6	87.6	44.7	133.2	15.9	82.1	48.2
3 days	-	-	125.6	20.7	-	-	100.7	36.4	125.7	20.6	-	-	-	-
7 days	-	-	-	-	-	-	133.9	15.5	157.4	0.6	-	-	-	-

\*reference test obtained by Gomes (2017)

The results attained for the evolution of the percentage of Zn (II) adsorbed throughout one day in the tests executed with the application of halloysite nanoclay are illustrated in Figure 9.

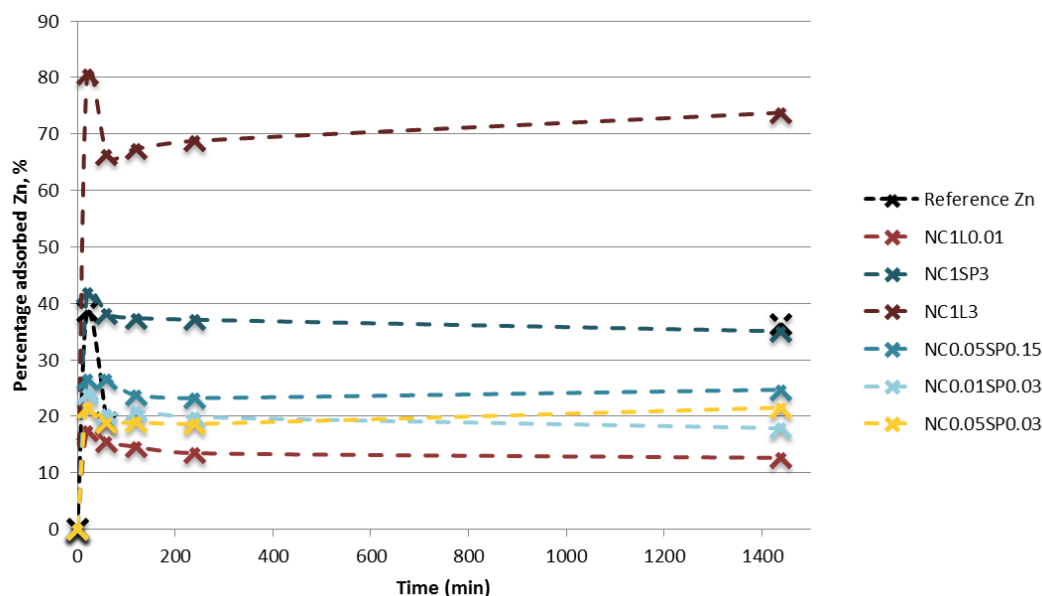


**Figure 9:** Evolution of the percentage of Zn (II) adsorbed over time in the soil suspension tests with the application of halloysite nanoclay.

Examining all the experiments executed in this study with the application of halloysite nanoclay, it is clear that after 24 hours, only the experiment NC1L3 (using 3% of LigniOx-LB as surfactant) was effective in retaining Zn (II) and the equilibrium concentration was achieved after approximately 2 hours of contact, which is in accordance with the findings of Yavuz et al. (2003). Furthermore, the application of nanoclay to the soil showed that the highest adsorption capacity for Zn (II) occurred always after 20 minutes of contact time.

In the experiment with 0.01% (w/w) of halloysite nanoclay formerly dispersed with 0.03% (w/w) of SDBS + Pluronic F-127 the adsorption capacities obtained throughout time demonstrated that Zn (II) was not effectively adsorbed, showing lower results than the reference test, 17.9% compared to 36.3%, respectively. The increase in the concentration of halloysite nanoclay from 0.01% to 0.05% (w/w), maintaining the same concentration of surfactants (0.03% (w/w)), resulted in a slight increase in the adsorption capacity obtained after 24h to 21.5%, which was still very low. The improvement in the immobilization of Zn (II) was more noticeable in the experiment where the concentration of nanoclay and surfactants was increased to 0.05% (w/w) and 0.15% (w/w), respectively, as it would be expected since the nanoclay should be better dispersed given the higher concentration of surfactants. The increase verified in the adsorption capacity of the heavy metals, in this case Zn (II), may be attributed to the rise in the soil's pH and the consequent limitation of the



metal's ions mobility in soil (Świercz et al., 2016), as it also occurred with the addition of biochar. Furthermore, the heavy metal's ions present in the suspension may form stable complexes with the siloxane and hydroxyl groups present in the outer surface of the halloysite nanoclay, therefore enhancing their adsorption efficiency (Liu et al., 2019b; Soleimani & Amini, 2017; Yavuz et al., 2003). However, the adsorption may be limited by the electrostatic repulsions between the heavy metal's cations and the positively charged inner surface of the nanoclay (Glotov et al., 2019).

The 5-time increment in both the concentrations of nanoclay and surfactant (from NC0.01SP0.03 to NC0.05SP0.15) improved the adsorption capacity over time, being the only experiment where the adsorption capacity increased from the first to the seventh day. Despite the immobilization of Zn (II) obtained on the seventh day for the NC0.05SP0.15 experiment, it is apparent that the concentrations of 0.01% and 0.05% (w/w) of halloysite nanoclay were not sufficient to efficiently retain Zn (II), since the results after 1 day of adsorption are lower than the reference test.

Comparing with the results obtained by Liu et al. (2019c), it can be seen that the experiments performed with 0.05% (w/w) of halloysite nanoclay (NC0.05SP0.03 and NC0.05SP0.15) achieved a higher immobilization of Zn (II) after 24h of contact than their control experiment and the amendment with sediment and  $\text{Ca(OH)}_2$  at a ratio of 1:10 (w/w). Nonetheless, the concentration of 0.05% (w/w) of halloysite nanoclay was not enough to overcome the Zn (II) immobilization reached by Liu et al. (2019c) when they enriched the halloysite nanotubes with carboxylic groups alone and with carboxylic groups and  $\text{Ca(OH)}_2$  at a ratio of 1:10 (w/w), proving the importance of these types of groups in the adsorption of heavy metals, and thus of the modification of the halloysite nanoclay.

The increase in the concentrations of halloysite nanoclay to 1% (w/w) and of the SDBS + Pluronic F-127 to 3% (w/w), which is 100 times higher than the first experiment (NC0.01SP0.03), resulted in a better adsorption capacity of Zn (II), achieving 35.1% after 24h of contact and 61.2% after 3 days. However, none of these experiments led to a very high adsorption capacity demonstrating, once again, that the concentrations used were not appropriate to effectively remediate the majority of the Zn (II) present in soil, or that the halloysite nanoclay needs to be functionalized to be effective for this task. This experiment attained a higher retention of Zn (II) than the raw sediment,  $\text{Ca(OH)}_2$  and HNTs@CRC amendments done by Liu et al. (2019c), showing an improvement in comparison to the previous test, thus indicating an interest in a possible further increase in the concentrations of halloysite nanoclay and SDBS + Pluronic F-127.

The effect of the time of contact was evaluated in three different experiments. The only experiment carried out for 7 days was the one with a nanoclay concentration of 5% (w/w) previously dispersed with 0.15% (w/w) SDBS + Pluronic F-127, and the adsorption capacity increased from 24.7% to 25.3% and 65.1% on the first, third and seventh day, respectively. Nevertheless, the results obtained after the first and third day were lower than the reference test. The NC0.01SP0.03 test showed a lower adsorption capacity for Zn (II) after 3 days than the reference test, 12% compared to 32.3% respectively, however the NC1SP3 test resulted in a clear improvement since it retained 61.2% of the Zn (II) present in the suspension after 3 days. Thus, the results indicate that Zn (II) may be effectively adsorbed over time when the concentration of nanoclay is sufficient and they are efficiently dispersed with SDBS + Pluronic F-127.

Considering the results obtained with the mixture of surfactants SDBS + Pluronic F-127, in the study performed with the application of LigniOx-LB to the halloysite nanoclay, 1% (w/w) of nanoclay was used. Using 0.01% (w/w) of LigniOx-LB, proved that this concentration of surfactant was not enough to obtain an efficient adsorption capacity, since the result achieved after 24h was 12.6%, having decreased from 17.4% registered after 20 minutes. Thus, a test with a higher concentration of LigniOx-LB was performed (3% - test NC1L3). Comparing the NC1SP3 and NC1L3 tests to better evaluate the performance of the surfactants in dispersing the soil suspension with nanoclay, it is clear that LigniOx-LB provides a better adsorption of Zn (II) than SDBS + Pluronic F-127, 73.8% compared to 35.1%, respectively, after one day of adsorption. This is in agreement with previous studies, since Zn (II) presents a strong affinity towards the organic matter, as mentioned previously (Fontes & Gomes, 2003; Nascimento, 2018).

Comparing with the results obtained by other authors, the NC1L3 test achieved a higher immobilization of Zn (II) than all the amendments studied by Liu et al. (2019c), while the NC1SP3 obtained a similar adsorption capacity to the one achieved in the amendment enriched with carboxylic groups and  $\text{Ca}(\text{OH})_2$ . The difference verified between the adsorption capacities obtained by Liu et al. (2019c) and the ones achieved in this study may be due to the distinct properties of the applied nanoclay, i.e., surface area and pore diameter, and to the high affinity of Zn (II) towards organic matter. The tests performed by Hermawan et al. (2018) with the application of 2% or 5% of fly ash, zeolite or halloysite nanotubes showed a higher removal percentage of Zn (II), as presented in Table 12, than all the experiments executed in the present study with the addition of halloysite nanoclay. This may be attributed to the presence of various fine particles with a size lower than 0.075 mm in the Matauri Bay (MB)

and UltraHallopure (UHP) halloysite nanotubes applied in Hermawan et al. (2018) study, leading to a high surface area.

The values achieved for the evolution of the percentage of Ni (II) adsorbed over one day of contact time in the experiments performed with the addition of halloysite nanoclay are illustrated in Figure 10.

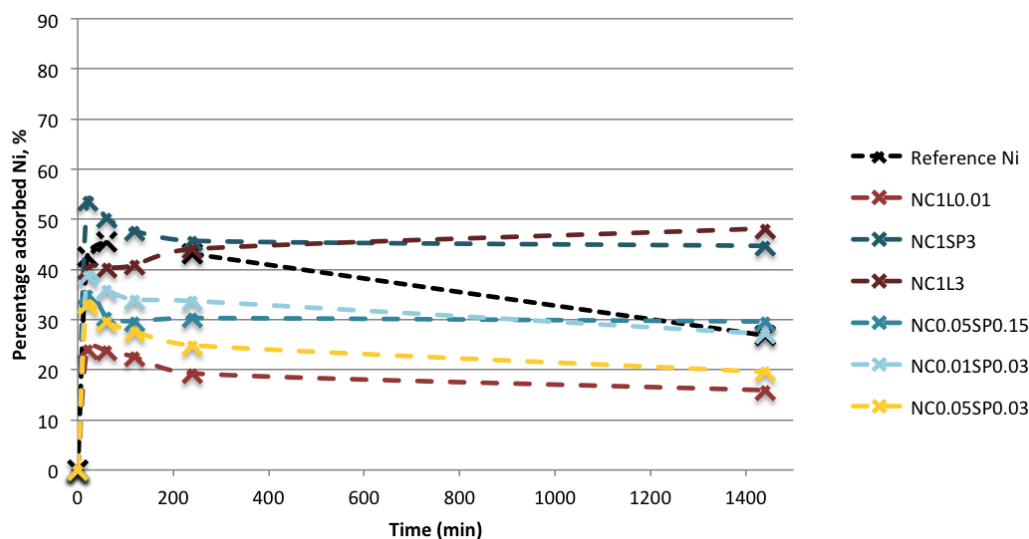


**Figure 10:** Evolution of the percentage of Ni (II) adsorbed over time in the soil suspension tests with the application of halloysite nanoclay.

The results obtained in the tests where halloysite nanoclay was added to the soil showed an improvement in the adsorption capacity of Ni (II) after 24h for all of the tests executed, except for the NC0.05SP0.03 and NC1L0.01 experiments, when compared to the reference test obtained by Gomes (2017) in similar conditions. Once more, this clearly demonstrated the importance of a good dispersion to attain an effective adsorption capacity. The equilibrium concentration was reached approximately after 2h, which is in agreement with the findings of Yavuz et al. (2003) obtained in the Zn (II) tests, as previously mentioned.

A five-time increment of the concentration of nanoclay to 0.05% (w/w) (from NC0.01SP0.03 to NC0.05SP0.03) did not result in an efficient adsorption since it only adsorbed 19.6% of Ni (II). This may be due to a poor dispersion ability of the surfactant considering its concentration remained the same. When the concentration of SDBS + Pluronic F-127 increased to 0.15% (w/w) (NC0.05SP0.15) the adsorption capacity of Ni (II) improved to 29.6%. However, the increase in the concentration of nanoclay and SDBS + Pluronic F-127 did not originate an efficient remediation of the soil contaminated with Ni (II). A further increase in the concentration of nanoclay and SDBS + Pluronic F-127 was studied. Rising the

concentrations to 1% (w/w) and 3% (w/w), respectively (NC1SP3), a 100-time increment from the NC0.01SP0.03 test, resulted in a clear improvement of the adsorption capacity after 24h, as 44.7% of Ni (II) was adsorbed. This may be due to the further increase in the pH of the suspension and, consequently, the lower mobility of the heavy metal's ions and its higher adsorption (Świercz et al., 2016). Yet again, desorption occurred throughout the time of the experiment, having reached the maximum adsorption value (53.6%) after 20 minutes of the beginning of the adsorption test.

In order to evaluate the impact of the time of contact on the adsorption capacity of Ni (II), three experiments were considered (NC0.01SP0.03, NC0.05SP0.15 and NC1SP3) and it is clear that the results were not satisfactory when compared to the reference experiment. Desorption occurred during these tests, though the highest adsorption capacity of Ni (II) in the NC0.05SP0.15 experiment was registered on the third day of contact, 36.4%, yet still lower than the one obtained on the third day for the reference test (41.4% - presented in Table 25). Assessing the adsorption capacity achieved after 3 days of contact for the NC0.01SP0.03 and NC1SP3 tests, it can be concluded that they are similar, 20.7% and 20.6%, respectively, indicating no clear advantage in the increase of concentration of nanoclay and SDBS + Pluronic F-127 for this time of contact.

The effect of the surfactant was studied by applying LigniOx-LB instead of the SDBS + Pluronic F-127 mixture. Its performance was assessed by testing two distinct concentrations, i.e. 0.01% and 3% (w/w) for dispersing a concentration of halloysite nanoclay of 1% (w/w). The former did not lead to an efficient adsorption due to the clearly low concentration of LigniOx-LB not being enough to effectively disperse the nanoclay present in the suspension, obtaining the lowest adsorption capacity after 24h, 15.9%. Therefore, the concentration of LigniOx-LB was increased to 3% (w/w), which substantially increased the adsorption capacity of Ni (II) after one day to 48.2%. The NC1L3 was the only test where Ni (II) adsorption increased throughout the 24 hours of the experiment. Comparing the tests with 1% (w/w) halloysite nanoclay previously dispersed with 3% (w/w) of the surfactant mixture SDBS + Pluronic F-127, it can be concluded that LigniOx-LB is more effective in the retention of Ni (II) after one day while SDBS + Pluronic F-127 obtained a highest adsorption capacity at the start of the experiment but it decreased thereafter. This might be explained by the increase in the total organic matter content and by the carboxylic and phenolic groups present in the suspension when using LigniOx-LB (Guo et al., 2008).

Comparing with previous studies, the NC1SP3 and NC1L3 tests immobilized Ni (II) better than all the amendments studied by Liu et al. (2019c) and NC0.05SP0.15 was more efficient than the raw sediment and Ca(OH)<sub>2</sub> amendments. Nonetheless, Hermawan et al.

(2018) obtained higher removal percentages of Ni (II) with the addition of 2 or 5% of the three types of fine materials (fly ash, zeolite and halloysite nanotubes), as presented in Table 12, than the ones achieved in this study, similarly to what occurred for Zn (II). The explanation behind this may be the distinct properties of the applied nanoclay, as aforementioned.

Matin et al. (2020) also studied the impact of adding 1% of nanoparticles (natural sodium montmorillonite nanoclay and nano-Fe) to biochar in the immobilization of Ni and Zn. In addition to the results listed in Table 12, Matin et al. (2020) obtained a cumulative leaching at the end of the experiment of 38.89% and 43.75% of Ni and Zn, respectively, upon the addition of 1% of nanoclay to 10% of almond biochar, compared to 29.7% and 31.3% with only 10% of almond biochar. Comparing all the results obtained by them with the experiments performed in this study with the application of 1% (w/w) of halloysite nanoclay, it is noteworthy that the NC1L3 test obtained a better adsorption capacity of both heavy metals after one day of contact than all the experiments executed by Matin et al. (2020). This may be due to the high content of organic matter present in the system and the fact that the metal ions have a great affinity towards the phenolic groups (Guo et al., 2008) which are present in LigniOx-LB. Conversely, the NC1SP3 test only performed better than the treatment with 10% almond biochar and 1% nano-Fe for Zn (II) and had a lower immobilization of Ni (II) than the treatment with 10% walnut biochar and 1% nanoclay. This may be due to the high surface area of the natural sodium montmorillonite nanoclay used by Matin et al. (2020) and to the application of biochar and nanomaterials together, therefore, increasing the number of active sites available for the immobilization of the heavy metals' cations.

Borggaard et al. (2019), Fontes & Gomes (2003) and Rifaey et al. (2017) refer that the heavy metals can be adsorbed to the soil solids by two types of sorption, i.e., specific sorption, by covalent interactions forming an inner-sphere complex, usually Cr (III), Cu (II) and Pb (II), or non-specific sorption, by electrostatic interactions, originating an outer-sphere complex, namely Ni (II), Zn (II) and Cd (II). The former type of sorption by organic and inorganic soil solids can firmly reduce the mobility of the heavy metals, while in the latter the heavy metals sorbed onto cation exchange sites on clay silicates can be easily desorbed. This may explain the desorption of Zn (II) and Ni (II) occurred throughout the experiments, when using nanoclay.



## 5. Conclusions and future work

### 5.1. Conclusions

In this work, oak wood bark biochar and halloysite nanoclay were dispersed by the application of surfactants and applied to a soil contaminated with heavy metals to evaluate their remediation performance.

Reviewing all the dispersions performed for the oak wood bark biochar with a size lower than 210  $\mu\text{m}$ , it is clear that the most favourable dispersion was obtained with 3% (w/w) of biochar and 0.03% (w/w) of LigniOx-LB. Contrarily, the dispersions achieved for the biochar with a size ranged between 210 and 345  $\mu\text{m}$  were not good, as there were multiple peaks present in the particle size distribution.

The soil affinity towards the heavy metals' ions was evaluated by percolation tests and it showed the following sequence: Cr (III) > Cu (II) > Ni (II) > Zn (II). The affinity order obtained is in agreement with previous studies, since it is a consequence of the atomic radii and electronegativity of the heavy metals and of their affinity towards the organic matter present in soil.

The application of 3% (w/w) of oak wood bark biochar (size < 210  $\mu\text{m}$ ) previously dispersed with 0.03% (w/w) of SDBS + Pluronic F-127 to a contaminated soil for a period of 7 days and the following execution of the percolation test showed a more significant improvement in the adsorption capacity of Ni (II) and Zn (II), as Cu (II) and Cr (III) were mostly adsorbed by the soil particles alone. However, the adsorption capacities using only the reference soil, were above 92% for all the heavy metals studied. Furthermore, the experiment with the same concentrations of adsorbent and surfactant but one day of contact produced a high adsorption capacity of Ni (II). Due to the consistently high adsorption capacities obtained throughout the tests for Ni (II) and Zn (II), when using only the reference soil, several analyses were made to find an explanation. The main conclusions were the shift in the soil's pH and grain size, being more acidic and showing a lower percentage of clay and sand than in the previous studies, in the research group, using the same soil. Therefore, it was decided to evaluate the impact of the parameters under study on heavy metals' adsorption by soil suspension tests, for which the soil grain size does not have such a high impact, since the soil is not compacted.

In the heavy metals' adsorption by soil suspension tests, the reference tests showed the same affinity order as obtained in the percolation test, as it was expected. Since Cr (III) and

Cu (II) showed an adsorption capacity above 98%, using the reference soil only, the remaining tests were only performed for Ni (II) and Zn (II).

The application of 3% (w/w) oak wood bark biochar previously dispersed with 0.03% SDBS + Pluronic F-127 improved the adsorption capacity of both heavy metals and it increased with the time of contact, showing the highest adsorption after 7 days. This may be due to the alkaline nature of biochar, since it increases the soil's pH and reduces the mobility and availability of the heavy metals' ions in the suspension.

The increase in the concentration of oak wood bark biochar from 3% (w/w) to 5% (w/w) and SDBS + Pluronic F-127 from 0.03% (w/w) to 0.05% (w/w) did not lead to an increment in the adsorption capacity of Zn (II) after one day for either sizes of the biochar. However, for the lower size biochar it resulted in an increment in the adsorption capacity achieved after 20 minutes of adsorption, but desorption occurred thereafter. For Ni (II) the higher concentration of biochar and surfactants, 5% (w/w) and 0.05% (w/w), respectively, originated a better adsorption capacity for the lower size oak wood bark biochar. The increment in both concentrations may have further increased the pH of soil, therefore decreasing the metal ions mobility and increasing the adsorption, and the number of available active sites.

The shift in surfactant from the SDBS + Pluronic F-127 mixture to LigniOx-LB (a natural surfactant) resulted in a clear enhancement of the adsorption capacity of Zn (II) after one day of contact, which may be due to the increase in the total organic matter content and its high affinity towards it. The adsorption capacity of Ni (II), when using LigniOx-LB as surfactant, is higher than the reference test yet lower than the one achieved with the SDBS + Pluronic F-127. This is in accordance to previous studies, since Ni (II) has a lower affinity towards organic matter than Zn (II).

The oak wood bark biochar with a size lower than 210  $\mu\text{m}$  originated better adsorption capacities of Zn (II) and Ni (II) than the biochar with a size ranged between 210 and 345  $\mu\text{m}$ , which could be expected according to the particle size distribution analyses previously performed and to the higher surface area of the lower size particles.

In the heavy metals' adsorption by soil suspension tests with the application of halloysite nanoclay it was concluded that a concentration lower than 1% (w/w) was not sufficient to effectively retain Zn (II) and Ni (II), since it produced lower adsorption capacities than the reference tests. The increase in the halloysite nanoclay concentration to 1% (w/w) and its former dispersion with 3% (w/w) of surfactant improved the adsorption capacity for both heavy metals. This may be attributed to the increase in the soil's pH and the formation of complexes between the heavy metal's ions and the siloxane and hydroxyl groups



present in the outer surface of the halloysite nanoclay. The adsorption capacity of Zn (II) on the third day of contact was significantly enhanced, however the results were not satisfactory in the case of Ni (II).

The change in surfactant towards LigniOx-LB improved the adsorption capacity achieved for both heavy metals, showing a more significant enhancement for Zn (II). The results obtained in this test were the highest of all the experiments performed, evidencing the potential for further investigation. The explanation for the results obtained may be the high affinity of the metals towards organic matter, as previously mentioned.

According to the results obtained in this study, the potential of oak wood bark biochar and halloysite nanoclay to remediate soils/sites polluted with heavy metals is clear. However, the conditions for their application should be further optimized and investigated.

### 5.2. Future work

The application of oak wood bark biochar derived from the Portuguese wildfires and of halloysite nanoclay achieved encouraging results in the remediation of soil contaminated with heavy metals. Accordingly, further experiments should be performed to better evaluate their remediation capacity and optimize the conditions of the test in order to attain the best result possible.

Regarding the application of oak wood bark biochar, it would be interesting to:

1. Study the effect of the pyrolysis temperature in its adsorption capacity;
2. Assess the influence of the time of contact in the percolation tests, since it was not accomplished in this work;
3. Analyse the effect of the soil and, consequently, its properties in the remediation capacity of the oak wood bark biochar;
4. Evaluate the adsorption capacity for cadmium, since other authors describe a similar behaviour to zinc.

In compliance with the results obtained in this study, further investigation should be done to study the impact of several parameters in the remediation potential of halloysite nanoclay, such as:

1. The application of higher concentrations of halloysite nanoclays and the appropriate concentration of surfactant to achieve a good dispersion;
2. The effect of the time of contact when using LigniOx-LB, as it was the formulation that produced the highest adsorption capacity achieved in this study;

3. The impact of the competitive adsorption of heavy metals with the application of halloysite nanoclay;
4. The performance of nanoclay in heavy metals' adsorption by soil percolation experiments;
5. The application of halloysite nanoclay and oak wood bark biochar simultaneously in the soil;
6. The adsorption capacity for cadmium using the halloysite nanoclay;
7. Compare the performance of halloysite nanoclay with other nanoclays.

## Bibliography

- Abundance of elements in Earth's crust. (2020, March 11). Retrieved March 15, 2020, from [https://en.wikipedia.org/wiki/Abundance\\_of\\_elements\\_in\\_Earth's\\_crust](https://en.wikipedia.org/wiki/Abundance_of_elements_in_Earth's_crust).
- Ali, U., Shaaban, M., Bashir, S., Gao, R., Fu, Q., Zhu, J., & Hu, H. (2020). Rice straw, biochar and calcite incorporation enhance nickel (Ni) immobilization in contaminated soil and Ni removal capacity. *Chemosphere*, *244*, 1–8.
- Alloway, B. J. (2013). Heavy Metals and Metalloids as Micronutrients for Plants and Animals. In B. J. Alloway (Ed.), *Heavy metals in Soils: Trace Metals and Metalloids in Soils and their Bioavailability* (3rd ed., Vol. 22, pp. 195–209). Springer Science+Business Media.
- Anastopoulos, I., Mittal, A., Usman, M., Mittal, J., Yu, G., Núñez-Delgado, A., & Kornaros, M. (2018). A review on halloysite-based adsorbents to remove pollutants in water and wastewater. *Journal of Molecular Liquids*, *269*, 855–868.
- Awa, S. H., & Hadibarata, T. (2020). Removal of Heavy Metals in Contaminated Soil by Phytoremediation Mechanism: a Review. *Water, Air, and Soil Pollution*, *231*(2), 1–15.
- Awasthi, A., Jadhao, P., & Kumari, K. (2019). Clay nano-adsorbent: structures, applications and mechanism for water treatment. *SN Applied Sciences*, *1*(9), 1–21.
- Bakshi, M., & Abhilash, P. C. (2020). Chapter 17 - Nanotechnology for soil remediation: Revitalizing the tarnished resource. In P. Singh, A. Borthakur, P. K. Mishra, & D. Tiwary (Eds.), *Nano-Materials as Photocatalysts for Degradation of Environmental Pollutants* (pp. 345–370). Elsevier.
- Beesley, L., Moreno-Jiménez, E., & Gomez-Eyles, J. L. (2010). Effects of biochar and greenwaste compost amendments on mobility, bioavailability and toxicity of inorganic and organic contaminants in a multi-element polluted soil. *Environmental Pollution*, *158*(6), 2282–2287.
- Bisht, A. S. (2019). Surfactants. In *Commercial Surfactants for Remediation* (1st ed., pp. 17–23). Springer Singapore.

- Biswas, B., Warr, L. N., Hilder, E. F., Goswami, N., Rahman, M. M., Churchman, J. G., Vasilev, K., Pan, G., & Naidu, R. (2019). Biocompatible functionalisation of nanoclays for improved environmental remediation. *Chemical Society Reviews*, *48*(14), 3740–3770.
- Borges, D. L. G., & Holcombe, J. A. (2017). Graphite Furnace Atomic Absorption Spectrometry. In *Encyclopedia of Analytical Chemistry* (pp. 1–20). John Wiley & Sons, Ltd.
- Borggaard, O. K., Holm, P. E., & Strobel, B. W. (2019). Potential of dissolved organic matter (DOM) to extract As, Cd, Co, Cr, Cu, Ni, Pb and Zn from polluted soils: A review. *Geoderma*, *343*(February), 235–246.
- Cha, J. S., Park, S. H., Jung, S. C., Ryu, C., Jeon, J. K., Shin, M. C., & Park, Y. K. (2016). Production and utilization of biochar: A review. *Journal of Industrial and Engineering Chemistry*, *40*, 1–15.
- Chai, Q., Lu, L., Lin, Y., Ji, X., Yang, C., He, S., & Zhang, D. (2018). Effects and mechanisms of anionic and nonionic surfactants on biochar removal of chromium. *Environmental Science and Pollution Research*, *25*(19), 18443–18450.
- Chen, X., Kumari, D., Cao, C. J., Plaza, G., & Achal, V. (2019). A review on remediation technologies for nickel-contaminated soil. *Human and Ecological Risk Assessment: An International Journal*, 1–15.
- Chowdhury, P., Elkamel, A., & Ray, A. K. (2015). Photocatalytic Processes for the Removal of Toxic Metal Ions. In S. Sharma (Ed.), *Heavy Metals in Water: Presence, Removal and Safety* (pp. 25–43). Royal Society of Chemistry.
- Clementi, E., Raimondi, D. L., & Reinhardt, W. P. (1967). Atomic screening constants from SCF functions. II. Atoms with 37 to 86 electrons. *The Journal of Chemical Physics*, *47*(4), 1300–1307.
- Dhaliwal, S. S., Singh, J., Taneja, P. K., & Mandal, A. (2020). Remediation techniques for removal of heavy metals from the soil contaminated through different sources: a review. *Environmental Science and Pollution Research*, *27*(2), 1319–1333.
- Dhasmana, A., Uniyal, S., Kumar, V., Gupta, S., Kesari, K. K., Haque, S., Lohani, M., & Pandey, J. (2019). Scope of Nanoparticles in Environmental Toxicant Remediation. In R.

- C. Sobti, N. K. Arora, & R. Kothari (Eds.), *Environmental Biotechnology: For Sustainable Future* (1st ed., pp. 31–44). Springer Singapore.
- Elbana, T. A., Magdi Selim, H., Akrami, N., Newman, A., Shaheen, S. M., & Rinklebe, J. (2018). Freundlich sorption parameters for cadmium, copper, nickel, lead, and zinc for different soils: Influence of kinetics. *Geoderma*, *324*, 80–88.
- Figueredo, N. A. de, Costa, L. M. da, Melo, L. C. A., Siebeneichler, E. A., & Tronto, J. (2017). Characterization of biochars from different sources and evaluation of release of nutrients and contaminants. *Revista Ciencia Agronomica*, *48*(3), 395–403.
- Figueiredo, D. T. R. (2014). *Characterization of Carbon Nanotubes dispersions for application in soil stabilization*. Universidade de Coimbra.
- Figueiredo, D. T. R., Correia, A. A. S., Hunkeler, D., & Rasteiro, M. G. B. V. (2015). Surfactants for dispersion of carbon nanotubes applied in soil stabilization. *Colloids and Surfaces A: Physicochemical and Engineering Aspects*, *480*, 405–412.
- Fiyadh, S. S., AlSaadi, M. A., Jaafar, W. Z., AlOmar, M. K., Fayaed, S. S., Mohd, N. S., Hin, L. S., & El-Shafie, A. (2019). Review on heavy metal adsorption processes by carbon nanotubes. *Journal of Cleaner Production*, *230*(4–5), 783–793.
- Floody, M. C., Theng, B. K. G., Reyes, P., & Mora, M. L. (2009). Natural nanoclays: applications and future trends – a Chilean perspective. *Clay Minerals*, *44*(2), 161–176.
- Fontes, M. P. F., & Gomes, P. C. (2003). Simultaneous competitive adsorption of heavy metals by the mineral matrix of tropical soils. *Applied Geochemistry*, *18*(6), 795–804.
- Fortuna, M. E., Simion, I. M., & Gavrilescu, M. (2011). Sustainability in environmental remediation. *Environmental Engineering and Management Journal*, *10*(December), 1987–1996.
- García, R., & Báez, A. P. (2012). Atomic Absorption Spectrometry (AAS). In M. A. Farrukh (Ed.), *Atomic Absorption Spectroscopy* (pp. 1–12). InTechOpen.
- Glotov, A., Stavitskaya, A., Novikov, A., Semenov, A., Ivanov, E., Gushchin, P., Darrat, Y., Vinokurov, V., & Lvov, Y. (2019). 4 - Halloysite Based Core-Shell Nanosystems:

- Synthesis and Application. In A. Wang & W. Wang (Eds.), *Nanomaterials from Clay Minerals* (pp. 203–256). Elsevier.
- Gomes, A. R. D. (2017). *Remediação da contaminação de um solo por metais pesados com recurso a nanopartículas*. Universidade de Coimbra.
- Gu, S., Kang, X., Wang, L., Lichtfouse, E., & Wang, C. (2018). Clay mineral adsorbents for heavy metal removal from wastewater: a review. *Environmental Chemistry Letters*, 17(2), 629–654.
- Guo, X., Zhang, S., & Shan, X. quan. (2008). Adsorption of metal ions on lignin. *Journal of Hazardous Materials*, 151(1), 134–142.
- Hale, S. E., Hanley, K., Lehmann, J., Zimmerman, A. R., & Gerard Cornelissen. (2011). Effects of chemical, biological, and physical aging as well as soil addition on the sorption of pyrene to activated carbon and biochar. *Environmental Science and Technology*, 45(4), 10445–10453.
- Halloysite nanoclay 685445. (n.d.). Retrieved February 18, 2020, from <https://www.sigmaaldrich.com/catalog/product/aldrich/>.
- Heavy Metals. (n.d.). Retrieved April 3, 2019, from <https://epi.envirocenter.yale.edu/2018-epi-report/heavy-metals>.
- Hermawan, A. A., Chang, J. W., Pasbakhsh, P., Hart, F., & Talei, A. (2018). Halloysite nanotubes as a fine grained material for heavy metal ions removal in tropical biofiltration systems. *Applied Clay Science*, 160 (September 2017), 106–115.
- Hickey, A. J., & Giovagnoli, S. (2018). Particle Size Measurement. In *Pharmaceutical Powder and Particles* (1st ed., pp. 43–53). Springer International Publishing.
- Hillel, D. (2008). Soil Physical Attributes. In *Soil in the Environment* (1st ed., pp. 55–77). Elsevier Inc.
- Inácio, M., Pereira, V., & Pinto, M. (2008). The Soil Geochemical Atlas of Portugal: Overview and applications. *Journal of Geochemical Exploration*, 98(1–2), 22–33.

- Ihsanullah, Abbas, A., Al-Amer, A. M., Laoui, T., Al-Marri, M. J., Nasser, M. S., Khraisheh, M., & Atieh, M. A. (2016). Heavy metal removal from aqueous solution by advanced carbon nanotubes: Critical review of adsorption applications. *Separation and Purification Technology*, *157*, 141–161.
- Jawed, A., Saxena, V., & Pandey, L. M. (2020). Engineered nanomaterials and their surface functionalization for the removal of heavy metals: A review. *Journal of Water Process Engineering*, *33*, 101009.
- Jiang, M. qin, Jin, X. ying, Lu, X. Q., & Chen, Z. liang. (2010). Adsorption of Pb(II), Cd(II), Ni(II) and Cu(II) onto natural kaolinite clay. *Desalination*, *252*(1–3), 33–39.
- Kalita, E., & Baruah, J. (2020). Environmental remediation. In S. Thomas, A. T. Sunny, & P. Velayudhan (Eds.), *Colloidal Metal Oxide Nanoparticles* (1st ed.). Elsevier Inc.
- Kalliola, A., Vehmas, T., Liitiä, T., & Tamminen, T. (2015). Alkali-O<sub>2</sub> oxidized lignin - A bio-based concrete plasticizer. *Industrial Crops and Products*, *74*, 150–157.
- Kananizadeh, N., Ebadi, T., Khoshniat, S. A., & Mousavirizi, S. E. (2011). The Positive Effects of Nanoclay on the Hydraulic Conductivity of Compacted Kahrizak Clay Permeated With Landfill Leachate. *Clean - Soil, Air, Water*, *39*(7), 605–611.
- Kastner, E., & Perrie, Y. (2016). Particle Size Analysis of Micro and Nanoparticles. In A. Müllertz, Y. Perrie, & T. Rades (Eds.), *Analytical Techniques in the Pharmaceutical Sciences* (pp. 677–699). Springer.
- Khalid, S., Shahid, M., Niazi, N. K., Murtaza, B., Bibi, I., & Dumat, C. (2017). A comparison of technologies for remediation of heavy metal contaminated soils. *Journal of Geochemical Exploration*, *182*, 247–268.
- Kruus, K., & Hakala, T. (2017, January 1). The Making of bioeconomy transformation. VTT Technical Research Centre of Finland. Retrieved May 27, 2020, from [https://cris.vtt.fi/ws/portalfiles/portal/23031110/The\\_Making\\_of\\_Bioeconomy\\_Transformation\\_2017.pdf](https://cris.vtt.fi/ws/portalfiles/portal/23031110/The_Making_of_Bioeconomy_Transformation_2017.pdf).
- Kumar, A., Balouch, A., Pathan, A. A., Jagirani, M. S., Mahar, A. M., Zubair, M., & Laghari, B. (2019). Remediation of Nickel ion from wastewater by applying various techniques: a review. *Acta Chemica Malaysia*, *3*(1), 1–15.

- Kumpiene, J., Lagerkvist, A., & Maurice, C. (2008). Stabilization of As, Cr, Cu, Pb and Zn in soil using amendments - A review. *Waste Management*, 28(1), 215–225.
- Li, C., Zhou, K., Qin, W., Tian, C., Qi, M., Yan, X., & Han, W. (2019a). A Review on Heavy Metals Contamination in Soil: Effects, Sources, and Remediation Techniques. *Soil and Sediment Contamination*, 28(4), 380–394.
- Li, H., Dong, X., da Silva, E. B., de Oliveira, L. M., Chen, Y., & Ma, L. Q. (2017). Mechanisms of metal sorption by biochars: Biochar characteristics and modifications. *Chemosphere*, 178, 466–478.
- Li, H., Li, J., Bodycomb, J., & Patience, G. S. (2019b). Experimental Methods in Chemical Engineering: Particle Size Distribution by Laser Diffraction—PSD. *Canadian Journal of Chemical Engineering*, 97(7), 1974–1981.
- Li, H., & Qiu, Y. (2019). Dispersion, sedimentation and aggregation of multiwalled carbon nanotubes as affected by single and binary mixed surfactants. *Royal Society Open Science*, 6(7), 190241.
- Lin, Q., & Xu, S. (2020). Co-transport of heavy metals in layered saturated soil: Characteristics and simulation. *Environmental Pollution*, 261, 114072.
- Lisuzzo, L., Cavallaro, G., Parisi, F., Riela, S., Milioto, S., & Lazzara, G. (2020). 4 - Colloidal stability and self-assembling behavior of nanoclays. In G. Cavallaro, R. Fakhrollin, & P. Pasbakhsh (Eds.), *Clay Nanoparticles* (1st ed., pp. 95–116). Elsevier.
- Liu, J., Xue, J., Yuan, D., Wei, X., & Su, H. (2019a). Surfactant Washing to Remove Heavy Metal Pollution in Soil: A Review. *Recent Innovations in Chemical Engineering (Formerly Recent Patents on Chemical Engineering)*, 13(1), 3–16.
- Liu, M., Cao, X., Liu, H., Yang, X., & Zhou, C. (2019b). 12 - Halloysite-Based Polymer Nanocomposites. In A. Wang & W. Wang (Eds.), *Nanomaterials from Clay Minerals* (1st ed., pp. 589–626). Elsevier.
- Liu, Y., Tang, Y., Wang, P., & Zeng, H. (2019c). Carbonaceous halloysite nanotubes for the stabilization of Co, Ni, Cu and Zn in river sediments. *Environmental Science: Nano*, 6(8), 2420–2428.



- Lu, K., Yang, X., Shen, J., Robinson, B., Huang, H., Liu, D., Bolan, N., Pei, J., & Wang, H. (2014). Effect of bamboo and rice straw biochars on the bioavailability of Cd, Cu, Pb and Zn to *Sedum plumbizincicola*. *Agriculture, Ecosystems and Environment*, *191*, 124–132.
- Malvern Instruments. (2010). Mastersizer 2000 user manual. Retrieved March 14, 2019, from [https://www.labmakelaar.com/fjc\\_documents/mastersizer-2000-2000e-manual-eng1.pdf](https://www.labmakelaar.com/fjc_documents/mastersizer-2000-2000e-manual-eng1.pdf).
- Malvern Instruments. (n.d.). *Zetasizer Nano Series*. Retrieved July 1, 2019, from <https://www.malvernpanalytical.com/br/products/product-range/zetasizer-range/zetasizer-nano-range/zetasizer-nano-zs>.
- Mao, X., Jiang, R., Xiao, W., & Yu, J. (2015). Use of surfactants for the remediation of contaminated soils: A review. *Journal of Hazardous Materials*, *285*, 419–435.
- Massaro M., Cavallaro G., Lazzara G. & Riela S. (2020). 13 - Covalently modified nanoclays: synthesis, properties and applications. In G. Cavallaro, R. Fakhrollin, & P. Pasbakhsh (Eds.), *Clay Nanoparticles* (1st ed., pp. 305–333). Elsevier.
- Mastersizer 2000 user manual. (2005) Retrieved March 14, 2019, from [https://www.labmakelaar.com/fjc\\_documents/mastersizer-2000-2000e-manual-eng1.pdf](https://www.labmakelaar.com/fjc_documents/mastersizer-2000-2000e-manual-eng1.pdf).
- Matin, N. H., Jalali, M., & Buss, W. (2020). Synergistic immobilization of potentially toxic elements (PTEs) by biochar and nanoparticles in alkaline soil. *Chemosphere*, *241*, 124932.
- Matos, M. P. S. R. (2016). *Utilização de nanomateriais na descontaminação de solos*. Universidade de Coimbra.
- Matos, M. P. S. R., Correia, A. A. S., & Rasteiro, M. G. (2017). Application of carbon nanotubes to immobilize heavy metals in contaminated soils. *Journal of Nanoparticle Research*, *19*(4).
- Merkus, H. G. (2009). *Particle Size Measurements: Fundamentals, Practice, Quality* (1st ed.). Springer Science+Business Media.

- Nakama, Y. (2017). Surfactants. In K. Sakamoto, R. Lochhead, H. Maibach, & Y. Yamashita (Eds.), *Cosmetic Science and Technology: Theoretical Principles and Applications* (1st edition, pp. 231–244). Elsevier Inc.
- Nascimento, L. B. A. do. (2018). *Análise de alternativas sustentáveis no tratamento de um solo contaminado*. Universidade de Coimbra.
- Pan, L., Ge, B., & Zhang, F. (2017). Indetermination of particle sizing by laser diffraction in the anomalous size ranges. *Journal of Quantitative Spectroscopy and Radiative Transfer*, *199*, 20–25.
- Pandey, S., & Mishra, S. B. (2011). Organic-inorganic hybrid of chitosan/organoclay bionanocomposites for hexavalent chromium uptake. *Journal of Colloid and Interface Science*, *361*(2), 509–520.
- Park, J. H., Choppala, G. K., Bolan, N. S., Chung, J. W., & Chuasavathi, T. (2011). Biochar reduces the bioavailability and phytotoxicity of heavy metals. *Plant and Soil*, *348*(1–2), 439–451.
- Pauling, L. (1973). *The nature of the chemical bond: And the structure of molecules and crystals: An introduction to modern structural chemistry* (3rd ed.). Ithaca, NY: Cornell U.P.
- Perry, R. H., & Green, D. W. (2008). *Perry's chemical engineers' handbook* (D. W. Green & R. H. Perry (eds.); 8th ed.). McGraw-Hill.
- Pulimi, M., & Subramanian, S. (2016). Chapter 8: Nanomaterials for Soil Fertilisation and Contaminant Removal. In S. Ranjan, N. Dasgupta, & E. Lichtfouse (Eds.), *Nanoscience in Food and Agriculture 1* (Vol 20, pp. 229–246). Springer International Publishing.
- Qayyum, S., Khan, I., Meng, K., Zhao, Y., & Peng, C. (2020). *A review on remediation technologies for heavy metals contaminated soil. 1*, 21–29.
- Radziemska, M., & Mazur, Z. (2016). Content of selected heavy metals in ni-contaminated soil following the application of halloysite and zeolite. *Journal of Ecological Engineering*, *17*(3), 125–133.

- Refaey, Y., Jansen, B., Parsons, J. R., de Voogt, P., Bagnis, S., Markus, A., El-Shater, A. H., El-Haddad, A. A., & Kalbitz, K. (2017). Effects of clay minerals, hydroxides, and timing of dissolved organic matter addition on the competitive sorption of copper, nickel, and zinc: A column experiment. *Journal of Environmental Management*, *187*, 273–285.
- Raja, M. A., & Husen, A. (2020). Chapter 20: Role of nanomaterials in soil and water quality management. In A. Husen & M. Jawaid (Eds.), *Nanomaterials for Agriculture and Forestry Applications* (1st ed., pp. 491–503). Elsevier Inc.
- Rizwan, M. S., Imtiaz, M., Huang, G., Chhajro, M. A., Liu, Y., Fu, Q., Zhu, J., Ashraf, M., Zafar, M., Bashir, S., & Hu, H. (2016). Immobilization of Pb and Cu in polluted soil by superphosphate, multi-walled carbon nanotube, rice straw and its derived biochar. *Environmental Science and Pollution Research*, *23*(15), 15532–15543.
- Saadatkah, N., Carillo Garcia, A., Ackermann, S., Leclerc, P., Latifi, M., Samih, S., Patience, G. S., & Chaouki, J. (2020). Experimental methods in chemical engineering: Thermogravimetric analysis—TGA. *Canadian Journal of Chemical Engineering*, *98*(1), 34–43.
- Saikia, J., Gogoi, A., & Baruah, S. (2019). Nanotechnology for Water Remediation. In N. Dasgupta, S. Ranjan, & E. Lichtfouse (Eds.), *Environmental Nanotechnology Volume 2* (1st ed., pp. 195–211). Springer International Publishing.
- Schwaferts, C., Niessner, R., Elsner, M., & Ivleva, N. P. (2019). Methods for the analysis of submicrometer- and nanoplastic particles in the environment. *TrAC - Trends in Analytical Chemistry*, *112*, 52–65.
- Selvi, A., Rajasekar, A., Theerthagiri, J., Ananthaselvam, A., Sathishkumar, K., Madhavan, J., & Rahman, P. K. S. M. (2019). Integrated Remediation Processes Toward Heavy Metal Removal/Recovery From Various Environments-A Review. *Frontiers in Environmental Science*, *7*(May).
- Shi, P., Zhang, H., Lin, L., Song, C., Chen, Q., & Li, Z. (2019). Molecular dynamics simulation of four typical surfactants in aqueous solution. *RSC Advances*, *9*(6), 3224–3231.

- Siyal, A. A., Shamsuddin, M. R., Low, A., & Rabat, N. E. (2020). A review on recent developments in the adsorption of surfactants from wastewater. *Journal of Environmental Management*, 254(October 2019), 109797.
- Skoog, D. A., Holler, F. J., & Crouch, S. R. (2007). *Principles of Instrumental Analysis* (6th ed.). Thomson Brooks/Cole.
- Soleimani, M., & Amini, N. (2017). Chapter 9: Remediation of Environmental Pollutants Using Nanoclays. In M. Ghorbanpour, M. Khanuja, & A. Varma (Eds.), *Nanoscience and Plant–Soil Systems* (Vol. 48, pp. 279–289). Springer International Publishing AG.
- Subramaniam, M. N., Goh, P. S., Lau, W. J., & Ismail, A. F. (2019). The roles of nanomaterials in conventional and emerging technologies for heavy metal removal: A state-of-the-art review. *Nanomaterials*, 9(4), 625.
- Świercz, A., Smorzewska, E., Słomkiewicz, P., & Suchanek, G. (2016). Possible use of halloysite in phytoremediation of soils contaminated with heavy metals. *Journal of Elementology*, 21(2), 559–570.
- Tomczyk, A., Sokołowska, Z., & Boguta, P. (2020). Biochar physicochemical properties: pyrolysis temperature and feedstock kind effects. *Reviews in Environmental Science and Biotechnology*, 19(1), 191–215.
- Tóth, G., Hermann, T., Da Silva, M. R., & Montanarella, L. (2016). Heavy metals in agricultural soils of the European Union with implications for food safety. *Environment International*, 88, 299–309.
- Trakal, L., Komárek, M., Száková, J., Zemanová, V., & Tlustoš, P. (2011). Biochar application to metal-contaminated soil: Evaluating of Cd, Cu, Pb and Zn sorption behavior using single- and multi-element sorption experiment. *Plant, Soil and Environment*, 57(8), 372–380.
- Uddin, F. (2008). Clays, nanoclays, and montmorillonite minerals. *Metallurgical and Materials Transactions A: Physical Metallurgy and Materials Science*, 39(12), 2804–2814.
- Van Liedekerke, M., Prokop, G., Rabl-Berger, S., Kibblewhite, M., & Louwagie, G. (2014). *Progress in management of contaminated sites — European Environment Agency*.

<http://www.eea.europa.eu/data-and-maps/indicators/progress-in-management-of-contaminated-sites/progress-in-management-of-contaminated-1>.

- Weber, K., & Quicker, P. (2018). Properties of biochar. *Fuel*, 217, 240–261.
- Wuana, R. A., & Okieimen, F. E. (2011). Heavy Metals in Contaminated Soils: A Review of Sources, Chemistry, Risks and Best Available Strategies for Remediation. *ISRN Ecology*, 2011, 1–20.
- Xu, Y., Liang, X., Xu, Y., Qin, X., Huang, Q., Wang, L., & Sun, Y. (2017). Remediation of Heavy Metal-Polluted Agricultural Soils Using Clay Minerals: A Review. *Pedosphere*, 27(2), 193–204.
- Yavuz, Ö., Altunkaynak, Y., & Güzel, F. (2003). Removal of copper, nickel, cobalt and manganese from aqueous solution by kaolinite. *Water Research*, 37(4), 948–952.
- Yousra, M., Mahmood-ul-Hassan, M., Sarwar, S., & Naeem, S. (2019). Adsorption of Lead, Cadmium, and Nickel on Benchmark Soils of Pakistan. *Eurasian Soil Science*, 52(9), 1063–1074.
- Zhang, X., Song, K., Liu, J., Zhang, Z., Wang, C., & Li, H. (2019). Sorption of triclosan by carbon nanotubes in dispersion: The importance of dispersing properties using different surfactants. *Colloids and Surfaces A: Physicochemical and Engineering Aspects*, 562, 280–288.
- Zhang, X., Wang, H., He, L., Lu, K., Sarmah, A., Li, J., Bolan, N. S., Pei, J., & Huang, H. (2013). Using biochar for remediation of soils contaminated with heavy metals and organic pollutants. *Environmental Science and Pollution Research*, 20(12), 8472–8483.
- Zheng, H., Zhang, C., Liu, B., Liu, G., Zhao, M., Xu, G., Luo, X., Li, F., & Xing, B. (2020). Biochar for Water and Soil Remediation: Production, Characterization, and Application. In G. Jiang & X. Li (Eds.), *A New Paradigm for Environmental Chemistry and Toxicology* (1st ed., pp. 153–196). Springer Singapore.



## Appendix A – Biochar dispersions'

Dispersions obtained for the experiments performed with oak wood bark biochar

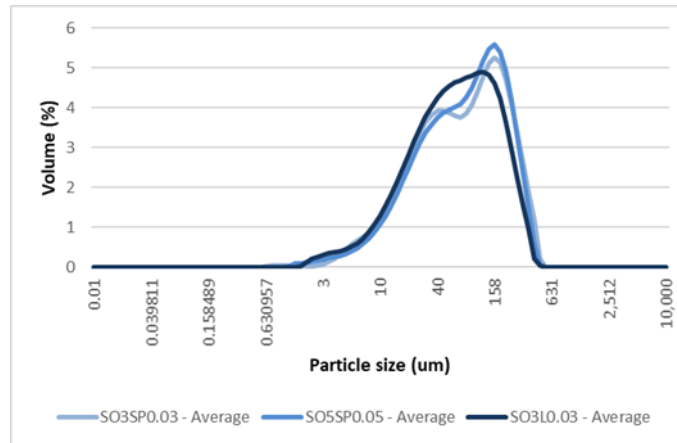


**Figure A1:** Comparison of the particle size distribution for the experiments performed with oak wood bark biochar with a size lower than 210  $\mu\text{m}$ , using different surfactants and concentrations.

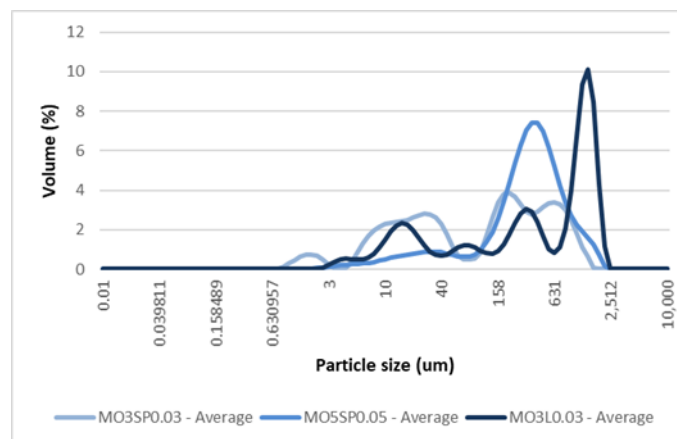


**Figure A2:** Comparison of the particle size distribution for the experiments performed with oak wood bark biochar with a size comprehended between 210 and 345  $\mu\text{m}$  using different surfactants and concentrations.

## Appendix B – Halloysite nanoclay dispersions'

Dispersions obtained for the experiments performed with halloysite nanoclay

0.01% (w/w) halloysite nanoclay and 0.03% (w/w) SDBS + Pluronic

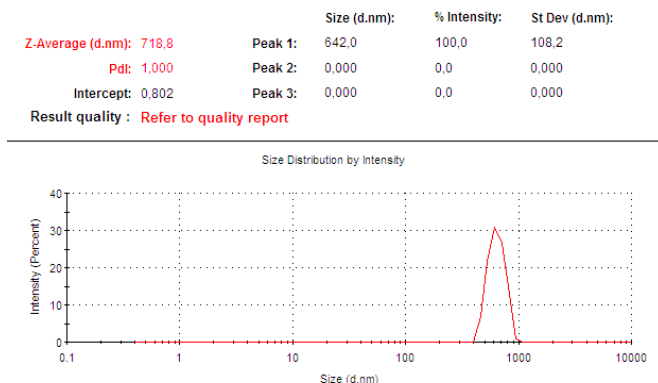


**Figure B1:** Particle size distribution of the dispersion of 0.01% (w/w) halloysite nanoclay with 0.03% (w/w) SDBS + Pluronic F-127.

0.05% (w/w) halloysite nanoclay and 0.15% (w/w) SDBS + Pluronic

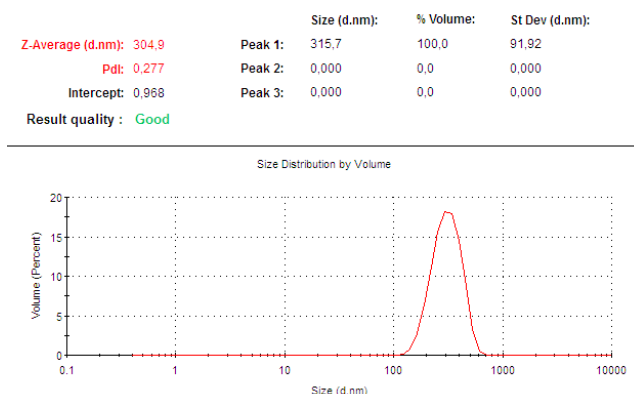


**Figure B2:** Particle size distribution of the dispersion of 0.05% (w/w) halloysite nanoclay with 0.15% (w/w) SDBS + Pluronic F-127.

1% (w/w) halloysite nanoclay and 3% (w/w) SDBS + Pluronic

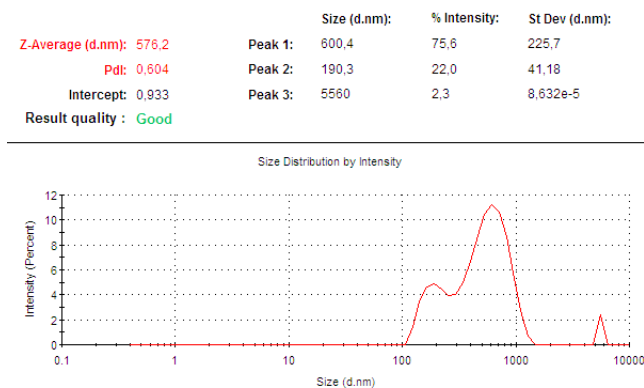


**Figure B3:** Particle size distribution of the dispersion of 1% (w/w) halloysite nanoclay with 3% (w/w) SDBS + Pluronic F-127.



## 1% (w/w) halloysite nanoclay and 3% (w/w) LigniOx-LB

	Size (r.nm):	% Intensity:	St Dev (r.nm):
Z-Average (r.nm): 422.8	Peak 1: 480.0	78.8	153.4
Pdl: 0.666	Peak 2: 79.48	12.2	15.32
Intercept: 0.935	Peak 3: 2612	9.0	230.7

Result quality : Good

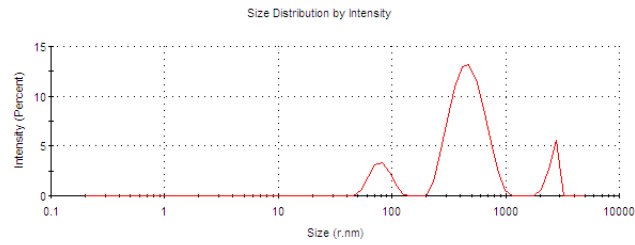


**Figure B4:** Particle size distribution of 1% (w/w) halloysite nanoclay with 3% (w/w) LigniOx-LB.

## Appendix C - Safety

### Copper (II) chloride dihydrate

Label elements:



Hazard Statements:

- H302 + H312 – Harmful if swallowed or in contact with.
- H315 – Causes skin irritation.
- H318 – Causes serious eye damage.
- H410 – Very toxic to aquatic life with life long lasting effects

Precautionary Statements:

- P273 – Avoid release to the environment.
- P280 – Wear protective gloves/ eye protection/ face protection.
- P302 + P352 – IF ON SKIN: Wash with plenty of soap and water.
- P305 + P351 + P338 – IF IN EYES: Rinse cautiously with water for several minutes. Remove contact lenses, if present and easy to do. Continue rinsing.
- P313 –Get medical advice/ attention.

### Chromium (III) nitrate nonahydrate

Label elements:



Hazard Statements:

- H272 – May intensify with fire; oxidizer.
- H332 – Harmful if inhaled.
- H317 – May cause an allergic skin reaction.
- H319 – Causes serious eye irritation.
- H411 – Toxic to aquatic life with long lasting effects.

Precautionary Statements:

- P280 – Wear protective gloves/ protective clothing/ eye protection/ face protection.
- P210 – Keep away from heat/sparks/open flames/hot surfaces. – No smoking.
- P221 – Take any precaution to avoid mixing with combustibles.
- P312 – Call a POISON CENTRE or a doctor/ physician if you feel unwell.

P302 + P352 – IF ON SKIN: Wash with plenty of soap and water.  
P337 + P313 – If eye irritation persists: Get medical advice/ attention.

### Nickel (II) nitrate hexahydrate

Label elements:



Hazard Statements:

H272 – May intensify with fire; oxidizer.  
H302 + H332 – Harmful if swallowed or if inhaled.  
H315 – Causes skin irritation.  
H317 – May cause an allergic skin reaction.  
H318 – Causes serious eye damage.  
H334 – May cause allergy or asthma symptoms or breathing difficulties if inhaled.  
H341 – Suspected of causing genetic defects.  
H350 – May cause cancer.  
H360 – May damage fertility or the unborn child.  
H372 – Causes damage to organs through prolonged or repeated exposure if inhaled.  
H410 – Very toxic to aquatic life with life long lasting effects

Precautionary Statements:

P201 – Obtain special instructions before use.  
P210 – Keep away from heat, hot surfaces, sparks, open flames and other ignition sources. No smoking.  
P273 – Avoid release to the environment.  
P280 – Wear protective gloves/ eye protection/ face protection.  
P305 + P351 + P338 + P310 – IF IN EYES: Rinse cautiously with water for several minutes.  
Remove contact lenses, if present and easy to do. Continue rinsing. Immediately call a POISON CENTRE/ doctor.  
P308 + P313 – IF exposed or concerned: Get medical advice/ attention.

### Zinc sulfate heptahydrate

Label elements:



Hazard Statements:

- H302 – Harmful if swallowed.
- H318 – Causes serious eye damage.
- H410 – Very toxic to aquatic life with life long lasting effects.

Precautionary Statements:

- P273 – Avoid release to the environment.
- P280 – Wear eye protection/ face protection
- P301 + P312 + P330 – IF SWALLOWED: Call a POISON CENTRE/ doctor if you feel unwell. Rinse mouth.
- P305 + P351 + P338 + P310– IF IN EYES: Rinse cautiously with water for several minutes.
- Remove contact lenses, if present and easy to do. Continue rinsing. Immediately call a POISON CENTRE/ doctor.

### Sodium dodecylbenzenesulfonate

Label elements:



Hazard Statements:

- H302 – Harmful if swallowed.
- H315 – Causes skin irritation.
- H318 – Causes serious eye damage.

Precautionary Statements:

- P280 – Wear protective eye protection/ face protection.
- P301 + P312 + P330 – IF SWALLOWED: Call a POISON CENTRE/ doctor if you feel unwell. Rinse mouth.
- P302 + P352 – IF ON SKIN: Wash with plenty of water.
- P305 + P351 + P338 + P310– IF IN EYES: Rinse cautiously with water for several minutes. Remove contact lenses, if present and easy to do. Continue rinsing.
- Immediately call a POISON CENTRE/ doctor.

### Pluronic F-127

Label elements:

Not a hazardous substance or mixture according to Regulation (EC) No. 1272/2008.

### Halloysite nanoclay

Label elements:

Not a hazardous substance or mixture according to Regulation (EC) No. 1272/2008.



